

UNIVERSITÀ DEGLI STUDI DI MILANO

---

FACOLTÀ DI SCIENZE E TECNOLOGIE



LAUREA MAGISTRALE IN FISICA

**Non-equilibrium dynamics and  
effective temperatures of  
a noisy quantum Ising chain**

MASTER'S DEGREE  
*in*  
THEORETICAL PHYSICS

*Author:*  
Giovanni Andrea FRIGERI  
Mat. n° 827495  
.....

*Supervisor:*  
Prof. Andrea GAMBASSI  
.....

*Internal Supervisor:*  
Prof. Sergio CARACCIOLO  
.....

October 6, 2015

*To my family*

*The purpose of thinking about the future is not to predict it but to raise people's hopes.*

Freeman Dyson

Motivated by recent experimental advances in the field of cold atoms, the theoretical study of the non-equilibrium dynamics of isolated quantum many-body systems is currently receiving increasing attention. One of the main question concerns the way in which a macroscopically large isolated system evolving with unitary quantum dynamics from a generic initial state approaches equilibrium. In this thesis we investigate the non-equilibrium dynamics of a quantum Ising chain perturbed by a time-dependent noise in the transverse field and driven out of equilibrium by a sudden change of the static component of this transverse field, we refer to this model as noisy quantum Ising chain. In previous work various equal-time quantities were calculated and it was found that, in the limit of weak noise, the system first attains an intermediate stationary non-thermal state in which the noise does not affect the dynamics, then the noise comes into play and drives the chain towards an infinite-temperature thermal state. Moreover, at long-times, the equal-time correlator of the transverse magnetization shows a diffusive behavior. In this work we extend the computation to two-time quantities and find the correlation and linear response functions of a noisy quantum Ising chain. We focus on the analysis of these expressions in the time range in which the noise has come in play; we find that at short time differences compared to the time elapsed from the quench, the two-time correlator of the transverse magnetization shows a diffusive behavior analogous to the one of the equal-time correlator. On the contrary, for much longer time differences, the qualitative behavior of the two-time correlator changes completely becoming ballistic. In addition, the knowledge of dynamic correlations gives us the opportunity to study the fluctuation-dissipation relations in non-equilibrium conditions. In particular, we extract an effective temperature of the noisy chain from the classical fluctuation-dissipation relation which provide information about its dynamics. In the case of short time differences compared to the time elapsed from the quench, the effective temperature grows towards infinity as time goes, according to the results obtained for the two-time correlator of the transverse magnetization. Instead, in the opposite case of much longer time differences we find an effective temperature that tends to zero: at the present this behavior is not understood and therefore more studies are required.

The thesis is organized as follows:

- In Chapter 1 we introduce the concept of quantum quench and the current understanding of quantum relaxation in integrable and non-integrable quantum many-body systems. Recent experiments involving non-equilibrium of these systems are illustrated.
- In Chapter 2 we review the equilibrium properties of the quantum Ising chain, paradigmatic example of integrable model undergoing a quantum phase transition, which is the basis of the model investigated in this thesis. We discuss after the non-equilibrium dynamics of a quantum Ising chain following a quench of the transverse field and we confirm the lack of thermalization using an approach based on fluctuation-dissipation relations.
- In Chapter 3 we first explain the Keldysh formalism employed in the following to derive the various results. The noisy quantum Ising chain is then introduced and its non-equilibrium dynamics is discussed in detail.
- In Chapter 4 we report the results obtained in this thesis for the two-time correlation and linear response functions of the transverse magnetization. The behavior for different times range is investigated. Finally, we extract an effective temperature of the noisy chain from the classical fluctuation-dissipation relation and we discuss the information provided by it.

Details about the calculations are reported in the Appendices.

## ACKNOWLEDGEMENTS

I would like to thank Prof. Andrea Gambassi for being my supervisor and for all the time he spent in additional explanations, corrections and advice.

I am grateful also to Prof. Sergio Caracciolo, one of the best teacher I met during my academic career, thanks to his lessons (and stories) physics becomes charming.

A special thank is for Jamir Marino for the help provided and the enthusiasm instilled in this work during these months.

My family has always supported me and I am very grateful for it.

Marina deserves heartfelt thanks for listening me even when I bored her with the details about my thesis.

I also want to thank SISSA students, with which I spent beautiful months in Trieste, and my friends in Bergamo for the carefree days.

Finally I am glad to Prof. Alessandro Silva for inspiring discussions and SISSA for financial support.

<b>Abstract</b>	<b>i</b>
<b>Acknowledgements</b>	<b>iii</b>
<b>1 Introduction to non-equilibrium dynamics</b>	<b>1</b>
1.1 Quantum quench . . . . .	1
1.2 Quantum thermalization . . . . .	3
1.2.1 Ergodicity in classical statistical mechanics . . . . .	3
1.2.2 Thermalization in quantum statistical mechanics . . . . .	5
1.2.3 Eigenstate thermalization hypothesis . . . . .	7
1.3 Integrable systems and generalized Gibbs ensemble . . . . .	9
1.4 The end of the story? . . . . .	11
1.5 Prethermalization . . . . .	12
1.6 Fluctuation-dissipation theorem and effective temperatures . . . . .	17
1.6.1 One-time quantities . . . . .	17
1.6.2 Two-time quantities . . . . .	19
<b>2 Quantum Ising Chain</b>	<b>22</b>
2.1 The model . . . . .	22
2.2 Diagonalization of the quantum Ising chain . . . . .	23
2.2.1 Even sector . . . . .	26
2.2.2 Odd sector . . . . .	29
2.2.3 Paramagnetic and ferromagnetic phase . . . . .	30

2.3	Quantum quench in the quantum Ising chain . . . . .	31
2.4	Effective temperatures for quantum Ising chain . . . . .	35
<b>3</b>	<b>Noisy Quantum Ising Chain</b>	<b>46</b>
3.1	The model, the motivation and the out of equilibrium protocol . . . . .	47
3.2	Keldysh formalism . . . . .	48
3.2.1	Closed time contour . . . . .	49
3.2.2	Green's function and non-equilibrium diagrammatics . . . . .	51
3.2.3	Langreth theorem . . . . .	54
3.2.4	Kinetic equations . . . . .	57
3.3	Prethermalization in a noisy quantum Ising chain . . . . .	58
3.3.1	Master equation . . . . .	58
3.3.2	Thermalization dynamics of observables . . . . .	63
<b>4</b>	<b>Dynamic correlations of the noisy quantum Ising chain and effective temperatures</b>	<b>70</b>
4.1	A toy model: two-level system . . . . .	70
4.1.1	The model and Green's function . . . . .	70
4.1.2	Equilibrium and fluctuation-dissipation theorem . . . . .	72
4.1.3	Effective temperatures . . . . .	73
4.2	Green's functions of noisy quantum Ising chain . . . . .	76
4.3	Correlator of the transverse magnetization . . . . .	77
4.4	Long-time behavior . . . . .	79
4.4.1	Two-time correlation and linear response functions . . . . .	79
4.4.2	Non-stationary two-time correlation function . . . . .	81
4.4.3	Effective temperature . . . . .	82
<b>5</b>	<b>Conclusions</b>	<b>86</b>
<b>A</b>	<b>Bogoliubov rotation</b>	<b>88</b>
<b>B</b>	<b>Green's functions of two-level system</b>	<b>90</b>
<b>C</b>	<b>Green's function of the noisy quantum Ising chain</b>	<b>94</b>
<b>D</b>	<b>Evaluation of integrals</b>	<b>99</b>

**References**

**101**

# CHAPTER 1

## INTRODUCTION TO NON-EQUILIBRIUM DYNAMICS

In this Chapter we illustrate the fundamental issues concerning non-equilibrium dynamics in closed quantum many-body systems. In particular, in Sec. 1.1 we introduce the simplest protocol to drive a system out of equilibrium, i.e., the so-called *quantum quench*. In Sec. 1.2 we discuss the definition of thermalization for closed quantum systems and the possible mechanism behind it. Then, in Sec. 1.3, we consider *integrable* quantum systems and their relaxation properties, introducing the generalized Gibbs ensemble. In Sec. 1.5 we present the concept of *prethermalization* and finally, in Sec. 1.6, we review the fluctuation-dissipation theorem and the associated *effective temperatures*, which will turn out to be a useful tool for investigating non-equilibrium dynamics. In addition to the relevant theoretical concepts, experiments involving non-equilibrium dynamics of isolated quantum systems are also illustrated here.

### 1.1 Quantum quench

The strength of thermodynamics consists in its effectiveness in describing a system composed by many degrees of freedom at *equilibrium* in terms of few macroscopic variables, such as temperature, volume, pressure etc. Moreover, these macroscopic variables are generally not independent, but they satisfy some relations, called equation of state, depending on the characteristics of the system considered. The underlying microscopic and probabilistic theory is statistical mechanics, which, starting from general and simple principles, successfully explains the equilibrium properties of systems with many degrees of freedom. This theory has been developed in the 18/19-th century and it is considered one of the greatest successes in physics for its general character and the broad range of applications. However, most systems found in nature are not in thermodynamic equilibrium; for they change over time, are subject to flux of matter and energy or to chemical reactions. Unfortunately, there is no general theory able to describe *non-equilibrium phenomena* and research in this direction proceeds mainly via a case by case study

forming a rapidly evolving research field.

In the past decade, experimental advances in the field of cold atoms [1–3] have made it possible to realize artificial systems which are accurately described by theoretical models (e.g., Hubbard, Kondo, Ising and Luttinger models): internal parameters are tunable with high precision and, in addition, they exhibit an unprecedented degree of isolation from the surrounding environment, i.e., their dynamics is unitary and genuinely quantum many-body effects (e.g., linear superposition of states, entanglement) are preserved by the dynamics during the time scales of the experiments. The availability of these systems provides an invaluable opportunity to explore theoretically and experimentally the non-equilibrium dynamics of closed quantum many-body systems [4]. Among the many ways in which a system can be driven out of equilibrium, in this thesis we concentrate on the simplest protocol, the so-called *quantum quench*. It consists in preparing the system in the ground state  $|0\rangle_{g_0}$  of its quantum many-body Hamiltonian  $H(g_0)$ , characterized by a parameter  $g_0$ , and in suddenly switching the parameter to a different value  $g \neq g_0$ , letting the system evolve according to the post-quench Hamiltonian  $H(g)$ , i.e.,

$$|\psi(t)\rangle = e^{-iH(g)t} |0\rangle_{g_0}, \quad (1.1)$$

where  $|\psi(t)\rangle$  is the state of the system after a time  $t$  from the quench. The ground state  $|0\rangle_{g_0}$  of the pre-quench Hamiltonian  $H(g_0)$  is not an eigenstate of the post-quench Hamiltonian  $H(g)$  and it has a finite overlap with all the post-quench eigenstates  $|n\rangle_g$  (see Fig. 1.1), making the dynamics of the system highly non-trivial.

A sudden change of a parameter is a theoretical idealization, since from an experimental point of view it is not possible to modify the characteristics of a system instantaneously. Let us call  $\tau_r$  the relaxation time of the system, i.e., the time scale which governs the response of the system to external perturbations, and  $\tau_g = g/\dot{g}$  the typical time associated with the variation of the parameter  $g$  in our experiment. For  $\tau_r \ll \tau_g$  the system is given sufficient time to adapt to the altered conditions and it can be thought of as being almost at equilibrium at every moment: this is known as adiabatic transformation. On the other hand, if  $\tau_g \ll \tau_r$  the system is not able to respond to the external perturbation and therefore lags behind: this is what we mean by a sudden change and what constitutes a quantum-quench.

There are different kinds of quantum quenches: the abrupt change of the parameter can involve only a spatially localized part of the extended system (local quench) or the whole system (global quench); it is possible to "quench" the parameter across a quantum phase transition, suddenly switching on interactions, or modify the geometry of the system (geometric quench). It is natural to ask oneself if the system long after a quantum quench approaches a steady state, what the characteristics of this state are and if the eventual relaxation process occurs uniformly in time or if it consists of many stages. We address these questions in the next Sections.

## Quantum quench $H(g)$ (global)

$$|\psi(t)\rangle = e^{-iH(g)t}|0\rangle_{g_0}$$

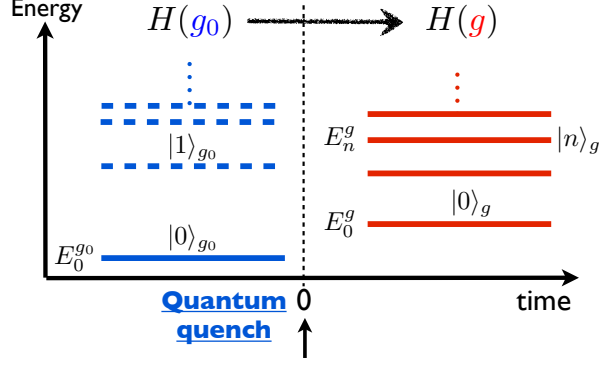


**Figure 1.1:** Schematic representation of the energy spectrum of the pre-quench (blue) and post-quench (red) Hamiltonian. The state  $|0\rangle_{g_0}$  in which the system is initially prepared is not an eigenstate of the post-quench Hamiltonian  $H(g)$ , resulting in a non trivial quantum evolution (see Eq. (1.1)). [Courtesy of A. Gambassi]

## 1.2 Quantum thermalization

### 1.2.1 Ergodicity in classical statistical mechanics

In classical physics the concept behind thermalization is *ergodicity*. Consider a classical system of  $N$  particles in  $d$  spatial dimensions, with volume  $V$  and constant energy  $E$ . The system is characterized by a time-independent Hamiltonian  $H(\vec{x})$ , where  $\vec{x} = (\vec{q}, \vec{p})$  is a point in a  $2dN$ -dimensional phase space  $\Gamma$ . The value of  $\vec{x}$  determines the microscopic state of the system and, because of energy conservation, it belongs to the constant energy surface  $\Sigma_E$ , defined as the set of points  $\vec{x} \in \Gamma$  such that  $H(\vec{x}) = E$ . The point  $\vec{x}$  evolves in time according to Hamilton's equations

$$\begin{aligned} \frac{dq_i(t)}{dt} &= \frac{\partial H}{\partial p_i}, \\ \frac{dp_i(t)}{dt} &= -\frac{\partial H}{\partial q_i}, \\ H(\vec{q}, \vec{p}) &= E, \end{aligned} \tag{1.2}$$

with  $i = 1, \dots, 2dN$ , drawing a trajectory  $\vec{x}(t)$  on the surface  $\Sigma_E$ . In order to describe the properties of the system, we are interested in the value of some observable  $O(\vec{x}(t))$ , which depends on the dynamical state of the system. In experiments done in equilibrium conditions, one is actually measuring the time average  $\bar{O}$  of the observable  $O$ , defined as

$$\bar{O} \equiv \lim_{T \rightarrow +\infty} \frac{1}{T} \int_{t_0}^{t_0+T} dt O(\vec{x}(t)). \tag{1.3}$$

Despite the conceptual simplicity of this definition, it cannot be used for practical purposes. Indeed, determining the dynamics of  $\vec{x}(t)$  requires solving as many differential equations (1.2) as the number of degrees of freedom (of the order of Avogadro number  $N_A \sim 10^{23}$  for macroscopic systems), which is clearly an impossible task. One needs a different approach and equilibrium statistical mechanics is the viable one. Instead of considering its time evolution, the idea is to take a large number of copies of the same system and to assign to this set a time-independent<sup>1</sup> probability distribution  $\rho(\vec{x})$  that determines the probability for the system to be in the state  $\vec{x}$ . The set of the copies is known as *statistical ensemble* and  $\rho(\vec{x})$  is the associated probability distribution. The choice of the ensemble and of the corresponding probability distribution  $\rho$  depends on the macroscopic conditions of the system. If, for example, it has a fixed number  $N$  of particles, a given volume  $V$  and a given value of the energy within the range  $E$  and  $E + \Delta E$ , the probability distribution  $\rho(\vec{x})$  has to be nonzero only at the points  $\vec{x} \in \Gamma$  which are consistent with these constraints, i.e.,

$$\rho_{mc}(\vec{x}) = \begin{cases} 1/\Omega, & \text{if } H(\vec{x}) = E, \\ 0 & \text{otherwise.} \end{cases} \quad (1.4)$$

In Eq. (1.4) we indicate by  $\Omega$  the area of the surface  $\Sigma_E$  and assume that each point  $\vec{x}$  in  $\Sigma_E$  is equally probable. This kind of ensemble is known as the *microcanonical* one. Once the probability distribution  $\rho$  is chosen, we define the ensemble average of the observable  $O$  as

$$\langle O \rangle_\rho \equiv \int_\Gamma d\vec{x} \rho(\vec{x}) O(\vec{x}). \quad (1.5)$$

This average is more easily computable than the time average (1.3), because one does not need to solve all the equations of motions but instead it is sufficient to know the macroscopic properties of the system and define a consistent probability distribution. The connection between these two approaches is provided by the concept of *ergodicity*. A system is said to be ergodic if, for any observable  $O$  and for almost all initial states  $\vec{x}_0$ , the time average (1.3) is equivalent to the microcanonical average (1.4 and 1.5):

$$\bar{O} = \langle O \rangle_\rho. \quad (1.6)$$

Another equivalent definition is that a system is said to be ergodic if during its motion  $\vec{x}(t)$  passes arbitrarily close to all points of the surface  $\Sigma_E$  of the phase space compatible with energy conservation. An important class of systems which are *not* ergodic is constituted by *integrable* systems. By definition a classical system with  $f$  degrees of freedom is integrable if there are  $f$  independent integrals of motion which are Poisson-commuting; this means that the Hamilton's equations can be exactly integrated via action-angle variables. The presence of additional conservation laws in integrable systems constrains the dynamics of the system to a subregion of the energy surface  $\Sigma_E$  and so the evolution is not able to uniformly cover the surface at constant energy.

---

<sup>1</sup>We are considering here equilibrium cases.

### 1.2.2 Thermalization in quantum statistical mechanics

In the early days of quantum mechanics, von Neumann realized that the most obvious generalization of the notion of ergodicity to the quantum realm is arduous [5]. In quantum mechanics the counterpart of the state  $\vec{x}$  is the wavefunction  $|\psi\rangle \in \mathcal{H}$ , where  $\mathcal{H}$  is the Hilbert space of the system considered. The time evolution of this state is now governed by the Schrödinger equation

$$i\frac{\partial}{\partial t}|\psi(t)\rangle = H|\psi(t)\rangle, \quad (1.7)$$

where we set  $\hbar = 1$  and  $H$  is the Hamiltonian operator of the system. If we choose the basis of the normalized eigenstates  $|\alpha\rangle$  of the Hamiltonian,  $H|\alpha\rangle = E_\alpha|\alpha\rangle$ , it is possible to decompose the state as

$$|\psi\rangle = \sum_{\alpha} c_{\alpha}|\alpha\rangle, \quad (1.8)$$

where the normalization condition  $\langle\psi|\psi\rangle = 1$  implies

$$\sum_{\alpha} |c_{\alpha}|^2 = 1. \quad (1.9)$$

The solution of the evolution equation (1.7) is then given by

$$|\psi(t)\rangle = \sum_{\alpha} c_{\alpha} e^{-iE_{\alpha}t} |\alpha\rangle. \quad (1.10)$$

The expectation value of an observable  $O$  at time  $t$  is

$$\langle O(t)\rangle = \langle\psi(t)|O|\psi(t)\rangle = \text{Tr}[\rho(t)O] = \sum_{\alpha,\beta} c_{\alpha}c_{\beta}^* e^{-i(E_{\alpha}-E_{\beta})t} \langle\beta|O|\alpha\rangle, \quad (1.11)$$

where the density matrix  $\rho(t)$  associated with the pure state  $|\psi\rangle$  is given by

$$\rho(t) = |\psi(t)\rangle\langle\psi(t)|. \quad (1.12)$$

Accordingly, the time average calculated according to Eq. (1.3) is

$$\overline{O} = \lim_{T \rightarrow +\infty} \frac{1}{T} \int_{t_0}^{t_0+T} dt \langle O(t)\rangle = \text{Tr}[\overline{\rho(t)}O], \quad (1.13)$$

where  $\overline{\rho(t)}$  is the time average of the density matrix. Also in this case the computation of Eq. (1.11) is practically impossible for a macroscopic system and we need to introduce a statistical description.

Similarly to the classical case, it is possible to introduce the suitable ensembles and the corresponding operator density matrix  $\rho$ . The ensemble expectation value of an observable  $O$  is

$$\langle O\rangle_{\rho} = \text{Tr}[\rho O]. \quad (1.14)$$

The quantum equivalent of the microcanonical ensemble (system with constant energy within the range  $[E, E + \Delta E]$ ) is defined by the density matrix  $\rho_{mc}$

$$\rho_{mc} = \frac{1}{\mathcal{N}} \sum_{\alpha \in S_E} |\alpha\rangle\langle\alpha|, \quad (1.15)$$

where  $S_E$  is the set of eigenstates  $|\alpha\rangle$  of  $H$  such that  $E \leq E_\alpha \leq E + \Delta E$  and  $\mathcal{N}$  is a normalization factor, counting the total number of eigenstates within the microcanonical shell  $[E, E + \Delta E]$ . The microcanonical expectation of an observable is obtained from Eqs. (1.14) and (1.15) as:

$$\langle O \rangle_{mc} = \text{Tr} [\rho_{mc} O] = \frac{1}{\mathcal{N}} \sum_{\alpha \in S_E} \langle \alpha | O | \alpha \rangle. \quad (1.16)$$

A naive extension of the concept of ergodicity to the quantum realm should require that, chosen a generic initial condition  $|\psi_0\rangle$  made out of states in the microcanonical shell

$$|\psi_0\rangle = \sum_{\alpha \in S_E} c_\alpha |\alpha\rangle, \quad (1.17)$$

the time average of the density matrix is equal to the microcanonical one. Proceeding along this line, the time average of the density matrix is

$$\begin{aligned} \overline{|\psi(t)\rangle\langle\psi(t)|} &= \lim_{T \rightarrow +\infty} \frac{1}{T} \int_{t_0}^{t_0+T} dt \sum_{(\alpha, \beta) \in S_E} c_\alpha c_\beta^* e^{-i(E_\alpha - E_\beta)t} |\alpha\rangle\langle\beta| \\ &= \sum_{\alpha \in S_E} |c_\alpha|^2 |\alpha\rangle\langle\alpha| + \lim_{T \rightarrow +\infty} \frac{1}{T} \int_{t_0}^{t_0+T} dt \sum_{(\alpha \neq \beta) \in S_E} c_\alpha c_\beta^* e^{-i(E_\alpha - E_\beta)t} |\alpha\rangle\langle\beta| \\ &= \sum_{\alpha \in S_E} |c_\alpha|^2 |\alpha\rangle\langle\alpha| + i \lim_{T \rightarrow +\infty} \sum_{(\alpha \neq \beta) \in S_E} \left( \frac{c_\alpha c_\beta^* |\alpha\rangle\langle\beta|}{E_\alpha - E_\beta} \right) \left( \frac{e^{-i(E_\alpha - E_\beta)(T+t_0)} - e^{-i(E_\alpha - E_\beta)t_0}}{T} \right) \\ &= \sum_{\alpha \in S_E} |c_\alpha|^2 |\alpha\rangle\langle\alpha| \equiv \rho_{diag}, \end{aligned} \quad (1.18)$$

where we use Eqs. (1.10) and (1.17), then split the sum and finally perform the integration. In the last equality, we could neglect the second term of the previous line under the assumption that the eigenstates of the system are not degenerate, i.e.,  $E_\alpha \neq E_\beta$  if  $\alpha \neq \beta$ , while we define the *diagonal* density matrix  $\rho_{diag}$ . The equivalence between the diagonal density matrix  $\rho_{diag}$  and the microcanonical one  $\rho_{mc}$  requires that

$$|c_\alpha|^2 = \frac{1}{\mathcal{N}}, \quad (1.19)$$

as it is evident from the comparison of Eqs. (1.15) and (1.18). But Eq. (1.19) is a very special condition, satisfied by a very restricted class of initial states.

Another argument showing that the concept of quantum thermalization is peculiar in several respects, consists in the fact that the trace of the density matrix is constant during a unitary time evolution (this follows from the cyclic property of the trace). Hence, if we take a pure state  $|\psi_0\rangle$  as a starting point of the evolution, the trace of the square of its density matrix  $\rho = |\psi_0\rangle\langle\psi_0|$  is identically one at any time, i.e.,

$$\mathrm{Tr}[\rho^2(t)] = \mathrm{Tr}[\rho^2] = \mathrm{Tr}[\rho] = 1. \quad (1.20)$$

On the other hand, we expect that thermalization occurs and therefore the properties of the system should be described by a thermal density matrix  $\rho_{th}$  with inverse temperature  $\beta > 0$

$$\rho_{th} = \frac{1}{Z} e^{-\beta H}, \quad (1.21)$$

which, however, has  $\mathrm{Tr}[\rho_{th}^2] < 1$  in contrast to Eq. (1.21). Accordingly, it seems that true thermalization in closed systems never occurs. But our common sense makes us believe that macroscopic systems should reach an equilibrium thermal state, unless some special conditions are met (e.g., integrability, see below for details). In order to solve this apparent puzzle, we restrict our attention to a finite and spatially compact subpart  $A$  of the original system, so that the complementary part  $\bar{A}$  can act as an effective bath, leading the subsystem to thermalization. Adopting this point of view, the key quantity in which we are interested is the *reduced density matrix*  $\rho_A$

$$\rho_A = \mathrm{Tr}_{\bar{A}}[\rho], \quad (1.22)$$

obtained from  $\rho$  by tracing over the degrees of freedom of the bath. We can now claim that a closed quantum many-body system relaxes to an equilibrium thermal state at inverse temperature  $\beta$ , or in other words thermalizes, if, in the thermodynamic limit and for any subsystem  $A$ , the long-time limit of  $\rho_A$  equals the appropriate Gibbs density matrix  $\rho_{th}$ , i.e.,

$$\lim_{t \rightarrow +\infty} \rho_A(t) = \rho_{A,mc} = \mathrm{Tr}_{\bar{A}}[\rho_{mc}] = \rho_{th} = \frac{e^{-\beta H}}{Z}. \quad (1.23)$$

In this case, the outcome of measurement of *local* observable  $O_A$  can be evaluated either as the time average or as an ensemble average

$$\lim_{t \rightarrow +\infty} \langle \psi(t) | O_A | \psi(t) \rangle = \mathrm{Tr}[\rho_{A,mc} O_A] = \frac{1}{Z} \mathrm{Tr} \left[ e^{-\beta H} O_A \right]. \quad (1.24)$$

### 1.2.3 Eigenstate thermalization hypothesis

One of the most debated issue in the literature about non-equilibrium many-body systems is the mechanism underlying quantum thermalization. The most accepted conjecture regarding the mechanism underlying the emergence of a thermal state in isolated quantum systems is the so-called eigenstate thermalization hypothesis (ETH). It states that thermalization happens at the level of individual energy eigenstates and that the time evolution plays just an auxiliary role (see Fig. 1.2); in order to compute thermal

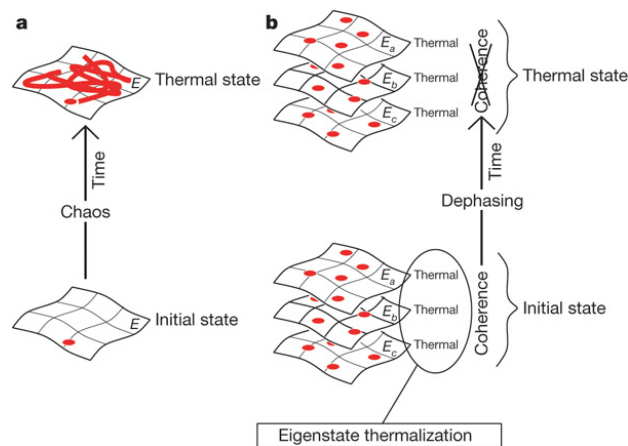


**Figure 1.2:** (a): In classical systems thermalization is made possible by dynamical chaos. The system evolves in time and visits all the available phase space, such that it can be correctly described with a microcanonical ensemble. (b): It has been conjectured that the mechanism responsible for thermalization in quantum systems is the eigenstate thermalization hypothesis. The thermalization happens at the level of individual energy eigenstates (see Eq. (1.26)) and time evolution does not construct the thermal state as in the classical case but it only reveals it. In fact, the thermal state exists already at time  $t = 0$ , but the quantum coherence, which is suppressed as times passes, hides it. [Figure taken from Ref. [6]]

averages it is sufficient to know the average over a single energy eigenstate within the microcanonical energy window. Below we will be more specific and we clearly explain how ETH works. Consider an observable  $O$ : its time average  $\bar{O}$  is given by Eq. (1.13) and therefore, proceeding in the same way as done before to derive Eq. (1.18), it can be computed as a diagonal ensemble average, i.e.,

$$\bar{O} = \sum_{\alpha \in S_E} |c_\alpha|^2 \langle \alpha | O | \alpha \rangle. \quad (1.25)$$

The value predicted for the observable by the microcanonical ensemble is instead given by Eq. (1.16). The averages (1.25) and (1.16) have to be equal and the only possibility for this to happen is to assume that the diagonal elements  $\langle \alpha | O | \alpha \rangle = O_{\alpha\alpha}$  are constant in the energy window  $[E, E + \Delta E]$ . Under this hypothesis and from Eqs. (1.16) and (1.25), we can assert that thermalization happens at the level of individual eigenstates of the Hamiltonian, i.e.,

$$O_{\alpha\alpha} = \langle O \rangle_{mc} = \bar{O}; \quad (1.26)$$

in other words, each eigenstate implicitly contains a thermal state. The role of time evolution is only to suppress the off-diagonal elements  $\langle \beta | O | \alpha \rangle$  with  $\beta \neq \alpha$  appearing in  $\bar{O}$  (similarly to Eq. (1.18)), leaving behind only the ones with  $\beta = \alpha$ . This idea was introduced by Deutsch in 1991 [7] and Srednicki in 1994 [8]. In Ref.[8] the author considered an isolated quantum hard-sphere gas, whose classical counterpart has chaotic dynamics, and showed that the momentum distribution of each constituent particle approaches its thermal equilibrium value. In Ref. [7], instead, the ETH has been shown to hold for integrable systems with a small perturbation in the form of a random

matrix. More recently, supporting evidence for ETH has been collected in non-integrable models investigated via numerical methods [6, 9] while its breakdown was demonstrated in integrable models [10].

### 1.3 Integrable systems and generalized Gibbs ensemble

As we mentioned above, integrability plays an important role in determining the asymptotic properties of a system. However, defining a quantum counterpart of integrability is a non-trivial task [11]. For instance, it is not clear what should be considered as number of degrees of freedom in a system with a finite dimensional Hilbert space, e.g., a spin chain: if the number of spins, which is proportional to the size of the system or, instead, the dimension of the Hilbert space which grows exponentially with the size of the system. Moreover, the existence, analogously to the classical case, of a maximal set of independent and commuting operators cannot be considered the hallmark of integrability. Indeed, such a set can be built by considering the projectors on the eigenstates of the Hamiltonian, but this can be done for any system and therefore does not discriminate if a quantum system is integrable or not. A better definition is the one given by Sutherland [12]: a quantum system is integrable if any multi-body scattering process can be decomposed in a series of binary collisions; this implies that quasi-particles can scatter only elastically and their identity is preserved upon collisions.

In addition to energy, an extensive number of non-trivial independent conserved quantities  $I_n$  is present in quantum integrable systems; these quantities constrain the dynamics and prevent any relaxation towards a thermal state. Indeed, starting from an initial state  $|\psi_0\rangle$ , the expectation value of integrals of motion is conserved during the dynamics:

$$\langle \psi_0(t) | I_n | \psi_0(t) \rangle = \langle \psi_0 | I_n | \psi_0 \rangle, \quad (1.27)$$

and the system retains information about the initial state at any time. On the contrary, a thermal state has no memory of the initial state. For quantum *integrable* systems it was supposed [13] that relaxation actually occurs towards a non-thermal steady state described by the so-called *generalized Gibbs ensemble* (GGE)

$$\rho_{gge} = \frac{1}{Z_{gge}} e^{-\sum_n \lambda_n I_n}, \quad (1.28)$$

where  $\{I_n\}$  is the set of the independent local conserved quantities with

$$[I_n, I_m] = 0 \quad \text{and} \quad [I_n, H] = 0, \quad \forall n, m, \quad (1.29)$$

while the constants  $\lambda_n$  are fixed by imposing that the expectation value over the GGE coincides with the (conserved) value that these quantities have in the initial state (see Eq. (1.27)):

$$\langle I_n \rangle_{gge} = \text{Tr} [I_n \rho_{gge}] = \lim_{t \rightarrow \infty} \langle \psi_0(t) | I_n | \psi_0(t) \rangle = \langle \psi_0 | I_n | \psi_0 \rangle. \quad (1.30)$$

In this case, it follows that the long-time limit of the expectation value of a local observable  $O_A$  will be

$$\lim_{t \rightarrow \infty} \langle \psi_0(t) | O_A | \psi_0(t) \rangle = \text{Tr} [O_A \rho_{gge}]. \quad (1.31)$$

It is worth noting that the only assumption behind the GGE density matrix (1.28) is the maximum-entropy principle [14] according to which the density matrix  $\rho$  is the one which maximizes the von Neumann entropy

$$S[\rho] = -\text{Tr} [\rho \ln \rho], \quad (1.32)$$

taking in account the conservation of the quantities  $I_n$ . Mathematically, one has to look for  $\rho$  which maximizes the functional  $F[\rho]$ :

$$F[\rho] = S[\rho] - \xi [\text{Tr}[\rho] - 1] - \sum_n \lambda_n [\text{Tr}[I_n \rho] - \langle \psi_0 | I_n | \psi_0 \rangle], \quad (1.33)$$

which is composed by the entropy  $S$ , a term imposing the normalization of the density matrix and a final term taking in account that the integrals  $I_n$  of motion in the steady state are equal to their initial value. The solution of this minimization problem is the GGE density matrix (1.28) in which we can interpret the coefficients  $\lambda$ 's as Lagrange multipliers. Moreover, one assumes that only local integrals of motion have to be included in the GGE because, as explained in Sec. 1.2, we focus only on a subpart of the system and so we are interested in its local properties. The generalized Gibbs ensemble has been tested successfully in various models, such as Luttinger liquids [15], Ising chains [16, 17], integrable hard-core bosons [13] and Hubbard-like models [18, 19].

As we anticipated in Sec. 1.1, the non-equilibrium dynamics following a quantum quench can be investigated also experimentally thanks to cold atomic gases. We now illustrate the important experiment performed by Kinoshita et al. [20], known as the quantum Newton's cradle. In this experiment arrays of tightly confined tubes of ultracold  $^{87}\text{Rb}$  atoms were prepared in a superposition of states of opposite momentum. The imparted kinetic energy was small compared to the energy required to excite the atoms to the higher transverse states and the gases remained effectively one dimensional along the axis of elongation. The system was then allowed to evolve for a certain time before the momentum distribution was sampled (see Fig. 1.3). It was observed that, after thousands of collisions, the momentum distribution remained non-Gaussian, signaling that the non-equilibrium Bose gas did not equilibrate on the time scales of the experiment (see Fig. 1.3). The explanation of this unexpected behavior is that this experimental setup is close to be represented by the Lieb-Liniger model [21, 22], which describes a gas of one-dimensional Bose particles interacting via a repulsive delta-function potential. This model is a notable example of integrable quantum many-body system and so the associated non-trivial conservation laws prevent relaxation towards a Gibbs thermal ensemble.

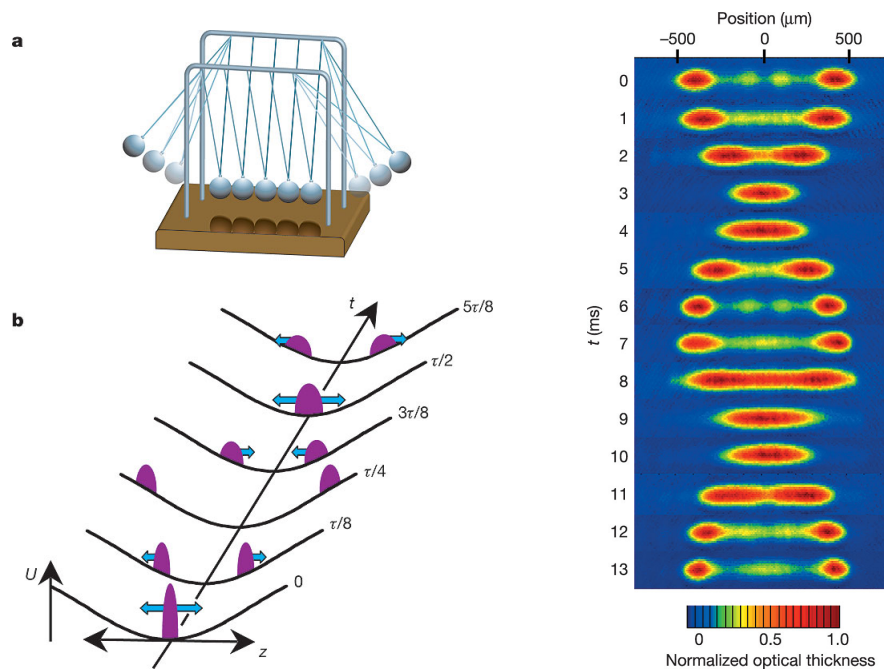


**Figure 1.3:** (a) The classical Newton cradle and (b) its quantum counterpart considered in the experiment of Ref. [20]. Right: Absorption image as a function of the time  $t$  elapsed from the quench during the first oscillation cycle for the quantum Newton cradle, showing the absence of relaxation towards a steady state and an almost periodic motion [Figure taken from Ref. [20]]

## 1.4 The end of the story?

Until now, it seems that the current knowledge about the relaxation of closed quantum many-body systems following a quantum quench can be summarized as follows: non-integrable systems relax to a thermal Gibbs ensemble, while integrable models attain a non-thermal state described by a generalized Gibbs ensemble. However, the actual dynamics towards quantum relaxation could be more involved, as some recent works suggest. For example, in Ref. [23] the dynamics of a Bose-Hubbard model following a quench from the superfluid to the Mott insulator regime was investigated in this respect. It was found that for large values of the post-quench interaction strength between the particles the system approaches a distinctly non-equilibrium steady state which bears strong memory of the initial conditions. By contrast, if the post-quench interaction strength is comparable to the hopping between neighboring sites, the correlations are rather well approximated by those at thermal equilibrium. The explanation behind this strange behavior was given in terms of the ineffectiveness of quasi-particles interactions deep in the Mott regime, with a suppression of thermalization, because of the impossibility of redistributing the energy injected into the system after the quench. Instead, a more pronounced dependence of the evolution on the initial state was observed in a numerical study of integrability breaking in a one-dimensional quantum Ising chain [24]

$$H = - \sum_i [\sigma_i^z \sigma_{i+1}^z + g \sigma_i^x] - h \sum_i \sigma_i^z. \quad (1.34)$$

Numerical results for the out of equilibrium evolution of the reduced density matrix of this model showed the existence of three different regimes occurring depending on the initial states. The initial configuration was chosen to be a translation invariant product states, determined by the state of an individual spin,

$$|\psi\rangle = \cos\left(\frac{\theta}{2}\right)|0\rangle + e^{i\phi}\sin\left(\frac{\theta}{2}\right)|1\rangle, \quad (1.35)$$

for  $|0\rangle$  ( $|1\rangle$ ) the  $+1$  ( $-1$ ) eigenstates of  $\sigma^z$ . If the initial state has all spins aligned along the positive  $y$  direction ( $\theta = \phi = \pi/2$ ), then the reduced density matrix approaches the thermal canonical ensemble (strong thermalization), while for initial states with spins pointing along the positive  $z$  direction ( $\theta = 0$ ) the system shows convergence to thermal values only after time averaging (weak thermalization). Remarkably, if the initial spins point along the  $x$  direction ( $\theta = \pi/2, \phi = 0$ ) relaxation is fast, but the distance between the evolved state and the thermal one is different from zero even in the long-time limit. In Ref. [25] it was established that when certain models which are far from being integrable reach the steady state, they have memory of the initial conditions, resulting in a lack of thermalization but being instead described by a generalized Gibbs ensemble.

In spite of these evidences in favor of the role played by the GGE in the dynamical evolution of quantum many-body systems, its explicit construction for general interacting integrable models remains an open problem, and there are examples of integrable systems where the GGE seemingly fails to describe correctly the steady state [26, 27]. A thorough understanding of the non-equilibrium dynamics of closed quantum many-body system has not yet been reached and research in this field is one of the most active and growing activity in statistical physics and condensed matter.

## 1.5 Prethermalization

In the previous Sections we concentrated on the state attained by a closed quantum system long after a quantum quench, but it is certainly interesting to investigate also the intermediate dynamics and understand whether the relaxation occurs uniformly or via a sequence of different stages. In fact, it is possible that a system driven out of equilibrium initially approaches an intermediate quasi-steady state and then approaches the eventual stationary state of the dynamics at a later time. A notable instance of this case is provided by the so-called *prethermalization*.

This multi-stage dynamics was first mentioned in the study of relativistic heavy-ions collisions [28]. It was observed that, on a time scale  $\tau_{pt}$ , a dephasing mechanism leads to the equipartition of energy between kinetic and potential component and to the establishment of a time-independent equation of state  $P = P(\epsilon)$  relating the pressure  $P$  and the energy density  $\epsilon$ , even if the system is still far from equilibrium. This process is independent of the details of the interaction and is very rapid; for this first non-thermal steady state was introduced the term prethermalization. Inelastic collisions are responsible for the existence of a second, longer time scale  $\tau_{damp}$  which characterizes the relaxation of the mode occupation numbers; most of the dependence on the initial

conditions is already lost at this stage, even if the momentum distribution function still does not look thermal. True equilibration happens only at later times  $t \sim \tau_{eq}$ . A similar scenario emerges also in condensed matter, as highlighted in Ref.[29] where the authors investigated the non-equilibrium dynamics of a Fermi-Hubbard model at half filling (with Fermi energy  $\epsilon_F = 0$ ) in more than one spatial dimension (such that the system is not integrable and thermalization is expected) after a sudden interaction quench. This model is described by the following Hamiltonian

$$H(t) = \sum_{k,\sigma} \epsilon_k : c_{k\sigma}^\dagger c_{k\sigma} : + \theta(t) U \sum_i \left( n_{i\uparrow} - \frac{1}{2} \right) \left( n_{i\downarrow} - \frac{1}{2} \right), \quad (1.36)$$

where  $\sigma \in \{\uparrow, \downarrow\}$  indicates the spin value,  $k$  the momentum,  $c$  and  $c^\dagger$  are canonical fermionic annihilation and creation operators, respectively,  $n_{i,\uparrow(\downarrow)} = c_{i,\uparrow(\downarrow)}^\dagger c_{i,\uparrow(\downarrow)}$  represents the occupation number of the site  $i$  with spin value  $\sigma = \uparrow(\downarrow)$ , while  $\theta(t)$  is defined as  $\theta(t < 0) = 0$ ,  $\theta(t > 0) = 1$  and it accounts for the sudden interactions switch-on. Three clearly separated time regimes were found: a first stage for times  $0 < t \lesssim \rho_F^{-1} U^{-2}$ , where  $\rho_F = \rho(\epsilon = 0)$  is the density of states at the Fermi level, during which one observe a fast reduction of the Fermi surface discontinuity with oscillations decaying as  $1/t$  in the momentum distribution function. This short-time regime has been interpreted as the formation of quasi-particles from the free electrons of the initial non-interacting Fermi gas. Then for times  $t \gtrsim \rho_F^{-1} U^{-2}$  the system relaxes towards an intermediate quasi-steady regime, where there are no further changes in the momentum distribution function, but this distribution does not resemble the equilibrium one. This is a clear instance of prethermalization and if the system was integrable, this regime of dynamics would become stable and last forever, but the inelastic interaction processes at later times drive this metastable state towards the true equilibrium distribution function. Finally, in the late stage of the dynamics for  $t \gtrsim \rho_f^{-3} U^{-4}$ , a Boltzmann equation description is expected to hold and the authors have been able to show that the resulting momentum distribution function of the system approaches a Fermi-Dirac one with temperature  $T \sim U$ : in other words, the system has reached a thermal state.

Another important aspect of prethermalization is its possible connection with the GGE: in fact, GGE stationary states for integrable systems could be seen as prethermal plateaus which never decay and, conversely, the prethermal intermediate state of nearly integrable models can be seen as if it was the GGE asymptotic state of the "closest" integrable model constructed with specific quasi-conserved quantities [30]. To be more specific, consider as starting point an integrable Hamiltonian

$$H(t = 0) = H_0 = \sum_{\alpha} \epsilon_{\alpha} I_{\alpha}, \quad (1.37)$$

where  $\epsilon_{\alpha}$  is the "energy" of the level labeled by the quantum number  $\alpha$ ,  $\{I_{\alpha}\}$  is a set of integrals of motion with corresponding eigenvectors  $|n\rangle$ ,  $I_{\alpha}|n\rangle = n_{\alpha}|n\rangle$ , and suddenly switch on a small integrability-breaking term  $H_1$

$$H(t > 0) = H_0 + gH_1 \quad \text{with} \quad |g| \ll 1. \quad (1.38)$$

Because of the smallness of the parameter  $g$ , the evolution after the quench of this system can be investigated using unitary perturbation theory, for details see Ref. [30]. We expect that the dynamics is strongly influenced by the near integrability of  $H(t > 0)$  and the conservation laws possessed by  $H_0$  are not totally lost. In this case the system prethermalizes and an observable  $\langle A(t) \rangle$  relaxes first to a non-thermal quasi-stationary value  $A_{preth}$ . The expectation value of  $A$  within the prethermalization plateau can be obtained as long-time average

$$\overline{\langle A(t) \rangle} = \lim_{T \rightarrow \infty} \frac{1}{T} \int_0^T dt' \langle A(t') \rangle, \quad (1.39)$$

assuming that  $g$  is so small that the scale  $1/|g|$  and  $1/|g|^2$ , related to the perturbative character of the calculations, are well separated and the limit  $T \rightarrow \infty$  is taken in the sense that  $1/|g| \ll T \ll 1/|g|^2$ . It turns out that Eq. (1.39) can be written as [30]

$$A_{preth} = \overline{\langle A(t) \rangle} = 2\langle A \rangle_{\tilde{0}} - \langle A \rangle_0 + O(g^3), \quad (1.40)$$

where the averages  $\langle \bullet \rangle_0$  and  $\langle \bullet \rangle_{\tilde{0}}$  are respectively taken on the initial state  $|0\rangle$ , ground state of the integrable Hamiltonian  $H_0$ , and on the perturbative ground state  $|\tilde{0}\rangle$  of  $H(t > 0)$ . Being close to integrability is reflected by the fact that a set of approximate integrals of motion  $\tilde{I}_\alpha$  can be constructed and that the Hamiltonian (1.38) can be cast in the following form

$$H = \sum_\alpha \epsilon_\alpha \tilde{I}_\alpha + \sum_{\tilde{n}} |\tilde{n}\rangle (gE_n^{(1)} + g^2 E_n^{(2)}) \langle \tilde{n}| + O(g^3), \quad (1.41)$$

where  $|\tilde{n}\rangle$ ,  $E_n^{(1,2)}$  are the perturbed eigenvectors and eigenvalues of  $H(t > 0)$ . For approximate integrals of motion we mean quantities  $\tilde{I}_\alpha$  which commute among themselves and with the full Hamiltonian at least up to second order, i.e.,

$$[\tilde{I}_\alpha, \tilde{I}_\beta] = 0 \quad \text{and} \quad [H, \tilde{I}_\alpha] = O(g^3). \quad (1.42)$$

This set of approximate constant of motions are then used to build the corresponding GGE

$$\rho_{\tilde{G}} = \frac{1}{Z} \exp \left[ - \sum_\alpha \lambda_\alpha \tilde{I}_\alpha \right] \quad (1.43)$$

with the constrain

$$\langle \tilde{I}_\alpha \rangle_{\tilde{G}} = \text{Tr} \left[ \rho_{\tilde{G}} \tilde{I}_\alpha \right] = \langle \tilde{I}_\alpha \rangle_0. \quad (1.44)$$

Phrased in these terms, the main result of Ref. [30] is that the prethermal values (1.40) can be actually predicted as GGE averages with the density matrix (1.43), i.e.,

$$A_{preth} = \langle A \rangle_{\tilde{G}} + O(g^3). \quad (1.45)$$

The scenario described in Ref. [30] is expected to hold for intermediate time scales  $1/g \ll t \ll 1/g^2$ , as a natural limitation coming from perturbative computations, and therefore the prethermal metastable state is expected to be long lived as much as the integrable point is weakly perturbed. If thermalization eventually occurs, it is due to the  $O(g^3)$  terms, which are expected to become relevant on time scales of the order  $1/g^3$ . Prethermalization occurs also in systems of quenched spinor condensates [31], non-integrable quantum spin chains after a quench [32] and weakly interacting bosons following an interaction quench [33]. In Chapter 3 we report in some detail the study of the non-equilibrium dynamics of a noisy quantum Ising chain, which shows prethermalization [34].

We now present the recent experiment performed by Schmiedmayer's group [35] thanks to which it has been possible to directly observe a system in a prethermal state. The experiment considers a single one-dimensional Bose gas cloud of  $^{87}\text{Rb}$  atoms in the quasi-condensate regime and with an elongated shape: because of this geometrical constraint and reduced dimensionality many longitudinal modes are populated with a consequent rich spatial structure and dynamics of the local phase of the "condensate" wave function, in contrast to three-dimensional condensates in which the existence of a genuine long-range order implies a quantum state with a single global phase. The initial state is prepared by rapidly and coherently splitting the single one-dimensional gas, producing a system of two uncoupled and elongated one-dimensional Bose gases in a double-well potential. After the splitting, the two gases have almost identical longitudinal phase profile  $\phi_{1,2}(z)$  (where  $z$  is the coordinate along the elongation), and are therefore strongly correlated in their phases (see Fig. 1.4). By contrast, two independent quasi-condensates have different and uncorrelated phase profiles  $\phi_1$  and  $\phi_2$ . The strongly correlated phases of the two gases after splitting reflects the memory of their common parent quasi-condensate. The experiment studies how this memory evolves, decays in time, and, in particular, whether a thermal equilibrium state corresponding to two independent separated quasi-condensates is reached at long times. After the splitting, the system evolves in the double-well potential for some time  $t_e$  before the two gases are released from the trap and allowed to interfere. The interference pattern along the longitudinal direction is integrated over a variable length  $L$  and the so-called integrated contrast  $C(L)$  is extracted

$$C^2(L) = \frac{1}{L} \left| \int_{-L/2}^{L/2} dz e^{i\Delta\phi(z,t)} \right|^2, \quad (1.46)$$

where  $\Delta\phi = \phi_1 - \phi_2$  is the phase difference between the two gases and  $C(L)$  is a direct measure of the strength of the relative phase fluctuations. In the initial state this quantity is large, because essentially  $\Delta\phi = 0$ ; during the evolution, instead, the phase difference varies, resulting in a decreasing of  $C(L)$  as a function of time. Repeated experimental runs can be used in order to measure the mean squared contrast  $\langle C^2 \rangle$  of the system. Fig. 1.5 (taken from Ref. [35]) shows an initial rapid decay of  $\langle C^2 \rangle$ , after which a quasi-steady state emerges which slowly evolves further on a second, much

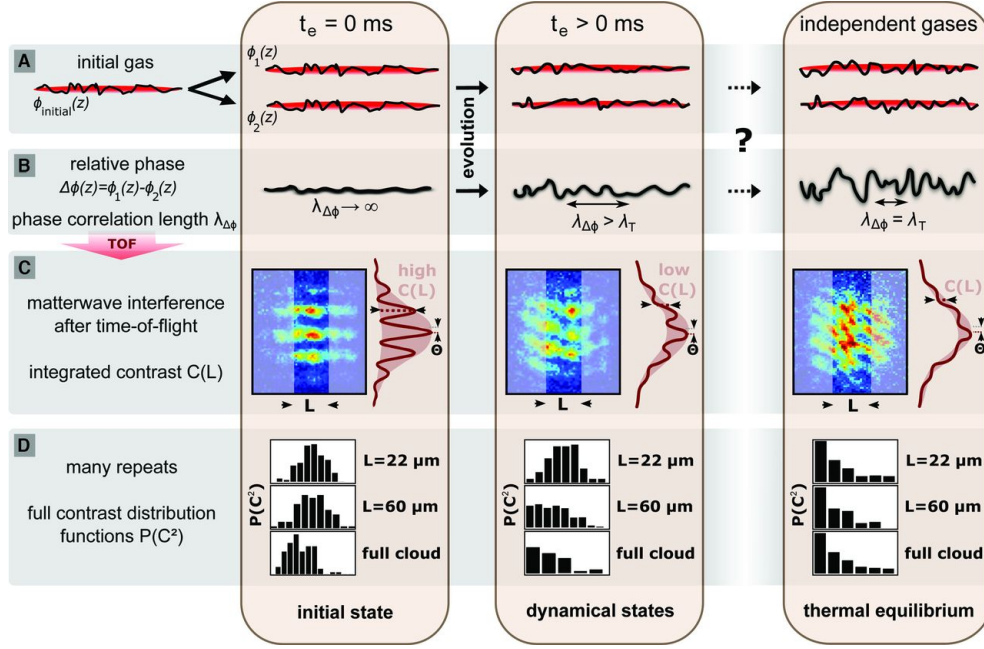


**Figure 1.4:** (A): An initial phase fluctuating one-dimensional Bose gas formed by an elongated cloud (with longitudinal coordinate  $z$ ) is split into two uncoupled gases with almost identical phase distributions  $\phi_1(z)$  and  $\phi_2(z)$  and allowed to evolve for a time  $t_e$ . (B): At  $t_e = 0$ , fluctuations in the local phase difference  $\Delta\phi(z)$  between the two gases are very small, and the corresponding phase correlation length  $\lambda_{\Delta\phi}$  is very large. During the evolution, these relative-phase fluctuations increase, and  $\lambda_{\Delta\phi}$  decreases. The main goal of the experiment is to understand whether or when this system will reach the corresponding thermal equilibrium of uncorrelated phases as characterized by the initial temperature  $T$  and thermal coherence length  $\lambda_T$ . (C): Matter-wave interference patterns obtained letting the two gas clouds interfere after different evolution times. The contrast  $C(L)$  (see Eq. (1.46)) is a direct measure of the strength of the relative-phase fluctuations. (D): Repeated experimental runs provide a characteristic distribution  $P(C^2)$  of contrasts, which allows one to distinguish between the initial state, an intermediate prethermalized state, and the eventual thermal equilibrium of the system. [Figure taken from Ref. [35]]

slower time scale. In order to verify if the quasi-steady state is thermal or not, the probability distribution function  $P(C^2)dC^2$ , which gives the probability that  $C^2$  takes values within the range  $[C^2, C^2 + dC^2]$ , is computed and compared with a thermal equilibrium distribution at temperature  $T_{eff}$ . It was found that the experimental data are well described by an equilibrium distribution with an effective temperature which, however, is a factor of five smaller than the initial temperature of the unsplit system (see Fig. 1.5). The conclusion is that the observed steady-state cannot be the true thermal equilibrium state of the system, but it is instead a prethermal state. These experimental facts can be rationalized theoretically on the basis of an integrable theory, i.e., the Tomonaga-Luttinger liquid formalism which provides predictions in very good agreement with the experimental data; for details see Ref. [35].

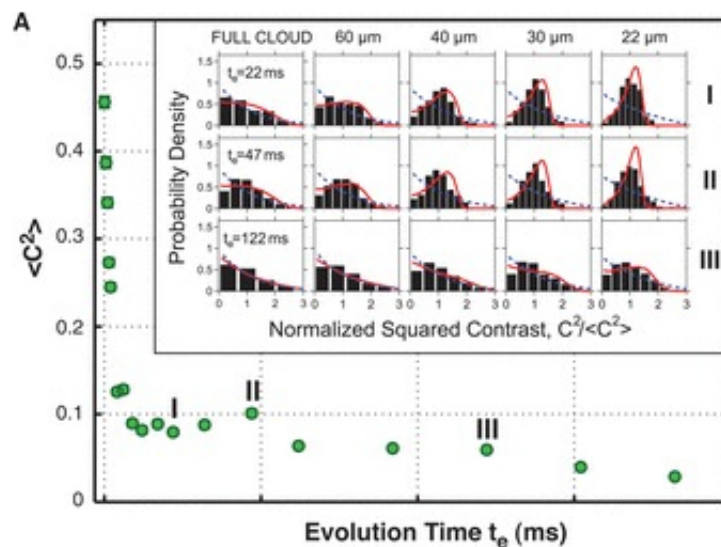


**Figure 1.5:** (A): Evolution of the mean squared-contrast  $\langle C^2 \rangle$  (see Eq. (1.46)) of the interference patterns integrated over the whole length of the quasi one-dimensional clouds. Rapid decay is followed by a much slower one. Inset: experimental distributions of the squared contrast for three different values of the evolution time  $t_e$ . Red lines are the best fit with equilibrium distributions from which  $T_{eff}$  is extracted, while the blue dashed lines are the equilibrium distributions at the actual setup temperature. The evident discrepancy with the experimental data indicates that the steady state is non-thermal. [Figure taken from Ref. [35]]

## 1.6 Fluctuation-dissipation theorem and effective temperatures

In the previous Sections we illustrated how the non-equilibrium dynamics of closed quantum many-body systems following a quantum quench is actually understood and described. One can distinguish two classes of systems: non-integrable ones, whose asymptotic local properties are described by the usual Gibbs distribution, and integrable systems, which, instead, relaxes to the so-called generalized Gibbs ensemble, accounting for the additional local conserved quantities in the system. However, it has been suggested in Refs. [36, 37] that, depending on the system's parameters and the specific quantity under study, a conventional Gibbs ensemble might effectively describe some relevant features of the non-equilibrium dynamics even in integrable case and therefore their study would not reveal the non-equilibrium nature of the dynamics. Therefore, a different approach is required in order to assess the real thermalization of a system and in this Section we discuss this novel method [38, 39].

### 1.6.1 One-time quantities

Consider a system in the initial state  $|\psi_0\rangle$  subject to the sudden quench of its Hamiltonian from  $H(g_0)$  to  $H(g)$  (see Fig. 1.1). The post-quench Hamiltonian governs the unitary dynamics of the system, characterized by the state  $|\psi(t)\rangle$ . Usually, one-time

quantities are studied in this kind of problems in order to understand the relaxation properties. Among them, a special role is played by the energy of the system; indeed the average energy  $E(t)$

$$E(t) \equiv \langle \psi(t) | H(g) | \psi(t) \rangle = \langle \psi_0 | e^{iH(g)t} H(g) e^{-iH(g)t} | \psi_0 \rangle = \langle \psi_0 | H(g) | \psi_0 \rangle = E(t=0), \quad (1.47)$$

is conserved in the dynamics because of unitary evolution. We can define an effective inverse temperature  $\beta_{eff}^E$  associated to the energy as

$$\langle \psi_0 | H(g) | \psi_0 \rangle = \frac{1}{Z} \text{Tr} \left[ e^{-\beta_{eff}^E H(g)} H(g) \right], \quad (1.48)$$

where the quantity on the l.h.s is the average energy of the system after the quench while the one on the r.h.s is the average energy of an equilibrium state of  $H(g)$  at a temperature  $T = T_{eff}^E = 1/\beta_{eff}^E$  (we set to 1 the Boltzmann constant  $k_B$ ). In other words, we can imagine the system as if it was in an equilibrium thermal state at temperature  $T_{eff}^E$  fixed by the amount of energy injected into the system upon quenching. However, one would like to check that a Gibbs state with the temperature thus defined also describes the stationary limit of the average value of other observables. Considering an observable  $O$ , one can compare the stationary value of the average of the observable after the quench  $\langle O(t = \infty) \rangle$  with the expectation value that the same observable would have in an equilibrium Gibbs ensemble at the effective temperature  $T_{eff}^O$  and determine  $T_{eff}^O$  in such a way that these two averages coincide, i.e.,

$$\lim_{t \rightarrow \infty} \langle \psi_0 | O(t) | \psi_0 \rangle = \frac{1}{Z} \text{Tr} \left[ e^{-\beta_{eff}^O O} \right] = \langle O \rangle_{T=T_{eff}^O}. \quad (1.49)$$

An effective thermal-like behavior of the system in the stationary state would require these temperatures  $T_{eff}^O$  to be independent of the observable  $O$  considered and to coincide with  $T_{eff}^E$  defined by Eq. (1.48), because a real thermal state is described by a unique temperature. This approach is useful also in order to understand better the difference between the canonical Gibbs ensemble and the generalized Gibbs ensemble. Consider an Hamiltonian that can be written in the diagonal form

$$H_{int} = \sum_k \epsilon_k I_k = \sum_k H_k, \quad (1.50)$$

where  $\{I_k\}$  is a set of non-trivial conserved quantities and  $\epsilon_k$  is the energy of the level labeled by the quantum number  $k$ . Therefore, the dynamics after the quench is constrained by a large number of integrals of motion and in Sec. 1.3 we argued that the asymptotic properties of these kind of systems are captured by a generalized Gibbs ensemble (see Eq. (1.28)) and that the Lagrange multipliers  $\lambda_k$  can be determined by imposing the condition (1.30). Equation (1.30) is analogous to Eq. (1.48), but with a set of effective temperatures  $\{T_{eff}^k\} = \{\epsilon_k/\lambda_k\}$  determined by the condition

$$\langle \psi_0 | I_k | \psi_0 \rangle = \frac{1}{Z_{gge}} \text{Tr} \left[ e^{-\sum_k \lambda_k I_k} I_k \right] = \frac{1}{Z_{gge}} \text{Tr} \left[ e^{-\sum_k \beta_{eff}^k H_k} I_k \right] = \langle I_k \rangle_{T=T_{eff}^k}. \quad (1.51)$$

In a sense, the generalized Gibbs ensemble is characterized by a variety of different effective temperatures, one for each eigenstate, opposite to the canonical Gibbs ensemble which is described by only one temperature. A signal of possible thermalization of the system is the equality of all  $k$ -dependent effective temperatures  $T_{eff}^k$  to  $T_{eff}^E$ .

### 1.6.2 Two-time quantities

In the stationary state one-time quantities are by definition time-independent, whereas two-time quantities are not and therefore they carry information on how the dynamics occurs even in equilibrium. Moreover, the analysis of one-time observable could be misleading [17, 36, 37] and therefore one is naturally led to consider two-time correlation function between two generic operators  $A$  and  $B$ , defined by

$$C^{AB}(t, t') = \langle A(t)B(t') \rangle = \text{Tr} [\rho A(t)B(t')], \quad (1.52)$$

where the generic operator  $O$  evolves according to the Heisenberg representation ( $\hbar = 1$ )

$$O(t) = e^{iHt} O e^{-iHt}. \quad (1.53)$$

Clearly, generic  $A$  and  $B$  do not commute and therefore  $\langle A(t)B(t') \rangle \neq \langle B(t')A(t) \rangle$ ; it is then natural to define symmetric and antisymmetric correlation functions as

$$C_{\pm}^{AB}(t, t') = \langle [A(t), B(t')]_{\pm} \rangle, \quad (1.54)$$

where  $[X, Y]_{\pm} = (XY \pm YX)/2$ . Without loss of generality, it is possible to consider either operators with zero average or to subtract the latter from the definition of the generic operator  $O$ :  $O(t) \rightarrow O(t) - \langle O(t) \rangle$ . In addition to  $C^{AB}$ , the other fundamental dynamic quantity is the linear response function  $R^{AB}$  which quantifies, up to linear term, how much the expectation value  $\langle A(t) \rangle$  varies after a perturbation  $h_B(t)$  which couples linearly to the operator  $B$  in the Hamiltonian of the system:

$$R^{AB}(t, t') = \left. \frac{\delta \langle A(t) \rangle}{\delta h_B(t')} \right|_{h_B=0}, \quad (1.55)$$

where  $A(t)$  is obtained by evolving  $A$  with the time-dependent perturbed Hamiltonian  $H_{h_B}(t) \equiv H - h_B(t)B$ . The Kubo formula [40], which holds in and out of equilibrium, relates the linear response function  $R^{AB}(t, t')$  to the antisymmetric correlation  $C_{-}^{AB}(t, t')$  defined in Eq. (1.54)

$$\hbar R^{AB}(t, t') = 2i\theta(t - t')C_{-}^{AB}(t, t'), \quad (1.56)$$

where  $\theta(t - t')$  enforces causality: if the perturbation is switched on at time  $t'$  the system will react to it only at later times  $t > t'$ . If we consider Hermitian operators,  $O^{\dagger} = O$ , the complex conjugate of the correlations function is  $[C^{AB}(t, t')]^* = \langle B(t')A(t) \rangle$  and the symmetric and antisymmetric correlators  $C_{\pm}^{AB}$  can be respectively expressed in terms

of  $C^{AB}$  alone, defined in Eq. (1.52), as

$$C_+^{AB}(t, t') = \text{Re } C^{AB}(t, t') \quad \text{and} \quad C_-^{AB}(t, t') = i \text{Im } C^{AB}(t, t'), \quad (1.57)$$

so that Eq. (1.56) yields

$$\hbar R^{AB}(t, t') = -2\theta(t - t') \text{Im } C^{AB}(t, t'). \quad (1.58)$$

In equilibrium, the dynamics is invariant under time translations and therefore correlation and response functions are stationary, i.e.,  $C_{\pm}^{AB}(t, t') = C_{\pm}^{AB}(t - t')$ , whereas out of equilibrium this is not necessarily the case. In the stationary case, we can consider Fourier transform of the correlation function, defining the Fourier transform (and its inverse) of a function as

$$f(\omega) = \int_{-\infty}^{\infty} dt e^{i\omega t} f(t) \quad \text{and} \quad f(t) = \int_{-\infty}^{\infty} \frac{d\omega}{2\pi} e^{-i\omega t} f(\omega). \quad (1.59)$$

In Gibbs equilibrium the stationary correlation function between any two observables is linked to the linear response of one of these observables to a linear perturbation applied to the other in a model-independent way. Indeed, while the functional forms of the correlation and linear response may depend on the pair of observables considered and of course by the model studied, the relation between them remains unaltered and it is just determined by the temperature of the environment. This remarkably universal relation is the statement of the fluctuation-dissipation theorem (FDT) that in time domain can be expressed as

$$R^{AB}(t) = \frac{i}{\hbar} \theta(t) \int_{-\infty}^{\infty} \frac{d\omega}{\pi} e^{-i\omega t} \tanh\left(\frac{\beta\hbar\omega}{2}\right) C_+^{AB}(\omega), \quad (1.60)$$

where  $\beta$  is the inverse temperature of the system at equilibrium. Taking the limit  $\hbar \rightarrow 0$  of (1.60), one can find the classical fluctuation-dissipation theorem

$$R^{AB}(t) = -\beta\theta(t) \frac{d}{dt} C^{AB}(t). \quad (1.61)$$

The quantum FDT can be cast in a compact form in the frequency domain by Fourier transforming Eq. (1.60)

$$\hbar \text{Im } R^{AB}(\omega) = \tanh\left(\frac{\beta\hbar\omega}{2}\right) C^{AB}(\omega). \quad (1.62)$$

At equilibrium, the relation between  $R^{AB}$  and  $C^{AB}$  is determined only by the inverse temperature  $\beta$  and it is independent of the model and the pair of observables  $A, B$  considered. Accordingly, the knowledge of  $R^{AB}$  and  $C_+^{AB}$  for a pair observables  $A$  and  $B$  allows the determination of the inverse temperature  $\beta$  of the system in equilibrium via Eqs. (1.60) and (1.62), whatever the observable  $A$  and  $B$  are. FDT provides a way

to 'measure' the temperature of a system, through the measurements of correlation and response functions.

The idea of the novel approach we pursue in the following Section (see also Refs. [38, 39]) is to test the relaxation to a thermal state determining the correlation and linear response of a chosen pair of observables and verifying whether FDT is satisfied. Out of equilibrium, we define an inverse *effective temperature*  $\beta_{eff}^{AB}(\omega)$  by enforcing the quantum fluctuation dissipation relations (FDR), i.e., via

$$\hbar \text{Im} R^{AB}(\omega) = \tanh\left(\frac{\beta_{eff}^{AB}(\omega)\hbar\omega}{2}\right) C_+^{AB}(\omega), \quad (1.63)$$

where we consider  $C_+^{AB}(t)$  and  $R^{AB}(t)$  within the stationary regime in order to perform Fourier transform (1.59). In complete generality  $\beta_{eff}^{AB}(\omega)$  defined from Eq. (1.63) depends both on the choice of the observables  $A$  and  $B$  and on the frequency  $\omega$ . Indeed, as the correlation  $C^{AB}$  and response  $R^{AB}$  functions are, in principle, unrelated out of equilibrium it is necessary to allow such dependence of  $\beta_{eff}^{AB}(\omega)$  in Eq. (1.63). The study of the effective temperatures  $\beta_{eff}^{AB}(\omega)$  obtained from Eq. (1.63) can provide important information on the eventual thermalization of the system after the quench; if the system thermalizes, in fact, the effective temperatures  $\beta_{eff}^{AB}(\omega)$  must become almost constant in the frequency domain and also independent of the quantities used to define them, i.e.,

$$\beta_{eff}^{AB}(\omega) = \beta, \quad (1.64)$$

in such a way that FDR (1.63) reduces to FDT (1.62) proving that the system is really in thermal equilibrium at inverse temperature  $\beta$ . We emphasize that the idea of using FDR in order to investigate thermalization properties in non-equilibrium systems is completely general. In Sec. 2.4 we report the results obtained by using this approach for the quench dynamics of a quantum Ising chain [38], for which it was originally argued that some one-time observable could equilibrate. Then in Chapter 4 we compute the correlation and response functions for a quantum Ising chain perturbed by a time-dependent delta correlated noise in the transverse direction and driven out of equilibrium also by a sudden quench of the static component of the transverse field and extract an effective temperature in order to better understand its relaxation dynamics.

In this Chapter we introduce and provide the necessary background about the one-dimensional quantum Ising chain (QIC), which the noisy quantum Ising chain we study in this thesis is based on. In Sec. 2.1 we introduce the Hamiltonian of QIC, describing its properties and the presence of a quantum phase transition. Then, in Sec. 2.2, we show in detail how it is possible, through Jordan-Wigner transformation and Bogolyubov rotation, to map the QIC onto non-interacting fermionic system. The quantum Ising chain is an example of integrable model and so it provides the opportunity to test the GGE hypothesis, discussed in Sec. 1.3, for the relaxation dynamics of the system. In Sec. 2.3, we review the results found in Refs. [16, 17] for the non-equilibrium dynamics of a quantum Ising chain following a quantum quench of the transverse field. Finally, in Sec. 2.4, we confirm the lack of thermalization of the QIC from a qualitative different approach, based on the computation of the correlation and linear response functions and the consequent failure of the fluctuation-dissipation theorem [38].

## 2.1 The model

We discuss the one-dimensional quantum Ising chain in a transverse field (QIC). This model is described by the Hamiltonian

$$H(g) = -J \sum_{j=1}^L [\sigma_{j+1}^x \sigma_j^x + g \sigma_j^z] \quad (2.1)$$

where  $\sigma_j^\alpha$  are the Pauli matrices at site  $j$  which commute at different sites. We assume a positive exchange constant  $J > 0$ , the length  $L$  of the chain to be even and we impose

periodic boundary conditions  $\sigma_{L+1}^\alpha = \sigma_1^\alpha$ . In an explicit representation:

$$\sigma^x = \begin{pmatrix} 0 & 1 \\ 1 & 0 \end{pmatrix}, \quad \sigma^y = \begin{pmatrix} 0 & -i \\ i & 0 \end{pmatrix}, \quad \sigma^z = \begin{pmatrix} 1 & 0 \\ 0 & -1 \end{pmatrix} \quad \text{with} \quad [\sigma_j^\alpha, \sigma_k^\beta] = 2i\delta_{jk}\epsilon^{\alpha\beta\gamma}\sigma_j^\gamma \quad (2.2)$$

where  $\epsilon^{\alpha\beta\gamma}$  is totally anti-symmetric symbol, such that  $\epsilon^{xyz} = 1$ , and  $\delta_{jk}$  is the Kronecker's delta. In Eq. (2.1) the term  $\sigma_{j+1}^x\sigma_j^x$  does not commute with  $\sigma_j^z$ , highlighting the quantum nature of the system. The Hamiltonian Eq. (2.1) displays a global  $\mathbb{Z}_2$  symmetry being invariant for a global rotation around the  $z$ -axis in spin space by an angle of  $\pi$ , i.e.,

$$\sigma_j^x \rightarrow -\sigma_j^x, \quad \sigma_j^y \rightarrow -\sigma_j^y, \quad \sigma_j^z \rightarrow \sigma_j^z \quad (2.3)$$

The quantum Ising chain is of fundamental importance because it is the paradigmatic example of a model which undergoes an equilibrium quantum phase transition by tuning the coupling  $g$  [41]: at *zero temperature* and in the thermodynamic limit it is characterized by two phases, a paramagnetic for  $g > 1$  and ferromagnetic one for  $g < 1$ , separated by a quantum critical point at  $g = 1$ . In the paramagnetic phase we have a vanishing order parameter  $\langle \sigma_i^x \rangle$ , while in the ferromagnetic one we have spontaneous  $\mathbb{Z}_2$ -symmetry breaking  $\langle \sigma_i^x \rangle \neq 0$  and long-range order along the  $x$  direction appears in the system,  $\lim_{r \rightarrow \infty} C_r^{xx} = \lim_{r \rightarrow \infty} \langle \sigma_i^x \sigma_{i+r}^x \rangle \neq 0$ . However the long-range order disappears as soon as the temperature  $T$  takes non-vanishing values. We want to emphasize that this phase transition, occurring at  $T = 0$ , is only due to the quantum fluctuations in the system. Phase transitions in classical models are driven by thermal fluctuations which weaken and cease as  $T \rightarrow 0$ ; in contrast, quantum fluctuations are controlled by the coupling  $g$  and they persist up to  $T = 0$  eventually triggering this phase transition. Accordingly the quantum nature of the system is crucial.

The model Eq. (2.1) is realized in solids [42] and in Ref. [43] a degenerate Bose gas of rubidium atoms confined in an optical lattice has been used to simulate the Hamiltonian Eq. (2.1) with a negative exchange constant  $J < 0$ ; in the latter case the system is isolated from the environment and its parameters are controlled with high accuracy making possible to investigate non-equilibrium dynamics of spin chains experimentally.

## 2.2 Diagonalization of the quantum Ising chain

Now we want to show that it is possible to map the Hamiltonian of the QIC Eq. (2.1) into one of non-interacting fermions. We introduce the raising and lowering spin operators  $\sigma_j^\pm$  at the site  $j$

$$\sigma_j^\pm = \frac{\sigma_j^x \pm i\sigma_j^y}{2} \quad (2.4)$$

For 1/2-spin operators we can use the explicit representation Eq. (2.2) and prove that

$$\{\sigma_j^+, \sigma_j^-\} = 1. \quad (2.5)$$

So anticommutation relations Eq. (2.5) suggest an analogy between the operators  $\sigma^\pm$  and canonical creation and annihilation fermionic operators  $c^\dagger, c$ , i.e.,

$$\sigma_j^+ \mapsto c_j \quad , \quad \sigma_j^- \mapsto c_j^\dagger \quad (2.6)$$

$$\text{with } \left\{ c_j, c_k^\dagger \right\} = \delta_{jk} \quad \text{and} \quad \left\{ c_j, c_k \right\} = \left\{ c_j^\dagger, c_k^\dagger \right\} = 0 \quad (2.7)$$

But this analogy fails for spins at different sites given that truly fermionic operators would anticommute,  $\{c_j, c_k^\dagger\} = 0$  if  $j \neq k$ , while instead  $\sigma^\pm$  commute,  $[\sigma_j^+, \sigma_k^-] = 0$  if  $j \neq k$ . However it is possible to modify the identification suggested above and express 1/2-spin operators in terms of fermions in order to reproduce the commutation relations Eq. (2.2). In general we have to introduce a phase factor

$$\sigma_j^+ = U(j)c_j \quad \sigma_j^- = c_j^\dagger U^\dagger(j) \quad (2.8)$$

where  $U(j)$  is a non-local function of  $c, c^\dagger$  which eventually takes the form of a "string" of operators.

For one-dimensional systems Jordan and Wigner [44] established the phase factor

$$U(j) = \prod_{l=1}^{j-1} \exp(i\pi c_l^\dagger c_l) = \prod_{l=1}^{j-1} [1 - 2c_l^\dagger c_l]. \quad (2.9)$$

The last equality in Eq. (2.9) follows from the fact that the only eigenvalues of the fermionic number operator  $n_j = c_j^\dagger c_j$  are 0 or 1 and so  $\exp(i\pi c_l^\dagger c_l) = 1 - 2c_l^\dagger c_l$ ; in this way the phase factor  $U(j)$  can also be interpreted as a "string" of operators.

The spin operators  $\sigma^\pm$  expressed in terms of canonical creation and annihilation fermionic operators  $c^\dagger, c$  through the Eq. (2.8) with the phase factor  $U(j)$  given by Eq. (2.9) now satisfy the correct commutation rules, i.e.,

$$\text{if } \left\{ c_j, c_k^\dagger \right\} = \delta_{jk} \quad \text{then} \quad \left\{ \sigma_j^+, \sigma_j^- \right\} = 1 \quad \text{and} \quad \left[ \sigma_j^+, \sigma_k^- \right] = 0 \quad \text{for } j \neq k. \quad (2.10)$$

Accordingly, using Eqs. (2.4), (2.8) and (2.9) the original spin operators  $\sigma_j^\alpha$  are given by

$$\sigma_j^x = \sigma_j^+ + \sigma_j^- = \prod_{l=1}^{j-1} [1 - 2c_l^\dagger c_l] [c_j + c_j^\dagger], \quad (2.11)$$

$$\sigma_j^y = (-i) [\sigma_j^+ - \sigma_j^-] = (-i) \prod_{l=1}^{j-1} [1 - 2c_l^\dagger c_l] [c_j - c_j^\dagger], \quad (2.12)$$

$$\sigma_j^z = [\sigma_j^+, \sigma_j^-] = 1 - 2c_j^\dagger c_j, \quad (2.13)$$

where in Eq. (2.13) we use  $[c_j, c_m^\dagger c_m] = 0$  if  $j \neq m$  and  $[1 - 2c_j^\dagger c_j]^2 = 1$ .

It follows from Eqs. (2.8), (2.9) and (2.13) that the inverse Jordan-Wigner transforma-

tion is

$$c_j = \prod_{l=1}^{j-1} \sigma_l^z \sigma_j^+, \quad (2.14)$$

$$c_j^\dagger = \prod_{l=1}^{j-1} \sigma_l^z \sigma_j^-, \quad (2.15)$$

and it is possible to prove that if the spin operators  $\sigma$  satisfy the commutation rules Eq. (2.2) then the operators  $c^\dagger, c$  are fermionic, that is they fulfill the anticommutation relations Eq. (2.7).

Trough Eq. (2.11), we can write the nearest-neighbor interaction term in Eq. (2.1) as

$$\begin{aligned} \sigma_j^x \sigma_{j+1}^x &= \prod_{l=1}^{j-1} [1 - 2c_l^\dagger c_l] [c_j + c_j^\dagger] \prod_{m=1}^j [1 - 2c_m^\dagger c_m] [c_{j+1} + c_{j+1}^\dagger] \\ &= [c_j + c_j^\dagger] [1 - 2c_j^\dagger c_j] [c_{j+1} + c_{j+1}^\dagger] = [c_j^\dagger - c_j] [c_{j+1} + c_{j+1}^\dagger], \end{aligned} \quad (2.16)$$

where we use the anticommutation relations Eq. (2.7) and  $[1 - 2c_j^\dagger c_j]^2 = 1$ . One important point to note concerns boundary conditions. We assume periodic boundary conditions for spin operators,  $\sigma_{L+1}^\alpha = \sigma_1^\alpha$ , however boundary conditions of the Jordan-Wigner operators  $\{c_j, c_j^\dagger\}$  are affected by the fermion parity  $(-1)^{N_F}$ , where the number of fermions  $N_F$  in the chain is defined as

$$N_F \equiv \sum_{j=1}^L c_j^\dagger c_j. \quad (2.17)$$

Indeed, let us look at the boundary term  $\sigma_L^x \sigma_{L+1}^x$ :

$$\begin{aligned} \sigma_L^x \sigma_{L+1}^x &= \sigma_L^x \sigma_1^x = \prod_{l=1}^{L-1} [1 - 2c_l^\dagger c_l] [c_L^\dagger + c_L] [c_1 + c_1^\dagger] \\ &= \prod_{l=1}^{L-1} \exp(i\pi c_l^\dagger c_l) [c_L^\dagger + c_L] [c_1 + c_1^\dagger] = e^{i\pi \sum_{l=1}^{L-1} c_l^\dagger c_l} [c_L^\dagger + c_L] [c_1 + c_1^\dagger] \\ &= (-) e^{i\pi \sum_{l=1}^L c_l^\dagger c_l} [c_L^\dagger - c_L] [c_1 + c_1^\dagger] = (-1)^{N_F+1} [c_L^\dagger - c_L] [c_1 + c_1^\dagger], \end{aligned} \quad (2.18)$$

where we use Eqs. (2.7), (2.9), (2.11) and (2.17) and we note that if we consider the creation operator  $c_L^\dagger$  we certainly have  $n_L = 1$ , while considering the annihilation operator  $c_L$  we have  $n_L = 0$ . By comparing Eq. (2.16) and Eq. (2.18), we define the Jordan-Wigner operators  $c_{L+1}$  as

$$c_{L+1} \equiv (-1)^{N_F+1} c_1, \quad (2.19)$$

which amounts to assuming periodic boundary conditions for the chain if  $N_F$  is odd and antiperiodic ones if  $N_F$  is even.

Therefore we use Eqs. (2.13), (2.16) and (2.18) to write Eq. (2.1) as

$$H(g) = -J \sum_{j=1}^{L-1} [c_j^\dagger - c_j] [c_{j+1} + c_{j+1}^\dagger] - Jg \sum_{j=1}^L [c_j c_j^\dagger - c_j^\dagger c_j] + J(-1)^{N_F} [c_L^\dagger - c_L] [c_1 + c_1^\dagger] \quad (2.20)$$

Looking at the structure of the Hamiltonian (2.20) we note that it is quadratic in the fermionic operators  $c, c^\dagger$  and so quasi-particles are either created/destroyed in pairs or they hop to the nearest neighboring site; this implies that the Hamiltonian (2.20) conserves the parity of the number of fermions  $(-1)^{N_F}$ . In mathematical terms the operators  $H$  and  $(-1)^{N_F}$  commute,  $[H, (-1)^{N_F}] = 0$ , and we can diagonalize them simultaneously. Accordingly the Hamiltonian is block diagonal,  $H(g) = H_e(g) \oplus H_o(g)$ , where  $H_{e/o}$  acts on the subspace of the Fock space with an even/odd number of fermions.

### 2.2.1 Even sector

Focusing on the sector with an even number  $N_F$  of fermions  $(-1)^{N_F} = 1$ , according to Eq. (2.19) fermions acquire antiperiodic boundary conditions on the fermions

$$c_{L+1} = -c_1. \quad (2.21)$$

In this way the Hamiltonian Eq. (2.20) can be written as

$$H_e(g) = -J \sum_{j=1}^L [c_j^\dagger - c_j] [c_{j+1} + c_{j+1}^\dagger] - Jg \sum_{j=1}^L [c_j c_j^\dagger - c_j^\dagger c_j]. \quad (2.22)$$

Being quadratic, it can be conveniently diagonalized via a Fourier transform

$$c_j = \frac{1}{\sqrt{L}} \sum_k e^{-ikj} c_k \quad \text{with} \quad k = \pm \frac{\pi(2n+1)}{L} \quad \text{and} \quad n = 0, \dots, \frac{L}{2} - 1. \quad (2.23)$$

The quantization of  $k$  is due to the antiperiodic boundary conditions Eq. (2.21) and this sector is generally referred to as Neveu-Schwarz sector (NS). In Fourier space Eq. (2.20) assume the form

$$\begin{aligned} H_e(g) &= 2J \sum_{k>0} [\cos k (c_{-k} c_{-k}^\dagger - c_k^\dagger c_k) + i \sin k (c_k^\dagger c_{-k}^\dagger - c_{-k} c_k)] + 2Jg \sum_{k>0} [c_k^\dagger c_k - c_{-k} c_{-k}^\dagger] \\ &= 2J \sum_{k>0} \Psi_k^\dagger H_k \Psi_k, \end{aligned} \quad (2.24)$$

where we have introduced the Nambu spinor  $\Psi_k$  and the  $2 \times 2$  matrix  $H_k$  according to

$$\Psi_k = \begin{pmatrix} c_k \\ c_{-k}^\dagger \end{pmatrix} \quad \text{and} \quad H_k = \begin{pmatrix} g - \cos k & i \sin k \\ -i \sin k & \cos k - g \end{pmatrix}, \quad \text{respectively.} \quad (2.25)$$

This Hamiltonian is eventually diagonalized via a Bogolyubov rotation (see Appendix A),

$$\begin{pmatrix} c_k \\ c_{-k}^\dagger \end{pmatrix} = \begin{pmatrix} u_k^g & -iv_k^g \\ -iv_k^g & u_k^g \end{pmatrix} \begin{pmatrix} \gamma_k^g \\ \gamma_{-k}^{g\dagger} \end{pmatrix} = \mathcal{R}(\theta_k^g) \begin{pmatrix} \gamma_k^g \\ \gamma_{-k}^{g\dagger} \end{pmatrix} \quad (2.26)$$

$$\text{where} \quad u_k^g = \cos \theta_k^g \quad \text{and} \quad v_k^g = \sin \theta_k^g. \quad (2.27)$$

The operators  $\gamma_k^{g\dagger}, \gamma_k^g$  represents fermionic quasi-particles that satisfy the canonical anticommutation relation  $\{\gamma_k^{g\dagger}, \gamma_{k'}^g\} = \delta_{k,k'}$  and  $\{\gamma_k^g, \gamma_{k'}^g\} = 0$ ; the Bogolyubov angle  $\theta_k^g$  fulfills the relation

$$\tan(2\theta_k^g) = \frac{\sin k}{g - \cos k}. \quad (2.28)$$

For  $k > 0$  this relation has to be inverted with  $2\theta_k^g \in [0, \pi]$ , whereas the values of  $\theta_k^g$  for  $k < 0$  are obtained by using the property  $\theta_{-k}^g = -\theta_k^g$ . As we use in the following, we anticipate that the Bogolyubov angle fulfills the following relations

$$\cos(2\theta_k^g) = \frac{2(g - \cos k)}{\epsilon_k^g} \quad \text{and} \quad \sin(2\theta_k^g) = \frac{2 \sin k}{\epsilon_k^g}. \quad (2.29)$$

In terms of Bogolyubov quasi-particles  $\gamma_k^{g\dagger}, \gamma_k^g$  the Hamiltonian  $H_e(g)$  Eq. (2.22) is diagonal and reads

$$H_e(g) = \sum_k \epsilon_k^g \left[ \gamma_k^{g\dagger} \gamma_k^g - \frac{1}{2} \right] = \sum_{k>0} \epsilon_k^g \left[ \gamma_k^{g\dagger} \gamma_k^g + \gamma_{-k}^{g\dagger} \gamma_{-k}^g - 1 \right], \quad (2.30)$$

with a dispersion relation

$$\epsilon_k^g = 2J\sqrt{1 + g^2 - 2g \cos k}. \quad (2.31)$$

In Fig. 2.1 we plot the dispersion relation  $\epsilon_k^g$  in Eq. (2.31) as a function of  $k \in [-\pi, \pi]$  in the case  $J = 1$  and  $g = 1.3$  (paramagnetic phase),  $g = 0.7$  (ferromagnetic phase) and  $g = 1$  (critical point). We note that the dispersion relation  $\epsilon_k^g$  is a function of  $k$  bounded both from above and from below

$$2J|g - 1| < \epsilon_k^g < 2J(1 + g). \quad (2.32)$$

A basis for the Fock space in the even sector is then given by

$$|k_1, \dots, k_{2m}; g\rangle_{NS} = \prod_{j=1}^{2m} \gamma_{k_j}^{g\dagger} |0, g\rangle_{NS} \quad \text{where} \quad k_j \in \text{NS}, m \in \mathbb{N}, \quad (2.33)$$

and  $|0, g\rangle_{NS}$  is the vacuum state annihilated by all  $\gamma_k^g$ :  $\gamma_k^g |0, g\rangle_{NS} = 0$  if  $k \in \text{NS}$ . The ground state of the system with an even number of fermions  $N_F$  is the vacuum state where no quasi-particle has been created

$$|\text{GS}\rangle_{NS} = |0, g\rangle_{NS}, \quad (2.34)$$

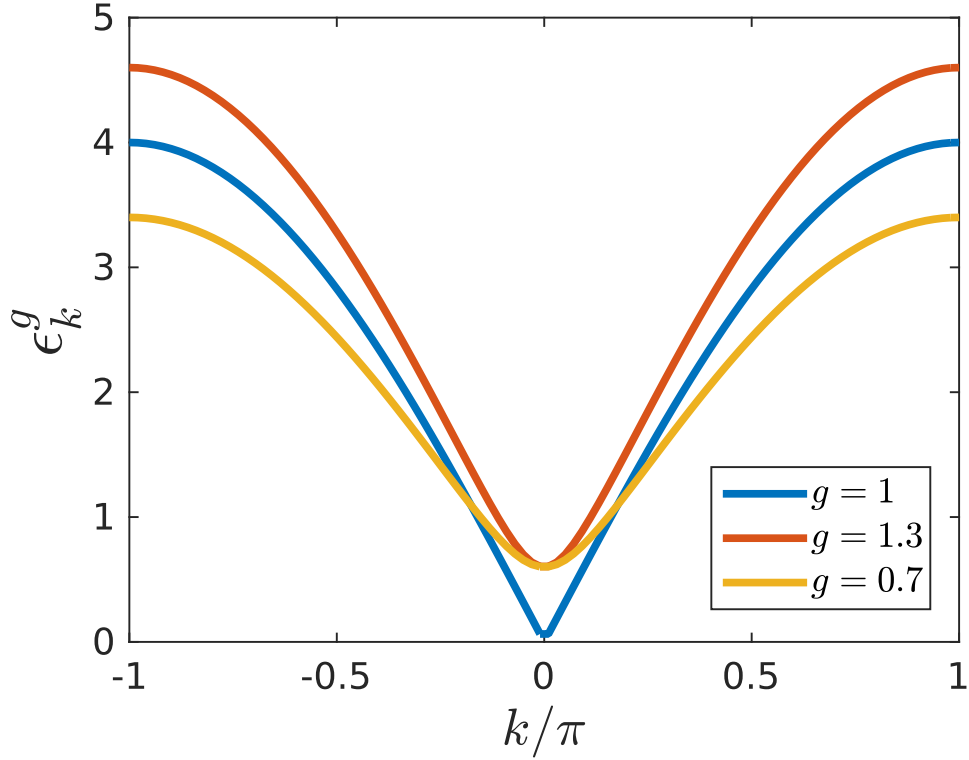


**Figure 2.1:** Dispersion relation  $\epsilon_k^g$  for  $J = 1$  [see Eq. (2.31)] as a function of  $k \in [-\pi, \pi]$  and three different values of the transverse field, indicated in the legend, chosen to correspond to the paramagnetic phase ( $g > 1$ ), ferromagnetic phase ( $g < 1$ ) and to the critical point  $g = 1$ .

from the Hamiltonian  $H_e(g)$  (2.30) and the property  $\gamma_k^g |0, g\rangle_{NS} = 0$ , the corresponding energy is

$$E_{0,NS}^g = -\frac{1}{2} \sum_k \epsilon_k^g. \quad (2.35)$$

It's possible to link the ground state with different transverse field through the relation [16]

$$|0, g_0\rangle_{NS} = \frac{1}{\mathcal{N}_{NS}} \exp \left[ i \sum_{p \in NS} K(p) \gamma_{-p}^{g_0\dagger} \gamma_p^{g\dagger} \right] |0, g\rangle_{NS} \quad (2.36)$$

where  $\mathcal{N}_{NS}$  is a normalization constant and the function  $K(p)$  is given by

$$K(p) = \tan(\Delta\theta_k), \quad (2.37)$$

and we defined the difference between Bogolyubov angles  $\Delta\theta_k$

$$\Delta\theta_k \equiv \theta_k^g - \theta_k^{g_0}. \quad (2.38)$$

The time evolution governed by the Hamiltonian  $H(g)$  of the ground state  $|0, g_0\rangle_{NS}$  is [16]

$$e^{-itH_e(g)} |0, g_0\rangle_{NS} = \frac{|B(t)\rangle_{NS}}{\sqrt{{}_{NS}\langle B|B\rangle_{NS}}} \quad (2.39)$$

where

$$|B(t)\rangle_{NS} = e^{-itE_{0,NS}^g} \exp \left[ i \sum_{0 < p \in NS} e^{-2it\epsilon_p^g} K(p) \gamma_{-p}^{g\dagger} \gamma_p^{g\dagger} \right] |0, g\rangle_{NS} \quad (2.40)$$

### 2.2.2 Odd sector

For an odd number  $N_F$  of fermions we have  $(-1)^{N_F} = -1$  and therefore, according to Eq. (2.19), we have to impose periodic boundary conditions on the fermions

$$c_{L+1} = c_1. \quad (2.41)$$

The Hamiltonian then takes the form

$$H_o(g) = -J \sum_{j=1}^L [c_j^\dagger - c_j] [c_{j+1} + c_{j+1}^\dagger] - Jg \sum_{j=1}^L [c_j c_j^\dagger - c_j^\dagger c_j] \quad (2.42)$$

and it can be diagonalized as in the NS case discussed above, i.e., doing a Fourier transform and then expressing the Hamiltonian in terms of suitable Bogolyubov fermions. The allowed quantized momenta are now

$$p = \frac{2\pi n}{L} \quad \text{with} \quad n = -\frac{L}{2}, \dots, \frac{L}{2} - 1, \quad (2.43)$$

because of the periodic boundary conditions on the fermions. The periodic sector is known as Ramond sector (R). By applying the Fourier transform, isolating the  $p = 0$  term and then using the Bogolyubov rotation the Hamiltonian in the R sector becomes

$$H_o(g) = \sum_{p \neq 0} \epsilon_p^g \left[ \gamma_p^{g\dagger} \gamma_p^g - \frac{1}{2} \right] - 2J(1-g) \left[ \gamma_0^{g\dagger} \gamma_0^g - \frac{1}{2} \right], \quad (2.44)$$

and a basis of the subspace of the Fock space with odd fermion numbers is

$$|p_1, \dots, p_{2m+1}; g\rangle = \prod_{j=1}^{2m+1} \gamma_{p_j}^{g\dagger} |0, g\rangle_R \quad \text{where} \quad p_j \in R, m \in \mathbb{N} \quad (2.45)$$

and  $|0, g\rangle_R$  is the vacuum state annihilated by all  $\gamma_p^g$ :  $\gamma_p^g |0, g\rangle_R = 0$  if  $p \in R$ . In the R sector, the state  $|0, g\rangle_R$  is not allowed by the condition that this sector must contain an odd number of fermions and therefore the lowest energy state fulfilling this condition is

$$|\text{GS}\rangle_R = \gamma_0^{g\dagger} |0, g\rangle_R, \quad (2.46)$$

with associated energy

$$H_o(g)\gamma_0^{g\dagger}|0,g\rangle_R = -\frac{1}{2}\left[\sum_{p\neq 0}\epsilon_p^g + 2J(1-g)\right]\gamma_0^{g\dagger}|0,g\rangle_R \equiv E_{0,R}^g\gamma_0^{g\dagger}|0,g\rangle_R, \quad (2.47)$$

where we used Eq. (2.44) and the anticommutation relations  $\{\gamma_p^g, \gamma_k^{g\dagger}\} = \delta_{pk}$ . Similarly to the NS sector, it's possible to show that [16]

$$e^{-itH_o(g)}|0,g_0\rangle_R = \frac{|B(t)\rangle_R}{\sqrt{R\langle B|B\rangle_R}} \quad (2.48)$$

where

$$|B(t)\rangle_R = e^{-itE_{0,R}^g} \exp\left[i\sum_{0<p\in R} e^{-2it\epsilon_p^g} K(p)\gamma_{-p}^{g\dagger}\gamma_p^{g\dagger}\right]|0,g\rangle_R \quad (2.49)$$

### 2.2.3 Paramagnetic and ferromagnetic phase

Noting that

$$\epsilon_0^g = 2J|1-g| > 0, \quad (2.50)$$

we can write the ground state energy  $E_{0,R}^g$  (2.47) in the R sector in the paramagnetic phase ( $g > 1$ ) and in the ferromagnetic phase ( $g < 1$ ), respectively, as

$$E_{0,R}^{g>1} = -\frac{1}{2}\sum_p \epsilon_p^g + \epsilon_0^g, \quad (2.51)$$

$$E_{0,R}^{g<1} = -\frac{1}{2}\sum_p \epsilon_p^g. \quad (2.52)$$

As long as  $L$  is finite one can verify numerically [see Fig. 2.2] that  $E_{0,NS}^g < E_{0,R}^g$  for any  $g$  and therefore  $|0,g\rangle_{NS}$  is the ground state in both phases.

However, in the thermodynamic limit  $L \rightarrow \infty$ , from Eqs. (2.35) and (2.52)

$$E_{0,NS}^g = -\frac{1}{2}\sum_k \epsilon_k^g \xrightarrow{L\rightarrow\infty} -\frac{L}{2}\int_{-\pi}^{\pi} \frac{dk}{2\pi} \epsilon_k^g, \quad (2.53a)$$

$$E_{0,R}^{g<1} = -\frac{1}{2}\sum_p \epsilon_p^g \xrightarrow{L\rightarrow\infty} -\frac{L}{2}\int_{-\pi}^{\pi} \frac{dp}{2\pi} \epsilon_p^g, \quad (2.53b)$$

and therefore  $E_{0,NS}^g = E_{0,R}^{g<1}$ .

From Eqs. (2.35), (2.50), (2.51) and (2.53), we conclude that, in the paramagnetic phase ( $g > 1$ ) and in the thermodynamic limit  $L \rightarrow +\infty$ ,  $E_{0,NS}^g < E_{0,R}^{g>1}$  and therefore the non degenerate ground state is always

$$|GS\rangle_{par} = |GS\rangle_{NS} = |0,g\rangle_{NS} \quad (2.54)$$

and  ${}_{par}\langle GS|\sigma_j^x|GS\rangle_{par} = \langle \sigma_j^x \rangle_{par} = 0$ .

Instead from Eqs. (2.35), (2.52) and (2.53) we can assert that, in the ferromagnetic phase ( $g < 1$ ) and in the thermodynamic limit  $L \rightarrow +\infty$ ,  $E_{0,NS}^g = E_{0,R}^{g<1}$  resulting in two degenerate ground states related by the  $\mathbb{Z}_2$  symmetry Eq. (2.3)

$$|GS\rangle_{fer} = \frac{1}{\sqrt{2}} [ |GS\rangle_{NS} \pm |GS\rangle_R ] = \frac{1}{\sqrt{2}} [ |0, g\rangle_{NS} \pm \gamma_0^{g\dagger} |0, g\rangle_R ]. \quad (2.55)$$

By spontaneous symmetry breaking the system selects a unique ground state in which spins align along the  $x$ -direction  $\langle \sigma_j^x \rangle_{fer} \neq 0$ .

Moreover, it is possible to see that the gap  $\Delta$  of the quantum Ising chain, defined as the difference between the energy of the ground state and the first excited state, is

$$\Delta = E_1^g - E_0^g = 2J|g - 1|, \quad (2.56)$$

and it vanishes at the critical point  $g = 1$ .

In the end we have seen that the quantum Ising chain in transverse field can be mapped into a system of non-interacting fermions and at zero temperature and in the thermodynamic limit it exhibits a quantum phase transition at the critical point  $g = 1$ .

## 2.3 Quantum quench in the quantum Ising chain

While in the previous Section we have briefly reviewed the equilibrium properties of the quantum Ising chain, here we focus on its dynamics following a global quantum quench of the transverse field. The quench protocol consists in preparing the system in the ground state  $|GS\rangle_{g_0}$  of the Hamiltonian  $H(g_0)$  and in suddenly switching at time  $t = 0$  the transverse field to a different value  $g$  such that the subsequent unitary time evolution of the system is determined by the new Hamiltonian  $H(g)$ . The time evolution of the initial state is then

$$|\psi(t)\rangle = e^{-iH(g)t}|GS\rangle_{g_0}. \quad (2.57)$$

Upon quenching the transverse field one injects an extensive amount of energy into the system and all excited states populates; this can be seen by looking immediately after the quench at the populations

$$\begin{aligned} {}_{g_0}\langle GS|\gamma_k^{g\dagger}\gamma_k^g|GS\rangle_{g_0} &= \sin^2(\Delta\theta_k), \\ {}_{g_0}\langle GS|\gamma_{-k}^g\gamma_{-k}^{g\dagger}|GS\rangle_{g_0} &= \cos^2(\Delta\theta_k), \end{aligned} \quad (2.58)$$

and the coherences

$$\begin{aligned} {}_{g_0}\langle GS|\gamma_k^{g\dagger}\gamma_{-k}^{g\dagger}|GS\rangle_{g_0} &= -\frac{i}{2}\sin(2\Delta\theta_k), \\ {}_{g_0}\langle GS|\gamma_{-k}^g\gamma_k^g|GS\rangle_{g_0} &= \frac{i}{2}\sin(2\Delta\theta_k), \end{aligned} \quad (2.59)$$

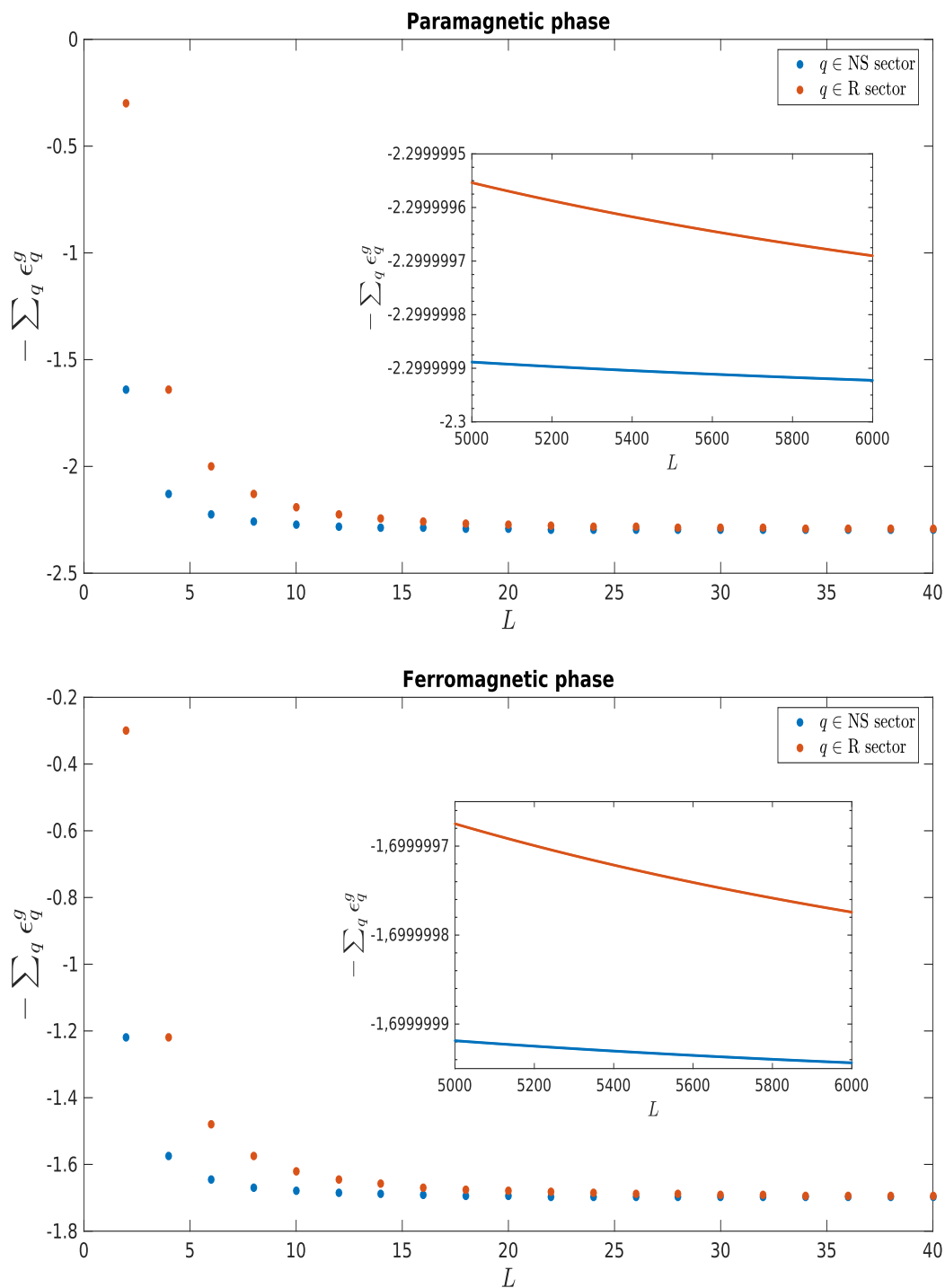


**Figure 2.2:** The quantity  $-\sum_q \epsilon_q^g$ , related to the ground-state energy  $E_0$  (see Eqs. (2.35), (2.51) and (2.52)), is plotted for even/odd number of fermions ( $q \in \text{NS/R}$ ) as a function of the chain length  $L$  for the paramagnetic (upper panel) and ferromagnetic (lower panel) phase. The insets show the behavior of  $-\sum_q \epsilon_q^g$  with  $q \in \text{NS/R}$  for large and finite values of the chain length  $L$  ( $5000 \leq L \leq 6000$ ) in the two phases. It can be seen that the values corresponding to the NS sector are always smaller than those of the R sector for finite  $L$ . A quantum phase transition occurs only in the thermodynamics limit.

where  $\Delta\theta_k$  is given by Eq. (2.38). Equations (2.58) and (2.59) can be obtained by expressing the fermionic operators  $\{\gamma_k^g, \gamma_{-k}^{g\dagger}\}$  in terms of  $\{\gamma_k^{g_0}, \gamma_{-k}^{g_0\dagger}\}$  through a Bogolyubov rotation  $\mathcal{R}(\theta_k^g)\mathcal{R}^\dagger(\theta_k^{g_0}) = \mathcal{R}(\Delta\theta_k)$  (see Eq. (2.26)) and then using the property of the initial state  $\gamma_k^{g_0}|GS\rangle_{g_0} = 0$ . It is natural to ask oneself if the energy pumped into the chain upon quenching will redistribute over the degrees of freedom and the system eventually reaches a thermal state.

This question has been addressed in 2012 by Calabrese et al. in Refs. [16, 17] with the conclusion that the presence of an extensive number of local conserved quantities  $n_k = \gamma_k^{g\dagger}\gamma_k^g$ <sup>1</sup> constrains the dynamics in such a way that the reduced density matrix  $\rho_A$ , defined in Eq. (1.22), after a sudden quench of the transverse field in the quantum Ising chain does not attain a Gibbs density matrix but in the stationary state it is rather equivalent to that of the *generalized Gibbs ensemble* (see Sec. 1.3):

$$\rho_A(t = \infty) = \rho_{GGE}, \quad (2.60)$$

where the GGE density matrix for the Ising chain is

$$\rho_{GGE} = \frac{1}{Z_{GGE}} \exp\left(-\sum_k \beta_k \epsilon_k^g \gamma_k^{g\dagger} \gamma_k^g\right), \quad (2.61)$$

with the Lagrange multipliers  $\beta_k$  fixed by the initial state through Eq. (1.30)

$${}_{g_0}\langle GS|\gamma_k^{g\dagger}\gamma_k^g|GS\rangle_{g_0} = \text{Tr}[\rho_{GGE}\gamma_k^{g\dagger}\gamma_k^g]. \quad (2.62)$$

For a quench in the Ising chain these conditions amount at

$$\beta_k \epsilon_k^g = 2 \operatorname{arctanh}[\cos(2\Delta\theta_k)], \quad (2.63)$$

where  $\epsilon_k^g$  and  $\Delta\theta_k$  are given by Eqs. (2.31) and (2.38), respectively. In this way arbitrary local multi-point spin correlation functions can be evaluated as averages within the GGE. In the following, we distinguish between *local* and *non-local* operators in terms of Jordan-Wigner fermions  $\{c, c^\dagger\}$ . From Eq. (2.13), it is evident that the transverse magnetization  $\sigma_j^z$  is a local operator, because it involves only Jordan-Wigner operators at the site  $j$ ; the order parameter  $\sigma_j^x$ , instead, is a non-local operator as can be seen from Eq. (2.11) which includes a string of Jordan-Wigner operators at the sites  $l \neq j$ . Although  $\sigma^x$  is a non-local operator we stress that correlation functions involving the order parameter can nevertheless be evaluated from GGE.

We focus on the correlation functions of the transverse spins  $\sigma_j^z$  and of the order parameter  $\sigma_j^x$ . First we consider the transverse spins because they are local in the fermionic representation and so their correlation functions and expectation values can be calculated rather easily. The expectation value of the on-site transverse magnetization in the

<sup>1</sup>the integrals of motion  $n_k = \gamma_k^{g\dagger}\gamma_k^g$  are non-local, but for the quantum Ising model is possible to show that local integrals of motion can be expressed as linear combinations of  $n_k$  [45]

thermodynamics limit  $L \rightarrow +\infty$  is

$$\langle \sigma_l^z \rangle \equiv \langle \psi(t) | \sigma_l^z | \psi(t) \rangle = \int_0^\pi \frac{dk}{\pi} \left[ \cos(2\theta_k^g) \cos(2\Delta\theta_k) + \sin(2\theta_k^g) \sin(2\Delta\theta_k) \cos(2\epsilon_k^g t) \right], \quad (2.64)$$

where  $\theta_k^g$ ,  $\epsilon_k^g$  and  $\Delta\theta_k$  are given in Eqs. (2.28), (2.31) and (2.38), respectively. Equation (2.64) displays a first constant term, which is the value in the stationary state and it agrees with the GGE prediction, and an oscillating term, describing the coherent evolution due to pairs of quasiparticles propagating after the quench from the initial state and decaying to zero for  $Jt \gg 1$  as a power law  $1/(Jt)^{3/2}$ . This behavior can be determined by a stationary phase approximation around the saddle points at  $k = 0$  and  $k = \pi$ . The power law decay of  $\langle \sigma_l^z \rangle$  towards the value prescribed by the GGE occurs through inhomogeneous dephasing, i.e., it results from the sum of many oscillating term with slightly different frequencies, and this picture agrees with the argument given in Ref. [46] for the relaxation dynamics of observables in integrable models.

The connected transverse two-point correlator in the thermodynamic limit and in the infinite time limit  $t \rightarrow \infty$  at fixed, finite separation between spins  $l$  is expressed as

$$\begin{aligned} C^{zz}(l, \infty) &\equiv \lim_{t \rightarrow +\infty} [\langle \psi(t) | \sigma_{j+l}^z \sigma_j^z | \psi(t) \rangle - \langle \psi(t) | \sigma_j^z | \psi(t) \rangle^2] \\ &= \int_{-\pi}^\pi \frac{dk}{2\pi} e^{ilk} e^{i\theta_k^g} \cos(2\Delta\theta_k) \int_{-\pi}^\pi \frac{dp}{2\pi} e^{ilp} e^{-i\theta_p^g} \cos(2\Delta\theta_p). \end{aligned} \quad (2.65)$$

The connected two-point function in an equilibrium Gibbs ensemble at temperature  $\beta^{-1}$  is

$$\langle \langle \sigma_j^z \sigma_{j+l}^z \rangle \rangle - \langle \langle \sigma_j^z \rangle \rangle^2 = \int_{-\pi}^\pi \frac{dk}{2\pi} e^{ilk} e^{i\theta_k^g} \tanh\left(\frac{\beta\epsilon_k^g}{2}\right) \int_{-\pi}^\pi \frac{dp}{2\pi} e^{ilp} e^{-i\theta_p^g} \tanh\left(\frac{\beta\epsilon_p^g}{2}\right), \quad (2.66)$$

where  $\langle \langle O \rangle \rangle$  denotes the thermal equilibrium expectation value at temperature  $1/\beta$ . In this way Eq. (2.65) resembles the finite temperature result in Eq. (2.66) provided that the temperature  $\beta$  is replaced by a mode-dependent inverse temperature  $\beta_k$  given in Eq. (2.63). Accordingly,  $C^{zz}(l, \infty)$  agrees with the GGE value given by Eqs. (2.61) and (2.63) and the GGE can be thought of as a system with mode-dependent temperatures. The reason for the appearance of mode-dependent temperatures is the *integrability* of the system; in this case the degrees of freedom do not interact among them and so each  $k$ -mode will "thermalize" at its own temperature  $\beta_k$ , determined by the energy injected into it upon quenching [Eq. (2.58)].

The order parameter  $\sigma_j^x$  is a *non-local* observable in the Jordan-Wigner representation and so its correlation functions are more difficult to compute. In order to obtain results for these quantity a determinant and form factor approach has been developed in Refs. [16, 17]. For quenches within the ferromagnetic phase the expectation value of the

order parameter  $\langle \sigma_l^x(t) \rangle$  turns out to relax to zero exponentially [16]

$$\langle \sigma_l^x(t) \rangle \equiv \langle \psi(t) | \sigma_l^x | \psi(t) \rangle \propto \exp \left[ t \int_0^\pi \frac{dk}{\pi} \epsilon_k^{g'} \log(\cos 2\Delta\theta_k) \right], \quad (2.67)$$

where  $\epsilon_k^{g'} = \frac{d}{dk} \epsilon_k^g$ ; the two-point function  $C^{xx}(l, t)$  decays exponentially in time and space [16]

$$\begin{aligned} C^{xx}(l, t) \equiv \langle \psi(t) | \sigma_{j+l}^x \sigma_j^x | \psi(t) \rangle &\propto \exp \left[ l \int_0^\pi \frac{dk}{\pi} \theta(2\epsilon_k^{g'} t - l) \log |\cos 2\Delta\theta_k| \right] \times \\ &\times \exp \left[ 2t \int_0^\pi \frac{dk}{\pi} \theta(l - 2\epsilon_k^{g'} t) \epsilon_k^{g'} \log |\cos 2\Delta\theta_k| \right], \end{aligned} \quad (2.68)$$

where the step function  $\theta(x)$  is defined as  $\theta(x < 0) = 0$  and  $\theta(x > 0) = 1$ . The exponential correlation length  $\xi$  of  $C^{xx}$  can be extracted from the first factor above which encodes the spatial dependence and it is equal to

$$\xi^{-1} = - \int_{-\pi}^\pi \frac{dk}{2\pi} \log |\cos 2\Delta\theta_k|. \quad (2.69)$$

As expected, the same expression for  $\xi^{-1}$  can be obtained from the GGE density matrix, i.e., by computing the thermal correlation length and then make the substitution in Eq. (2.63)). We can write the two-point correlation functions also as [16]

$$\frac{C^{xx}(l, t)}{(\langle \sigma^x(t) \rangle)^2} \sim \exp \left[ \int_0^\pi \frac{dk}{\pi} \left[ \frac{l}{\xi(k)} - \frac{2t}{\tau(k)} \right] \theta(2\epsilon_k^{g'} t - l) \right], \quad (2.70)$$

where we have defined mode dependent correlations lengths  $\xi(k)$  and decay times  $\tau(k)$  by

$$\xi^{-1}(k) = - \ln |\cos 2\Delta\theta_k| \quad \tau_k^{-1} = -\epsilon_k^{g'} \ln |\cos 2\Delta\theta_k|. \quad (2.71)$$

The step function in Eq. (2.70) means that a given  $k$ -mode contributes to the relaxation dynamics only if the distance  $l$  lies within its forward light cone, indicating that the quasiparticles emitted after the quench propagate ballistically.

## 2.4 Effective temperatures for quantum Ising chain

The first picture which emerged about the non-equilibrium dynamics of isolated quantum many-body systems was that non-integrable systems reach a thermal stationary state described by a Gibbs distribution with a single temperature (see Sec. 1.2); integrable systems, instead, are not expected to thermalize and the asymptotic properties of local observables are described by the so-called generalized Gibbs ensemble, discussed in Sec. 1.3, in which each conserved quantity is characterized by a different effective temperature. But this scenario seems to be richer; indeed it was suggested in Refs. [36, 37] that for small quenches in a quantum Ising chain observables that are non-local in terms

of Jordan-Wigner fermions display an effective thermal behavior. On the other hand, local quantities do not show thermal behavior, with the exception of quenches to the critical point for which all mode dependent temperatures become equal [17]. In fact, the critical point shows some noteworthy properties that can be attributed to the gapless spectrum (see Eq. (2.56)) and to the linearity of the dispersion relation  $\epsilon_k^{g=1}$  (see Eq. (2.31)) at low momenta. So it is desirable to develop a set of tools which allows one to test thermalization (or its lack) in isolated quantum systems beyond the one based on the analysis of stationary expectation values. One proposal is discussed in Sec. 1.6 which suggest to use the fluctuation-dissipation theorem in order to extract a time or frequency-dependent parameter that we call "effective temperature". The analysis of the effective temperatures can definitely inform us about the possible thermal character of the dynamics.

In this Section we study the effective temperatures for a quantum quench of the transverse field Ising chain [38] in order to demonstrate that equilibration never occurs in this model, in spite of some early evidence for the contrary, as mentioned above. In particular the attention is focused on quenches to the critical point and the observables taken in account are the transverse magnetization  $\sigma^z$ , local in the Jordan-Wigner fermions as it can be seen from Eq. (2.13), the global transverse magnetization  $M$  and the order parameter  $\sigma^x$ , which, instead, is non-local as it should be clear from Eq. (2.11). It is legitimate to restrict to the even sector because we consider expectation values of operators which are defined in terms of products of an even number of fermions operators and therefore they do not alter the parity of the state. The dynamic observables one is typically interested in can be expressed in terms of the operators  $\{\sigma_i^g\}$  and via Jordan-Wigner transformation in terms of the fermions  $\{c_k, c_k^\dagger\}$  or alternatively of  $\{\gamma_k, \gamma_k^\dagger\}$ . A practical way to compute the post-quench correlation functions is to express the time dependent operators  $\{c_k(t), c_k^\dagger(t)\}$  in terms of the operators  $\{\gamma_k^{g_0}\}$ ; the benefit of this approach is that the operators  $\{\gamma_k^{g_0}\}$  annihilate the state  $|GS\rangle_{g_0}$  in which the system has been initially prepared. On the other hand, the dynamics after the quench takes a simple form if the operators one is interested in are expressed in terms of the quasi particles  $\{\gamma_k^g, \gamma_k^{g\dagger}\}$  which diagonalize the post-quench Hamiltonian  $H(g)$ ; in fact their time evolution is trivially given by

$$\begin{pmatrix} \gamma_k^g(t) \\ \gamma_{-k}^{g\dagger}(t) \end{pmatrix} = \begin{pmatrix} e^{-i\epsilon_k^g t} & 0 \\ 0 & e^{i\epsilon_k^g t} \end{pmatrix} \begin{pmatrix} \gamma_k^g \\ \gamma_{-k}^{g\dagger} \end{pmatrix} \equiv \mathcal{U}(\epsilon_k^g, t) \begin{pmatrix} \gamma_k^g \\ \gamma_{-k}^{g\dagger} \end{pmatrix} \quad (2.72)$$

where we use Eq. (2.30), the Heisenberg equation of motion and we define the evolution operator  $\mathcal{U}(\epsilon_k^g, t)$  with dispersion relation  $\epsilon_k^g$  given in Eq. (2.31). It is evident that the number operator  $n_k^g = \gamma_k^{g\dagger} \gamma_k^g$  of each  $k$ -level, which appears in the GGE density matrix, is a constant of motion. In order to solve the dynamics, one first expresses the quasi particles  $\{\gamma_k^g, \gamma_{-k}^{g\dagger}\}$  in terms of  $\{\gamma_k^{g_0}, \gamma_{-k}^{g_0\dagger}\}$  through a Bogolyubov rotation  $\mathcal{R}(\theta_k^g) \mathcal{R}^\dagger(\theta_k^{g_0}) = \mathcal{R}(\Delta\theta_k)$  (see Eq. (2.26)). Then we apply the time evolution operator  $\mathcal{U}(\epsilon_k^g, t)$  to the quasi particles  $\{\gamma_k^g, \gamma_{-k}^{g\dagger}\}$  to obtain  $\{\gamma_k^g(t), \gamma_{-k}^{g\dagger}(t)\}$  and finally the time-dependent operators  $\{c_k^g(t), c_{-k}^{g\dagger}(t)\}$  are expressed in terms of the latter via a Bogolyubov

rotation  $\mathcal{R}^\dagger(\theta_k^g)$ . In summary, the total transformation is

$$\begin{pmatrix} c_k(t) \\ c_{-k}^\dagger(t) \end{pmatrix} = \mathcal{R}^\dagger(\theta_k^g) \mathcal{U}(\epsilon_k^g, t) \mathcal{R}(\Delta\theta_k) \begin{pmatrix} \gamma_k^{g_0} \\ \gamma_{-k}^{g_0\dagger} \end{pmatrix} \equiv \begin{pmatrix} u_k^{g,g_0}(t) & -[v_k^{g,g_0}(t)]^* \\ v_k^{g,g_0}(t) & [u_k^{g,g_0}(t)]^* \end{pmatrix} \begin{pmatrix} \gamma_k^{g_0} \\ \gamma_{-k}^{g_0\dagger} \end{pmatrix}, \quad (2.73)$$

where

$$u_k^{g,g_0}(t) = e^{-i\epsilon_k^g t} \cos \theta_k^g \cos \Delta\theta_k + e^{i\epsilon_k^g t} \sin \theta_k^g \sin \Delta\theta_k, \quad (2.74a)$$

$$v_k^{g,g_0}(t) = i e^{i\epsilon_k^g t} \cos \theta_k^g \sin \Delta\theta_k - i e^{-i\epsilon_k^g t} \sin \theta_k^g \cos \Delta\theta_k \quad (2.74b)$$

and  $\theta_k^g$ ,  $\epsilon_k^g$  and  $\Delta\theta_k$  are given by Eqs. (2.28), (2.31) and (2.38), respectively. In this way we can express the average

$$\langle \bullet \rangle = {}_{g_0} \langle GS | \bullet | GS \rangle_{g_0} \quad (2.75)$$

in terms of the functions  $u_k^{g,g_0}(t)$  and  $v_k^{g,g_0}(t)$ .

According to the philosophy of Sec. 1.6, we want to extract from various observable a set of effective temperatures in order to test an eventual effective thermal behavior. We start by analyzing the expectation value of  $\sigma^z(t)$  in the long-time stationary state after the quench Eq. (2.64)

$$\langle \sigma^z \rangle_{stat} \equiv \lim_{t \rightarrow \infty} \langle \sigma^z(t) \rangle = \int_0^\pi \frac{dk}{\pi} \cos(2\theta_k^g) \cos 2\Delta\theta_k. \quad (2.76)$$

As stated in the previous Section, this value differs from the one predicted by a Gibbs thermal ensemble at a unique temperature  $T$ , while it agrees with the GGE prediction with a suitable set of effective temperatures. However, at the critical point  $g = 1$ , it turns out that the effective temperature  $T_{eff}^z$  associated to the transverse magnetization, calculated from Eq. (1.49) with  $O = \sigma^z$ , is equal to the energy based effective temperature  $T_{eff}^E$ , defined by Eq. (1.48):

$$T_{eff}^z = T_{eff}^E. \quad (2.77)$$

Therefore Eq. (2.77) would suggest an effective thermalization within a Gibbs ensemble at temperature  $T_{eff}^E$ . In order to assess this apparent thermalization, according to the strategy discussed in Sec. 1.6, we now focus on the fluctuation and response functions of the system and extract from them a set of effective temperatures. The two-time symmetric, connected correlation and linear response functions  $C_+^{zz}$  and  $R^{zz}$ , respectively, for generic  $g$  and  $g_0$  are given by (see Eqs. (1.52), (1.54), (1.55), (1.57) and (1.58)) [38]

$$C_+^{zz}(t+t_0, t_0) = \frac{1}{2} \langle \{ \sigma_j^z(t+t_0), \sigma_j^z(t_0) \} \rangle - \langle \sigma_j^z(t+t_0) \rangle \langle \sigma_j^z(t_0) \rangle \quad (2.78)$$

$$= 4 \int_0^\pi \frac{dk}{\pi} \int_0^\pi \frac{dl}{\pi} \text{Re} [v_k(t+t_0) v_k^*(t_0) u_l(t+t_0) u_l^*(t_0)], \quad (2.79)$$

$$R^{zz}(t+t_0, t_0) = i\theta(t) \langle [\sigma_j^z(t+t_0), \sigma_j^z(t_0)] \rangle \quad (2.80)$$

$$= -8\theta(t) \int_0^\pi \frac{dk}{\pi} \int_0^\pi \frac{dl}{\pi} \text{Im} [v_k(t+t_0)v_k^*(t_0)u_l(t+t_0)u_l^*(t_0)], \quad (2.81)$$

with  $u_k(t) \equiv u_k^{g,g_0}(t)$  and  $v_k(t) \equiv v_k^{g,g_0}(t)$ . For critical quenches,  $g = 1$  and in the stationary regime  $t_0 \rightarrow \infty$ , Eqs. (2.79) and (2.81) become [38]

$$C_+^{zz}(t) \equiv \lim_{t_0 \rightarrow \infty} C_+^{zz}(t+t_0, t_0) = J_0^2(4t) - E^2(4t) + J_1^2(4t) - [E'(4t)]^2, \quad (2.82)$$

$$R^{zz}(t) \equiv \lim_{t_0 \rightarrow \infty} R^{zz}(t+t_0, t_0) = 4\theta(t) [J_0(4t)E(4t) - J_1(4t)E'(4t)], \quad (2.83)$$

where  $J_\alpha(t)$  is the Bessel function of the first kind and of order  $\alpha$ , while the function  $E(\tau)$  is defined as

$$E(\tau) \equiv \int_0^\pi \frac{dk}{\pi} \sin(\epsilon_k \tau / 4) \cos(2\Delta\theta_k), \quad (2.84)$$

with

$$\epsilon_k \equiv \epsilon_k^{g=1} = 4 \sin(k/2) \quad \text{and} \quad \Delta\theta_k = \theta_k^{g=1} - \theta_k^{g_0}. \quad (2.85)$$

The initial condition enters these expressions only via  $\cos(2\Delta\theta_k)$ . Remarkably, at the critical point  $g = 1$ , this quantity turns out to depend on the pre-quench value of the transverse field  $g_0$  only through the ratio [38]

$$\Upsilon = \left( \frac{1+g_0}{1-g_0} \right)^2 > 1. \quad (2.86)$$

We note that  $\Upsilon$  and consequently the stationary part of the correlation and response functions  $C_+^{zz}$  and  $R^{zz}$  are invariant under the transformation  $g_0 \rightarrow g_0^{-1}$  and therefore in the stationary regime we can restrict to initial conditions in the ferromagnetic phase  $g_0 < 1$ .

In Fig. 2.3 we report the stationary correlation and linear response functions  $C_+^{zz}$  and  $R^{zz}$ , respectively, as a function of time for quenches from  $g = 0, 0.5, 1$  to the critical point  $g = 1$ . In both panels the inset highlights on a double logarithmic scale the long-time algebraic decay of these functions. If the system is initially prepared deeply in the ferromagnetic phase  $g_0 = 0$  (or in the highly paramagnetic one with  $g_0 = \infty$ ),  $E(\tau) = J_1(\tau)$  and so Eqs. (2.82) and (2.83) become

$$C_+^{zz}(t) = J_0^2(4t) - \frac{1}{4} [J_0(4t) - J_2(4t)]^2, \quad (2.87)$$

$$R^{zz}(t) = 2\theta(t) J_1(4t) [J_0(4t) + J_2(4t)], \quad (2.88)$$

where we used the relation  $J_1'(\tau) = [J_0(\tau) - J_2(\tau)]/2$ . For  $g_0 \neq 0, \infty$  the function  $E(\tau)$  cannot be expressed in terms of Bessel functions, but its asymptotic behavior in the long-time limit  $t \gg 1$  can be determined analytically [38]

$$C_+^{zz}(t \gg 1) = -\frac{1}{8\pi t^2} \cos(8t) + \mathcal{O}(t^{-3}), \quad (2.89)$$

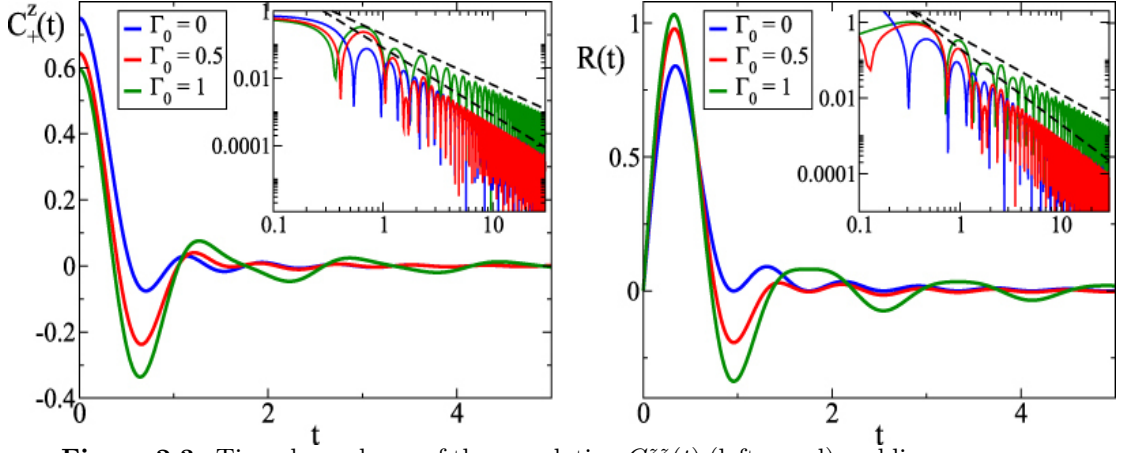


**Figure 2.3:** Time dependence of the correlation  $C_+^{zz}(t)$  (left panel) and linear response functions  $R^{zz}(t)$  (right panel) of the local transverse magnetization  $\sigma_j^z$  in the stationary regime after a quench to the critical point  $\Gamma = 1$ . The insets highlight the algebraic decay of the functions; if  $\Gamma_0 \neq \Gamma = 1$  (blue and red lines) the decay is  $\sim t^{-2}$  while in the case of equilibrium at zero temperature  $\Gamma = \Gamma_0 = 1$  (green line) we have a different power-law  $\sim t^{-3/2}$ . In the figures of this Section, the transverse magnetic field is indicated with  $\Gamma$  and not  $g$ . [Figure taken from Ref [38]]

$$R^{zz}(t \gg 1) = \frac{1}{4\pi t^2} \left[ \left( \frac{1-g_0}{1+g_0} \right)^2 - \sin(8t) \right] + \mathcal{O}(t^{-3}). \quad (2.90)$$

We recall that at equilibrium ( $g = g_0 = 1$ ) the leading algebraic decay of  $C_+^{zz}$  and  $R^{zz}$  is qualitatively different from the ones after the quench reported above, as it turns out to be  $\sim t^{-3/2}$  at zero temperature and  $\sim t^{-1}$  at finite temperature. This different algebraic decay is shown in the inset of Fig. 2.3.

Considering the Fourier transform of the functions Eqs. (2.82) and (2.83) (see Eq. (1.59)) it is possible to define a frequency-dependent effective temperature  $T_{eff}^z(\omega)$  through the fluctuation-dissipation relation (1.63) for  $C_+^{zz}(\omega)$  and  $R^{zz}(\omega)$ . Being  $\sigma^z$  quadratic in the fermions, the Fourier transform functions  $C_+^{zz}(\omega)$  and  $R^{zz}(\omega)$  receive contributions only from real values of the frequency  $\omega$  which coincide either with the sum  $\epsilon_k + \epsilon_l$  or with the difference  $\epsilon_k - \epsilon_l$  of the energies  $\epsilon_{k,l}$  of two quasi-particles. This results in a finite cut-off  $\omega_{max} = 2\epsilon_{k=\pi}$ ; moreover, due to the symmetry under time-reversal in the stationary state  $C_+^{zz}(t) = C_+^{zz}(-t)$ , the following symmetry properties holds

$$C_+^{zz}(\omega) = C_+^{zz}(-\omega) \quad \text{and} \quad \text{Im } R^{zz}(\omega) = -\text{Im } R^{zz}(-\omega). \quad (2.91)$$

In Fig. 2.4 we show the functions  $C_+^{zz}(\omega)$ ,  $R^{zz}(\omega)$  (left panel) and  $T_{eff}^z(\omega)$  (right panel) as obtained by numerical integration of Eqs. (2.82) and (2.83) and via Eq. (1.63). We note that  $T_{eff}^z(\omega)$  vanishes both for  $\omega \rightarrow \omega_{max}$  (with  $\omega_{max} = 2\epsilon_{k=\pi}(g=1) = 8$ ) and for  $\omega \rightarrow 0$ . We emphasize that there is no obvious relationship between  $T_{eff}^z$ , defined in Eq. (1.48), and  $T_{eff}^z(\omega)$  in the right panel of Fig. 2.4. A genuine thermal behavior, instead, would require  $T_{eff}^z(\omega)$  to be independent of  $\omega$  and  $T_{eff}^z = T_{eff}^E$ . The vanishing of the temperature  $T_{eff}^z(\omega \rightarrow 0)$  can be explained by the fact that for  $\omega \rightarrow 0$  the correlation and response functions are not only determined by the low  $k$ -modes, but

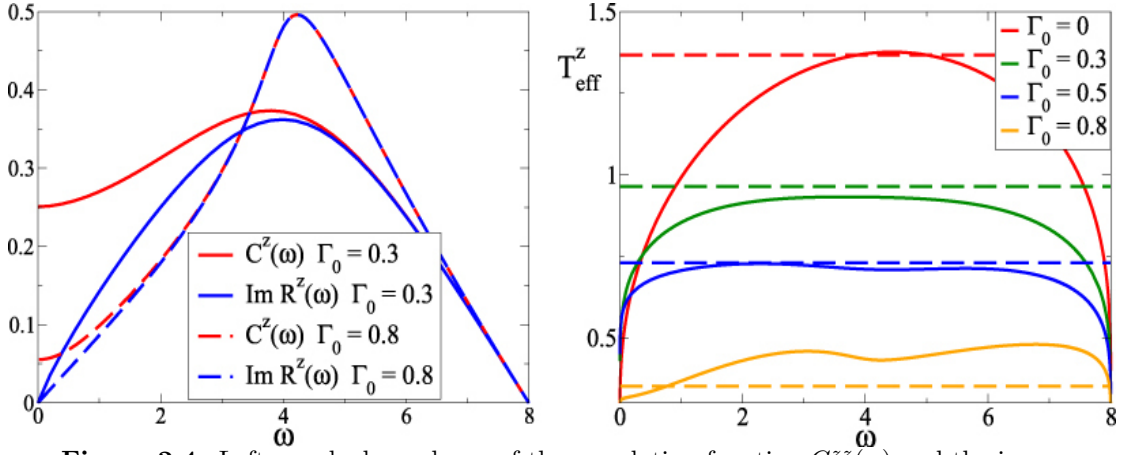


**Figure 2.4:** Left panel: dependence of the correlation function  $C_+^{zz}(\omega)$  and the imaginary part of the linear response function  $\text{Im} R^z(\omega)$  of  $\sigma^z$  on the frequency  $\omega$ , for  $\Gamma_0 = 0.3$  (solid lines) and  $0.8$  (dashed lines) at the critical point  $\Gamma = 1$ . Right panel: effective temperatures  $T_{\text{eff}}^z(\omega)$  defined on the basis of Eq. (1.63), for  $\Gamma = 1$  and various values of  $\Gamma_0$ . The corresponding dashed horizontal lines indicate the values of the effective temperature  $T_{\text{eff}}^E$  determined on the basis of the expectation value of the energy from Eq. (1.48). The comparison shows that there is no special relationship between these two possible effective temperatures, even though a thermal behavior was apparently observed when studying one-time quantities. In the figures of this Section, the transverse magnetic field is indicated with  $\Gamma$  and not  $g$ . [Figure taken from Ref [38]]

they also receive a contribution from the energy difference  $\epsilon_k - \epsilon_l$  between high-energy modes with  $k, l \simeq \pi$ , which are characterized by  $T_{k \simeq \pi} \simeq 0$ , where the mode-dependent temperature  $T_k$  is given in Eq. (2.63).

We conclude that, although  $\langle \sigma^z \rangle_{\text{stat}}$  takes a thermal value, the dynamics of  $\sigma^z$  is not compatible with a thermal behavior that would require  $T_{\text{eff}}^z(\omega)$  to be independent of  $\omega$  and  $T_{\text{eff}}^z = T_{\text{eff}}^E$ .

We now focus on the global transverse magnetization  $M$

$$M = \frac{1}{L} \sum_{j=1}^L \sigma_j^z. \quad (2.92)$$

The generic two-time connected correlation and response function of  $M(t)$  are, from Eqs. (1.52), (1.54), (1.55), (1.57) and (1.58), [38]

$$C_+^M(t+t_0, t_0) = L \left[ \frac{1}{2} \langle \{M(t+t_0), M(t_0)\} \rangle - \langle M(t+t_0) \rangle \langle M(t_0) \rangle \right] \quad (2.93)$$

$$= 8 \int_0^\pi \frac{dk}{\pi} \text{Re} [v_k(t+t_0) v_k^*(t_0) u_k(t+t_0) u_k^*(t_0)], \quad (2.94)$$

$$R^M(t+t_0, t_0) = iL \theta(t) \langle [M(t+t_0), M(t)] \rangle \quad (2.95)$$

$$= -16 \theta(t) \int_0^\pi \frac{dk}{\pi} \text{Im} [v_k(t+t_0) v_k^*(t_0) u_k(t+t_0) u_k^*(t_0)]. \quad (2.96)$$

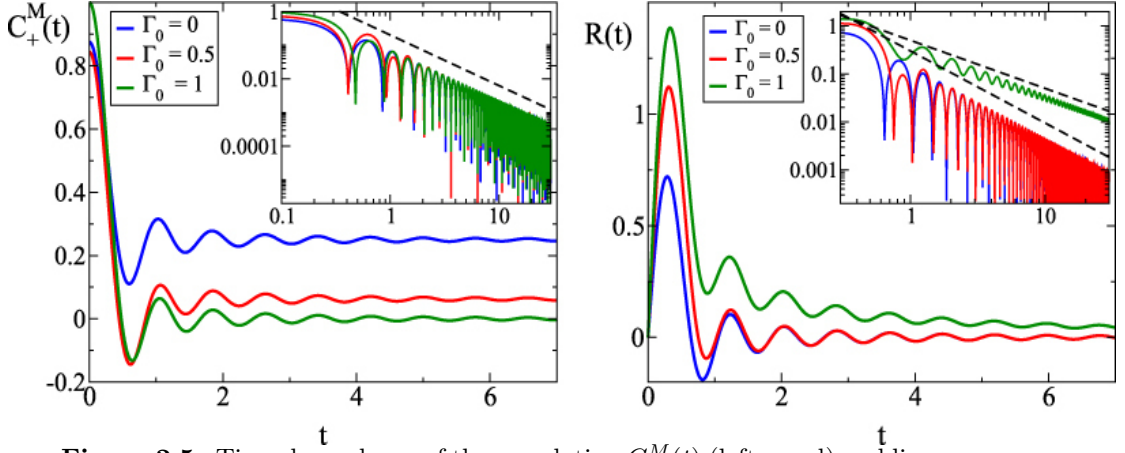


**Figure 2.5:** Time dependence of the correlation  $C_+^M(t)$  (left panel) and linear response functions  $R^M(t)$  (right panel) of the global transverse magnetization  $M$  (see Eq. (2.92)) in the stationary regime after the quench to the critical point  $\Gamma = 1$ . The insets show the algebraic decay of the functions  $\sim t^{-3/2}$  for initial conditions  $\Gamma_0 \neq \Gamma = 1$ ; in the case of equilibrium at zero temperature  $\Gamma_0 = \Gamma = 1$  (green solid lines),  $|C_+^M(t)|$  still decays as  $t^{-3/2}$  whereas  $|R^M(t)|$  decays more slowly, as indicated by the uppermost thin dashed line  $\sim t^{-1}$  in the inset of the right panel. In the figures of this Section, the transverse magnetic field is indicated with  $\Gamma$  and not  $g$ . [Figure taken from Ref [38]]

For critical quenches and in the stationary regime  $C_+^M$  and  $R^M$  become

$$C_+^M(t) \equiv \lim_{t_0 \rightarrow \infty} C^M = C + \frac{J_0(8t) + J_2(8t)}{2} + F(8t) + F''(8t). \quad (2.97)$$

$$R^M(t) \equiv \lim_{t_0 \rightarrow \infty} R^M(t + t_0, t_0) = 4\theta(t) [E(8t) + E''(8t)], \quad (2.98)$$

where we introduced the function  $F$  and the constant  $C$

$$F(\tau) \equiv \int_0^\pi \frac{dk}{\pi} \cos(\epsilon_k \tau / 4) \cos^2(2\Delta\theta_k) \quad \text{and} \quad C = \frac{(1 - g_0)^2}{4}. \quad (2.99)$$

In Fig. 2.5 we plot these stationary correlation and response functions of the global magnetization  $M$  for a critical quench  $g = 1$  from various initial conditions  $g_0 = 0, 0.5, 1$ . In the case of initial conditions deep in the ferromagnetic or paramagnetic phase (i.e.,  $g_0 = 0$  or  $g_0 = \infty$ ) the functions  $C_+^M(t)$  and  $R^M(t)$  can be expressed completely in terms of Bessel functions [38]

$$C_+^M(t) = \frac{1}{4} + \frac{5}{8}J_0(8t) + \frac{1}{2}J_2(8t) - \frac{1}{8}J_4(8t), \quad (2.100)$$

$$R^M(t) = \theta(t) [J_1(8t) + J_3(8t)]. \quad (2.101)$$

For generic quenches, instead, it is only possible to determine the long-time behavior of the stationary correlation and response functions:

$$C_+^M(t \gg 1) = C + \frac{1}{8\sqrt{\pi}t^{3/2}} \sin(8t - \pi/4) + \mathcal{O}(t^{-5/2}), \quad (2.102)$$

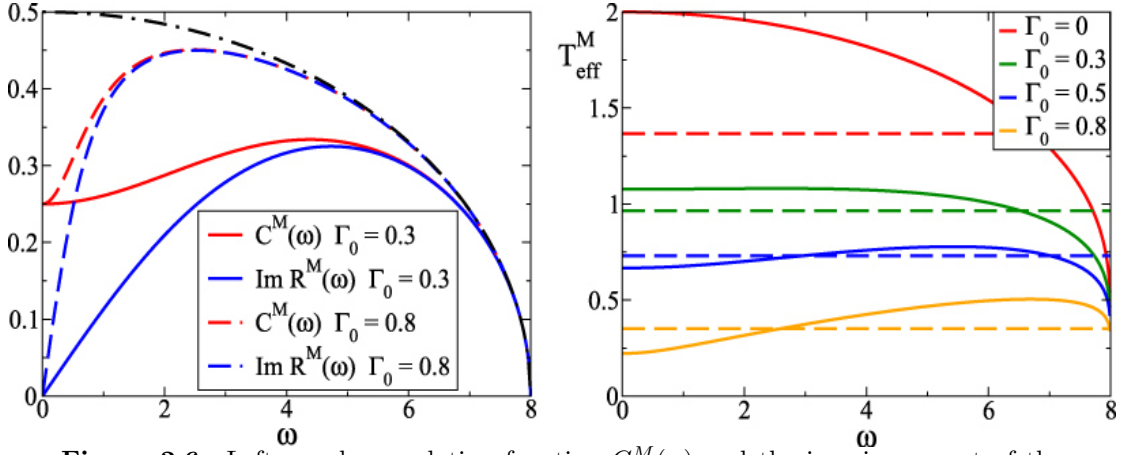


**Figure 2.6:** Left panel: correlation function  $C_+^M(\omega)$  and the imaginary part of the linear response function  $\text{Im} R^M(\omega)$  of  $M$  as functions of the frequency  $\omega$ , for  $\Gamma_0 = 0.3$  (solid lines) and  $0.8$  (dashed lines) at the critical point  $\Gamma = 1$ . The dot-dashed black line shows the limiting value of  $C_+^M(\omega)$  and  $\text{Im} R^M(\omega)$  for  $\Gamma_0 \rightarrow 1$ . Right panel: effective temperatures  $T_{\text{eff}}^M(\omega)$  for  $\Gamma = 1$  and various values of  $\Gamma_0$ . The corresponding dashed horizontal lines indicate the values of the effective temperature  $T_{\text{eff}}^E$  determined on the basis of the expectation value of the energy from Eq. (1.48). As in Fig. 2.4 the comparison between solid and dashed lines in the right panel shows that there is no special relationship between these two possible effective temperatures. Contrary to  $T_{\text{eff}}^z(\omega)$  [see Fig. 2.4], the effective temperature  $T_{\text{eff}}^M(\omega)$  takes a finite value at low frequencies  $\omega \rightarrow 0^+$ . In the figures of this Section, the transverse magnetic field is indicated with  $\Gamma$  and not  $g$ . [Figure taken from Ref [38]]

$$R_+^M(t \gg 1) = -\frac{1}{4\sqrt{\pi}t^{3/2}} \cos(8t - \pi/4) + \mathcal{O}(t^{-5/2}). \quad (2.103)$$

We note that the algebraic decay common to Eqs. (2.102) and (2.103) is slower than the one of the corresponding quantities for the local transverse magnetization in Eqs. (2.89) and (2.90); in addition, this leading-order decay  $\sim t^{-3/2}$  of both  $C_+^M$  and  $R^M$  for  $g_0 \neq g = 1$  is observed also at equilibrium at finite temperature [47].

Proceeding in the same way as we did for the local transverse magnetization we calculate the Fourier transforms of  $C_+^M(t)$  and  $R^M(t)$  and then we extract the effective temperatures  $T_{\text{eff}}^M(\omega)$  according to Eq. (1.63). The Fourier transform  $C_+^M(\omega)$  and  $R^M(\omega)$  receive a contribution only from frequencies  $\omega = \pm 2\epsilon_k$ , contrarily to  $C_+^{zz}(\omega)$  and  $R^{zz}(\omega)$ . The results are reported in Fig. 2.6. We note that for a certain frequency  $\omega$  the effective temperature  $T_{\text{eff}}^M(\omega)$  is equal to the mode dependent temperature  $T_k$  characterizing the GGE (see Eq. (2.63)),  $T_k = T_{\text{eff}}^M(\omega = 2\epsilon_k)$ . We emphasize that there is no obvious relationship between the effective temperature  $T_{\text{eff}}^E$  and the frequency-dependent  $T_{\text{eff}}^M(\omega)$ . The effective temperature  $T_{\text{eff}}^M(\omega)$  vanishes at  $\omega = \omega_{\text{max}}$  and it takes a finite value at low frequencies, contrary to what happens to the effective temperature  $T_{\text{eff}}^z(\omega)$ . The reason for this distinct low-frequency behavior of  $T_{\text{eff}}^M$  is that  $T_{\text{eff}}^M(\omega \rightarrow 0)$  is solely determined by the low-energy modes which are characterized by a finite effective temperature  $T_k$  given in Eq. (2.63). The difference between the various effective temperatures  $T_{\text{eff}}^M(\omega) \neq T_{\text{eff}}^z(\omega) \neq T_{\text{eff}}^E$  provides additional evidence of the lack of thermalization in the asymptotic long-time state.

The last observable we consider here is the order parameter  $\sigma^x$ . Its expectation value  $\langle \sigma^x(t) \rangle$  decays to zero at long times for any  $g \neq g_0$ ; this is similar to the equilibrium thermal behavior at finite temperature  $T > 0$  which is characterized by the absence of long-range order along the  $x$ -axis in spin space. In order to investigate the possible emergence of an effective thermal behavior we study the stationary two-time correlation function  $C^{xx}$ , defined as

$$C^{xx}(t+t_0, t) = \lim_{t_0 \rightarrow \infty} \langle \sigma_j^x(t+t_0) \sigma_j^x(t_0) \rangle, \quad (2.104)$$

which provides the symmetric correlation function  $C_+^{xx}$  and the linear response function  $R^{xx}$  using Eqs. (1.57) and (1.58). The order parameter correlation function can be written in terms of the determinant of a  $2L \times 2L$  matrix, where  $L$  is the chain length, and it is evaluated numerically in Ref. [38].

The dynamics of the operator  $\sigma^x$  shows a very different behavior compared to those of the previous observables considered, as we can see in Fig. 2.7. Both  $C_+^{xx}(t)$  and  $R^{xx}(t)$  decay *exponentially*, rather than algebraically, in the long-time limit, with the characteristic time  $\tau$  defined by

$$C_+^{xx}(t) \sim e^{-t/\tau} \quad \text{where} \quad \tau^{-1} = - \int_0^\pi \frac{dk}{\pi} \frac{d\epsilon_k^g}{dk} \ln \cos(2\Delta\theta_k). \quad (2.105)$$

We note that this time coincide with the one calculated in Ref. [16] (see Eq. (2.68)). It is very interesting to analyze the time dependence of the space-dependent stationary correlation  $C_+^{xx}(r, t)$  and response  $R^{xx}(r, t)$  functions of two spins  $\sigma^x$  separated by a distance  $r$ , calculated from  $C^{xx}(r, t+t_0, t) = \langle \sigma_{j+r}^x(t+t_0) \sigma_j^x(t_0) \rangle_{t_0=\infty}$  using Eqs. (1.57) and (1.58). We observe from Fig. 2.8 that the correlation and the response functions remain almost constant up to times  $t_m \simeq r/2$ ; then the correlation function oscillates and decays towards its asymptotic vanishing value whereas the response function first abruptly increases and takes non-negligible values and then decays as well. At short times,  $t < t_m$ ,  $C^{xx}(r, t)$  and  $R^{xx}(r, t)$  are constant because the quasi-particles emitted after the quench move ballistically with a finite maximum speed  $v_m \simeq 2$ . Accordingly, the correlation function will be constant until the point located at  $(r, t+t_0)$  does not belong to the light cone of the point  $(r=0, t_0)$ . This light-cone effect was already reported in Refs. [16, 17]. The long-time exponential decay of  $C^{xx}(r, t)$  and  $R^{xx}(r, t)$  is illustrated in Fig. 2.9, we observe that it is independent of  $r$  and it occurs with the rate  $\tau$  given by Eq. (2.105). Finally, in Ref. [38] a set of effective temperatures  $T_{eff}^x$  is extracted numerically from Eq. (1.63) and these temperatures turn out to have no relationship with the previous one, providing further evidence for the lack of thermal behavior.

In summary, we have seen that the quantum Ising chain does not thermalize as it is clearly shown not only by discrepancies in expectation values of one-time quantities, but also as revealed by the time-dependence of two-time correlation and response functions which do not satisfy the fluctuation-dissipation theorem proper to the Gibbs

ensemble. In fact, to assert the emergence of a thermal behavior solely on the basis of one-time quantities might be misleading and the effective temperatures extracted from fluctuation-dissipation relations result to be an extremely powerful tool to deeply understand the nature of the stationary state reached after the quench.

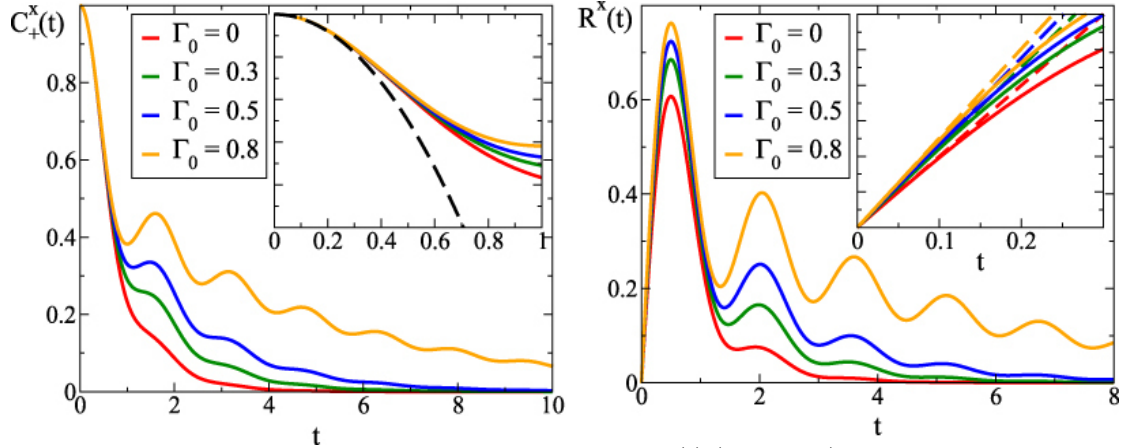


**Figure 2.7:** Time dependence of the correlation  $C_+^{xx}(t)$  (left panel) and linear response  $R^{xx}(t)$  (right panel) functions of the order parameter, in the stationary state after a quench to the critical point  $\Gamma = 1$  and for various values of  $\Gamma_0$ . The insets highlight the short-time behavior of these functions and the dashed curves correspond to the analytic expressions [38]  $1 - 2(\Gamma t)^2$  (left panel) and  $4\langle\sigma^z\rangle_{stat}\Gamma t$  (right panel). In the figures of this Section, the transverse magnetic field is indicated with  $\Gamma$  and not  $g$ . [Figure taken from Ref [38]]

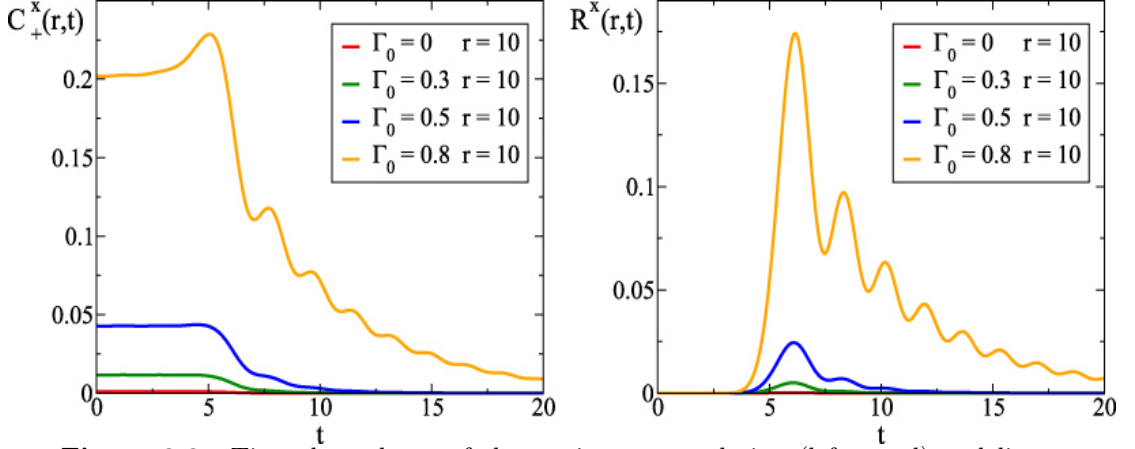


**Figure 2.8:** Time dependence of the stationary correlation (left panel) and linear response function (right panel) of two  $\sigma^x$  spins separated by a distance  $r = 10$  in units of the lattice spacing, after a quench to the critical point  $\Gamma = 1$ . Both  $C_+^{xx}(r = 10, t)$  and  $R^{xx}(r = 10, t)$  display clear light-cone effects, as discussed in the main text. In the figures of this Section, the transverse magnetic field is indicated with  $\Gamma$  and not  $g$ . [Figure taken from Ref [38]]

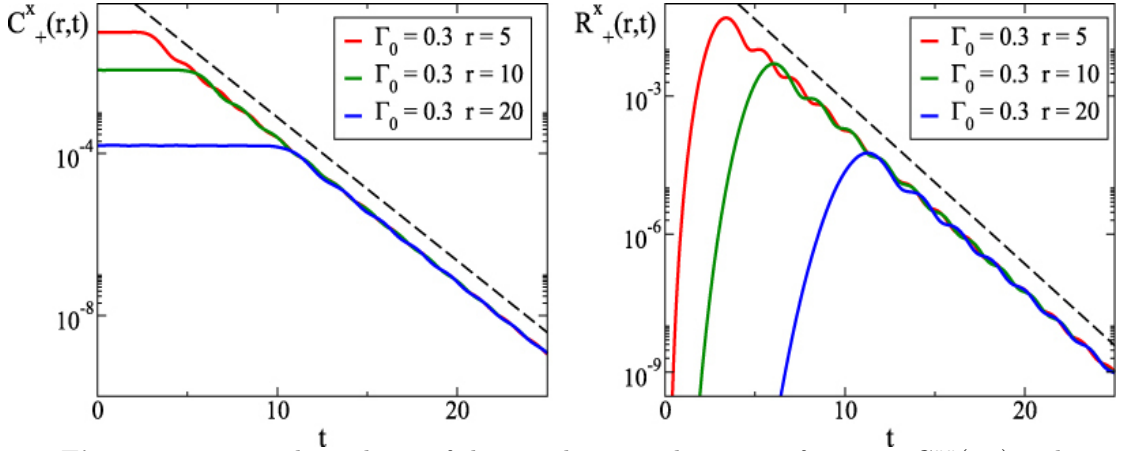


**Figure 2.9:** Time dependence of the correlation and response functions  $C_+^{xx}(r, t)$  and  $R_+^{xx}(r, t)$  for various values of  $r$  and  $\Gamma_0$  after a quench to the critical point  $\Gamma = 1$ . The behavior of both functions at short times is compatible with a light-cone effect with characteristic time  $r/v_m = r/2$  for the present case  $\Gamma = 1$ . Before this characteristic time, the correlation function is almost constant whereas the response function is negligible. The eventual exponential decay (highlighted by the logarithmic scale) is independent of  $r$  and the dashed lines correspond to a decay rate given by equation Eq. (2.105). The dependence on  $r$  of the correlation function at small times is compatible with a spatial exponential decay  $C_+^{xx}(r) \sim e^{-r/\xi}$  with correlation length  $\xi \simeq 2.3$  equal to the one predicted by Eq. (2.69). In the figures of this Section, the transverse magnetic field is indicated with  $\Gamma$  and not  $g$ . [Figure taken from Ref [38]]

It is interesting and important to know the asymptotic state reached by a quantum system driven out of equilibrium by a quantum quench [2, 13, 16, 20]. In addition to understanding which asymptotic state is attained by a quantum many-body system after a quantum quench, it is important to know how this develops in time, i.e., what are the time scales for thermalization, whether the process of thermalization occurs uniformly or it is composed by many stages and, eventually, which are the mechanisms behind thermalization. In this Chapter we answer these questions by studying the non-equilibrium dynamics of a quantum Ising chain perturbed by a time-dependent uncorrelated noise in the transverse field and driven out of equilibrium by a sudden quench of the mean value of this transverse field; we refer to this model as noisy quantum Ising chain. This model has been introduced in Ref.[34] in order to investigate the effect of integrability breaking on the non-equilibrium dynamics of a quantum Ising chain.

In Sec. 3.1 we introduce the model and the non-equilibrium protocol, illustrating the motivation which led to its formulation. In Sec. 3.2 we briefly review the Keldysh contour technique which allows us to treat conveniently quantum many-body systems governed by a time-dependent Hamiltonian. Finally, in Sec. 3.3 we show that it is possible to write down and solve analytically a master equation for the noisy quantum Ising chain using the Keldysh formalism; then we report the expressions of the time evolution of various and physically relevant observables obtained by employing the solution of the master equation. Remarkably, it turns out that the non-equilibrium dynamics of the system resulting from the interplay of a quantum quench and a time-dependent noise is characterized by three temporal stages. First, the system relaxes towards the asymptotic steady state of the quantum Ising chain after a sudden quench without noise; this phenomena is *prethermalization* discussed in Sec. 1.5. Later, a noise-induced dephasing occurs, suppressing exponentially the coherences on the time scale of the inverse noise strength. In the last stage, the noise heats up the system, driving it towards a thermal state but at infinite temperature. In addition, the correlation function of the transverse magnetization at equal times shows an interesting crossover from ballistic to diffusive

behavior as time goes by.

### 3.1 The model, the motivation and the out of equilibrium protocol

In Sec. 1.3 we discuss the peculiarity of the non-equilibrium dynamics of integrable systems. Generically, actual many-body systems are non-integrable and therefore the study of these systems is of fundamental importance in order to reach a complete and deep understanding of the non-equilibrium dynamics of quantum many-body systems. Unfortunately non-integrable systems are hard to treat analytically and their dynamics is almost never known beyond numerical simulations which, however, are still restricted to rather small systems and short times, especially in higher spatial dimensions. We now show heuristically that studying a quantum Ising chain perturbed by a Gaussian noise in the strength of the transverse field, which can be solved analytically as we see in the next Sections, can help us to understand the properties of a non-integrable Ising chain. Consider, in fact, the Hamiltonian

$$H(g, B) = \sum_i (\sigma_i^x \sigma_{i+1}^x + g \sigma_i^z) + B \sum_i \sigma_i^z \sigma_{i+1}^z, \quad (3.1)$$

where the first term is the integrable quantum Ising chain described in Chapter 2 while the second term, with coupling  $B$ , breaks the integrability of the model [24]. As in the Hubbard-Stratonovich transform, we consider the infinitesimal time evolution

$$e^{-i\epsilon H} = e^{-i\epsilon \sum_i [\sigma_i^x \sigma_{i+1}^x + g \sigma_i^z]} e^{-i\epsilon B \sum_i \sigma_i^z \sigma_{i+1}^z} + O(\epsilon^2), \quad (3.2)$$

where we employ the Baker-Campbell-Hausdorff formula

$$e^Z = e^X e^Y \quad \text{with} \quad Z = X + Y + \frac{1}{2} [X, Y] + \frac{1}{12} ([X, [X, Y]] - [Y, [X, Y]]) + \dots \quad (3.3)$$

We now introduce an auxiliary field  $\delta g$  and write the second term in Eq. (3.2) as a Gaussian integral

$$e^{-i\epsilon \sum_{m,n} B \sigma_m^z \sigma_n^z} \sim \int \prod_m d(\delta g_m) e^{-i\epsilon \sum_{m,n} \delta g_m B \delta g_n - i\epsilon \sum_m \sigma_m^z \delta g_m}, \quad (3.4)$$

where we considered generic indexes  $m$  and  $n$ . For nearest-neighbor interaction this representation requires the auxiliary field  $\delta g$  to be position dependent. Neglecting this fact and inserting Eq. (3.4) in Eq. (3.2), one can now interpret the integration over the auxiliary field  $\delta g$  as taking the expectation value on a random field which depends on time; in other words Eq. (3.4) can be read as an average over a time-dependent Gaussian white noise  $\delta g(t)$ . Accordingly, we end up with a quantum Ising chain perturbed by a

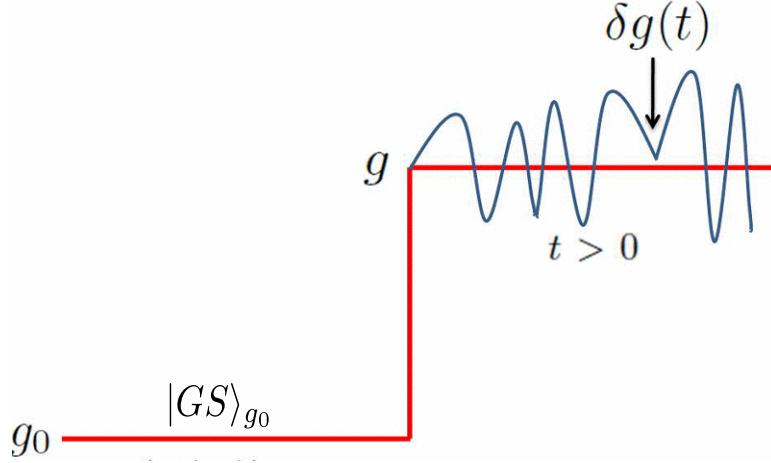


**Figure 3.1:** Out of equilibrium protocol studied for the quantum Ising chain: the system is prepared in the ground state of the unperturbed Ising chain (see Eq. (2.1)) with  $g_0 > 1$ ,  $|GS\rangle_{g_0}$ , and is evolved according to the noisy Ising Hamiltonian (3.5) with a different value of the transverse field  $g > 1$ , plus a Gaussian delta-correlated noise on top of it. [34]

time-dependent Gaussian white noise  $\delta g(t)$  along the transverse direction

$$H(g, t) = -J \sum_{i=1}^L [\sigma_i^x \sigma_{i+1}^x + g \sigma_i^z + \delta g(t) \sigma_i^z], \quad (3.5)$$

where the Gaussian noise  $\delta g(t)$  has zero average and delta temporal correlations, with an amplitude  $\Gamma$ , i.e.,

$$\begin{aligned} \langle \delta g(t) \rangle_{noise} &= 0, \\ \langle \delta g(t) \delta g(t') \rangle_{noise} &= \frac{\Gamma}{2} \delta(t - t'). \end{aligned} \quad (3.6)$$

We consider the dynamics of the system according to the following protocol: at time  $t < 0$  the chain is prepared in the ground state of the unperturbed Hamiltonian as in Eq. (2.1)], with a certain value  $g_0$  of the transverse magnetic field,  $|GS\rangle_{g_0}$ , and  $\delta g(t) = 0$ . At a later time  $t > 0$ , the chain is evolved according to the full Hamiltonian (3.5) with *both* a different value  $g$  of the transverse field *and* the noise  $\delta g(t)$ , as portrayed in Fig. 3.1. For simplicity, both  $g_0$  and  $g$  are chosen within the paramagnetic phase. In the following we focus on the interplay between the effect of the sudden quench  $g_0 \mapsto g$  of the transverse field and the time-dependent noise  $\delta g(t)$  driving the dynamics of the system.

## 3.2 Keldysh formalism

In this Section we review the Keldysh contour technique which we will use in Sec. 3.3 to solve the time-dependent Hamiltonian (3.5). For additional details and applications

the reader is referred to Refs. [48–51].

### 3.2.1 Closed time contour

Consider a quantum many-body system governed by a time-dependent Hamiltonian

$$H(t) = H_0 + V(t), \quad (3.7)$$

where  $H_0$  describes a system of non-interacting particles and  $V(t)$  is a time-dependent perturbation or interaction term between these particles. We assume that in the distant past  $t = -\infty$  the system is in a state specified by a density matrix  $\rho(-\infty)$  and that the particles are non-interacting, i.e.,  $V(-\infty) = 0$ . The density matrix  $\rho(t)$  evolves according to the von Neumann equation of motion

$$\partial_t \rho(t) = -i [H(t), \rho(t)], \quad (3.8)$$

where we set  $\hbar = 1$ . Equation (3.8) is formally solved with the help of the unitary evolution operator  $\mathcal{U}(t, t')$  as

$$\rho(t) = \mathcal{U}(t, -\infty) \rho(-\infty) \mathcal{U}^\dagger(t, -\infty) = \mathcal{U}(t, -\infty) \rho(-\infty) \mathcal{U}(-\infty, t), \quad (3.9)$$

where the evolution operator  $\mathcal{U}(t, t')$  obeys the differential equation

$$\begin{cases} \partial_t \mathcal{U}(t, t') = -i H(t) \mathcal{U}(t, t'), \\ \mathcal{U}(t, t) = \mathbf{1}, \end{cases} \quad (3.10)$$

and in the last equality of Eq. (3.9) we use the property  $\mathcal{U}^\dagger(t, t') = \mathcal{U}(t', t)$ . Due to the time-dependence of the perturbation  $V(t)$ , we note that the Hamiltonian operators taken at different times, in general, do not commute with each other. Accordingly, the solution of Eq. (3.10) is

$$\mathcal{U}(t, t') = \sum_{n=0}^{+\infty} \frac{(-i)^n}{n!} \int_{t'}^t dt_1 \dots \int_{t'}^t dt_n \mathcal{T} [H(t_1) \dots H(t_n)] = \mathcal{T} \exp \left[ -i \int_{t'}^t d\bar{t} H(\bar{t}) \right], \quad (3.11)$$

where the time-ordered product of operators, denoted by the symbol  $\mathcal{T}$ , is defined as

$$\mathcal{T} [O_1(t_1) O_2(t_2) \dots O_n(t_n)] = O_{i_1}(t_{i_1}) O_{i_2}(t_{i_2}) \dots O_{i_n}(t_{i_n}) \quad (3.12)$$

where  $i_1, i_2, \dots, i_n \in \{1, 2, \dots, n\}$  are such that  $t_{i_1} > t_{i_2} > \dots > t_{i_n}$ . One is usually interested in the expectation value of some observable  $O$  at a time  $t$  given by

$$\langle O(t) \rangle \equiv \text{Tr} [\rho(t) O] = \text{Tr} [\rho(-\infty) \mathcal{U}(-\infty, t) O \mathcal{U}(t, -\infty)], \quad (3.13)$$

where we use Eq. (3.9) and the cyclic property of the trace to move the evolution operator  $\mathcal{U}(t, -\infty)$  to the right of  $O$ . The last equality in Eq. (3.13) describes the evolution from the time  $t = -\infty$ , at which the initial density matrix  $\rho(-\infty)$  is specified, towards  $t$ ,

when the observable  $O$  is evaluated, and then back to the time  $t = -\infty$ . Accordingly, in order to calculate the expectation value of an observable  $O$  we have to evolve the initial state both forward and backward in time. At equilibrium, this forward-backward evolution can be avoided using the adiabatic theorem (see below) and in fact it can be reduced only to the forward one [50, 52, 53]. By considering systems at equilibrium at zero temperature, the expectation values have the form

$$\langle GS|O|GS\rangle, \quad (3.14)$$

where  $|GS\rangle$  is the ground state of the interacting many-body system described by the Hamiltonian  $H = H_0 + V$ . We assume to adiabatically switch the interactions on and off in the distant past and distant future, respectively, i.e.,

$$H(t) = H_0 + e^{-\epsilon|t|} V, \quad (3.15)$$

where  $\epsilon$  is a positive infinitesimal real number. Under the adiabatic assumption, the interacting ground state  $|GS\rangle$  is obtained from the ground state  $|0\rangle$  of the corresponding non-interacting system as

$$|GS\rangle = \mathcal{U}(0, -\infty)|0\rangle. \quad (3.16)$$

Moreover, one expects that

$$\mathcal{U}(+\infty, -\infty)|0\rangle = e^{i\phi}|0\rangle, \quad (3.17)$$

i.e., the time evolution of the non-interacting ground state upon adiabatic switching first on and then off the interactions brings the system back into the state  $|0\rangle$ , up to a phase factor  $e^{i\phi}$ . The idea behind Eqs. (3.16) and (3.17) is that the slow adiabatic perturbation keeps the system in its evolving ground state at all times. From Eq. (3.17) and the normalization of non-interacting ground state  $\langle 0|0\rangle = 1$ , we can write the phase factor as

$$e^{i\phi} = \langle 0|\mathcal{U}(+\infty, -\infty)|0\rangle. \quad (3.18)$$

Accordingly, Eq. (3.14) becomes

$$\begin{aligned} \langle GS|O|GS\rangle &= \langle 0|\mathcal{U}(-\infty, 0)O\mathcal{U}(0, -\infty)|0\rangle = e^{-i\phi}\langle 0|e^{i\phi}\mathcal{U}(-\infty, 0)O\mathcal{U}(0, -\infty)|0\rangle \\ &= \frac{\langle 0|\mathcal{U}(+\infty, -\infty)\mathcal{U}(-\infty, 0)O\mathcal{U}(0, -\infty)|0\rangle}{\langle 0|\mathcal{U}(+\infty, -\infty)|0\rangle} = \frac{\langle 0|\mathcal{U}(+\infty, 0)O\mathcal{U}(0, -\infty)|0\rangle}{\langle 0|\mathcal{U}(+\infty, -\infty)|0\rangle}, \end{aligned} \quad (3.19)$$

where we used Eqs. (3.16) and (3.18) and the group property for the evolution operator  $\mathcal{U}(t_1, t_2)\mathcal{U}(t_2, t_3) = \mathcal{U}(t_1, t_3)$ . The result of this procedure is that one needs to consider only the forward evolution  $\mathcal{U}(-\infty, +\infty)$  from the distant past to the distant future, as it is evident from the expression of the numerator in the last equality of Eq. (3.19): the evolution is from  $t = -\infty$  towards  $t = 0$ , where the observable  $O$  is evaluated, and then it continues to the distant future  $t = +\infty$ .

In non-equilibrium situation the procedure which take to Eq. (3.19) does not work. If the

Hamiltonian  $H(t)$  contains non-adiabatic time-dependent external fields the evolution drives the system away from the instantaneous ground state. Even if all such fields are eventually switched off in the distant future, there is no guarantee that the system returns to its initial ground state: acting with the operator  $\mathcal{U}(+\infty, -\infty)$  on the initial ground state results in an unknown superposition of excited states. As a result, the backward evolution  $\mathcal{U}(-\infty, t)$  cannot be eliminated and therefore, as it can be seen from Eq. (3.13), the evolution is along the closed time contour  $\mathcal{C}_t$  depicted in Fig. 3.2, which stretches from the distant past  $t = -\infty$  to the time  $t$ , where the observable  $O$  is evaluated, and then back to  $t = -\infty$ .

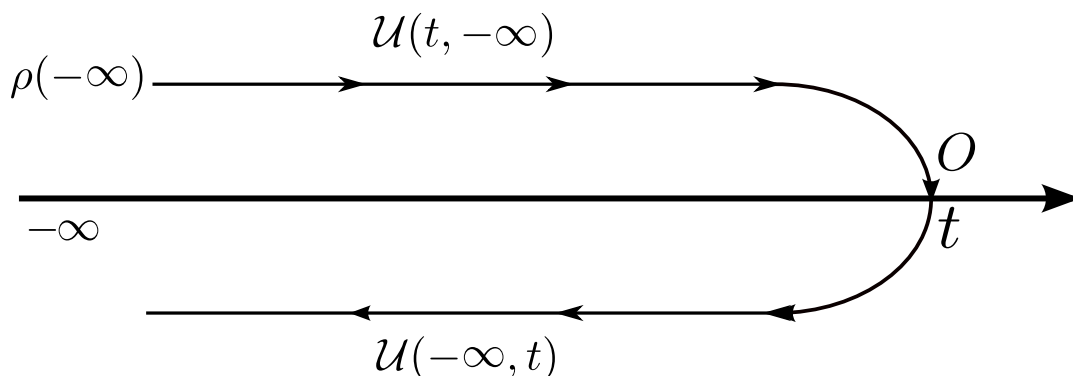


**Figure 3.2:** The closed time contour  $\mathcal{C}_t$  is illustrated. We consider the system to be driven out of equilibrium by a time-dependent perturbation  $V(t)$ ; in order to evaluate the expectation value of an observable  $O$  we need to evolve the initial state, specified by the density matrix  $\rho(-\infty)$ , along the forward branch from  $t = -\infty$  toward  $t$ , where the observable  $O$  is evaluated, and then back to the time  $t = -\infty$  (see Eq. (3.13)). In equilibrium situation, it is possible to reduce the evolution along the contour to real-time axis one using the adiabatic theorem (see Eqs. (3.16), (3.17) and (3.19)). On the other hand, in non-equilibrium situation the adiabatic does not hold and the contour evolution is necessary.

### 3.2.2 Green's function and non-equilibrium diagrammatics

As in the case of systems in equilibrium [52, 53], we define the Green's function from which we can obtain the physically relevant observables of the many-body system. However, as it is clear from the discussion above, we need to work on the closed time contour and we are thus led to study the contour-ordered Green's function  $G^c$ , also called propagator, defined as

$$G^c(1, 2) \equiv -i \left\langle \mathcal{T}_{\mathcal{C}}(\psi_H(1)\psi_H^\dagger(2)) \right\rangle = -i \text{Tr} \left[ \mathcal{T}_{\mathcal{C}}(\psi_H(1)\psi_H^\dagger(2))\rho(-\infty) \right], \quad (3.20)$$

where  $\psi_H, \psi_H^\dagger$  are the annihilation/creation field operators evolved in the Heisenberg representation according to the Hamiltonian (3.7), while we introduced the condensed notation  $i = (x_i, \tau_i)$  and promoted the temporal variable  $\tau$  to belong to the contour. In the following we refer by  $\tau_i$  to a time variable on the contour and by  $t_i$  to the corresponding real time variable (see Fig. 3.3). A contour ordering operator  $\mathcal{T}_{\mathcal{C}}$  has been introduced, which orders operators according to the position of their contour-time

argument on the closed contour; for example, for the case of two contour times,

$$\mathcal{T}_{\mathcal{C}}(\psi(\tau_1)\psi^\dagger(\tau_2)) = \begin{cases} \psi(\tau_1)\psi^\dagger(\tau_2), & \tau_1 \stackrel{\mathcal{C}}{>} \tau_2, \\ \pm\psi^\dagger(\tau_2)\psi(\tau_1), & \tau_2 \stackrel{\mathcal{C}}{>} \tau_1, \end{cases} \quad (3.21)$$

where the upper (lower) sign is for bosons (fermions) respectively. The notation  $\stackrel{\mathcal{C}}{\geq}$  for ordering along the contour has been introduced; for example,  $\tau_1 \stackrel{\mathcal{C}}{>} \tau_2$  means that  $\tau_1$  is further along the contour  $\mathcal{C}$  than  $\tau_2$  irrespective of their corresponding numerical values on the real axis and the symbol  $\stackrel{\mathcal{C}}{<}$  is defined analogously. We also introduce lesser  $G^{c,<}$  and greater  $G^{c,>}$  quantities for the contour ordered Green's function

$$G^{c,<}(1, 2) = G^c(1 \stackrel{\mathcal{C}}{<} 2), \quad (3.22)$$

$$G^{c,>}(1, 2) = G^c(1 \stackrel{\mathcal{C}}{>} 2). \quad (3.23)$$

It is possible to prove [48] that the Heisenberg evolution  $O_H(t)$  of an operator  $O$  can be expressed on closed contour form as

$$O_H(t) = \mathcal{T}_{\mathcal{C}_t} \left[ e^{-i \int_{\mathcal{C}_t} d\tau V_{H_0}(\tau)} O_{H_0}(t) \right], \quad (3.24)$$

where  $\mathcal{C}_t$  is the contour depicted in Fig. 3.2 stretching from  $t = -\infty$  to  $t$  and back again to  $t = -\infty$  and  $V_{H_0}(t)$  denotes the perturbation evolved in the Heisenberg representation according to the non-interacting Hamiltonian  $H_0$ . Using Eq. (3.24) we can write the contour-ordered Green's function in Eq. (3.20) as [48]

$$G^c(1, 2) = -i \text{Tr} \left[ \mathcal{T}_{\mathcal{C}} \left( e^{-i \int_{\mathcal{C}} d\tau V_{H_0}(\tau)} \psi_{H_0}(1)\psi_{H_0}^\dagger(2) \right) \rho(-\infty) \right], \quad (3.25)$$

and the contour  $\mathcal{C}$ , depicted in Fig. 3.3, stretches from  $t = -\infty$  to  $t = \min(t_1, t_2)$  and back to  $t = -\infty$  and then forward to  $\max(t_1, t_2)$  before finally returning back to  $t = -\infty$ . The contributions from the hatched parts in Fig. 3.3 cancel because for this part the field operators are not involved and a closed contour appears which gives the unit operator, or equivalently  $\mathcal{U}(t_1, -\infty)\mathcal{U}(-\infty, t_1) = \mathbf{1}$ . By the same argument, it is possible to extend the backward and forward branches of the contour to the infinite future  $t = +\infty$  obtaining the so-called Schwinger-Keldysh or real-time contour, which we illustrate in Fig. 3.4. We now assume that in the distant past  $t = -\infty$  the system was in thermal equilibrium with a density matrix

$$\rho(-\infty) = \rho_{th} = \frac{e^{-\beta H_0}}{Z}. \quad (3.26)$$

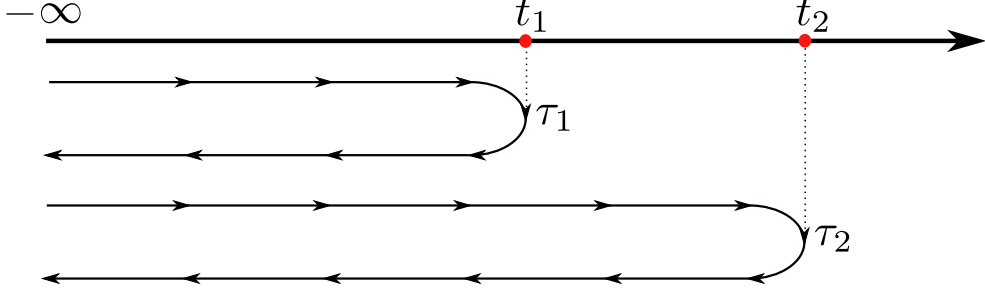


**Figure 3.3:** Contour  $\mathcal{C}$  stretches from  $t = -\infty$  to  $\min(t_1, t_2)$  and back to  $t = -\infty$  and then forward to  $\max(t_1, t_2)$  before finally returning back to  $t = -\infty$ . The contributions from the hatched parts cancel because the field operators are not involved in this part of the contour and so it gives the unit operator. We denote by  $\tau_i$  the time variable belonging to the contour (blue dot) and by  $t_i$  the associated variable on the real-axis (red dot).

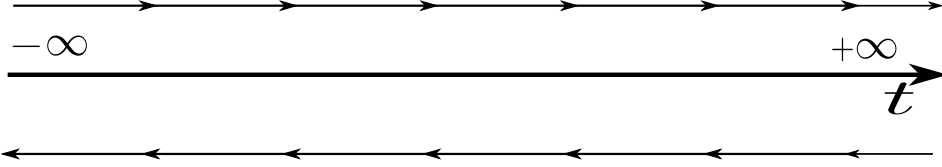


**Figure 3.4:** The Keldysh contour stretches from the far past  $t = -\infty$  to the distant future  $t = +\infty$  and back.

The contour-ordered Green's function takes the final form

$$\begin{aligned}
 G^c(1, 2) &= -i \text{Tr} \left[ \mathcal{T}_{\mathcal{C}} \left( e^{-i \int_{\mathcal{C}} d\tau V_{H_0}(\tau)} \psi_{H_0}(1) \psi_{H_0}^\dagger(2) \right) \rho_{th} \right] \\
 &= -i \left\langle \mathcal{T}_{\mathcal{C}} \left( e^{-i \int_{\mathcal{C}} d\tau V_{H_0}(\tau)} \psi_{H_0}(1) \psi_{H_0}^\dagger(2) \right) \right\rangle \\
 &= -i \frac{\left\langle \mathcal{T}_{\mathcal{C}} \left( e^{-i \int_{\mathcal{C}} d\tau V_{H_0}(\tau)} \psi_{H_0}(1) \psi_{H_0}^\dagger(2) \right) \right\rangle}{\left\langle \mathcal{T}_{\mathcal{C}} e^{-i \int_{\mathcal{C}} d\tau V_{H_0}(\tau)} \right\rangle},
 \end{aligned} \tag{3.27}$$

where in the last equality we introduced the trivial factor

$$\left\langle \mathcal{T}_{\mathcal{C}} e^{-i \int_{\mathcal{C}} d\tau V_{H_0}(\tau)} \right\rangle = 1, \tag{3.28}$$

in order to make Eq. (3.27) structurally equivalent to the equilibrium case [52, 53]. We have eliminated the complicated time evolution governed by the full Hamiltonian  $H(t)$  replacing it with simpler evolution determined by the non-interacting Hamiltonian  $H_0$ . We take advantage of this procedure because we can now apply Wick's theorem [48, 54], which applies only to quadratic Hamiltonians as  $H_0$ . Wick's theorem states that the expectation value of a contour-ordered string of operators  $\alpha$ , evolving with quadratic

Hamiltonian, can be obtained as

$$\langle \mathcal{T}_{\mathcal{C}} [\alpha_{H_0}(\tau_{2n}) \alpha_{H_0}(\tau_{2n-1}) \dots \alpha_{H_0}(\tau_2) \alpha_{H_0}(\tau_1)] \rangle = \sum_{\text{a.p.p}} \prod_{i \neq j} (\pm)^{\zeta_P} \langle \mathcal{T}_{\mathcal{C}} [\alpha_{H_0}(\tau_i) \alpha_{H_0}(\tau_j)] \rangle, \quad (3.29)$$

where the sum is over all possible pairs (a.p.p) of indices  $\{1, 2, \dots, 2n\}$ ,  $\alpha$  can be either a creation or an annihilation operator and the quantum statistical factor  $(\pm)^{\zeta_P}$  counts the number of transpositions relating the orderings on the two sides (upper sign for bosonic operators and lower sign for fermionic ones). By applying repeatedly Wick's theorem, we can construct the perturbative expansion of the contour ordered Green's function. Writing down the  $n$ -th order contribution from the expansion of the exponential in Eq. (3.27) containing the interaction, and employing Eq. (3.29), we obtain an expression for the full contour propagator  $G^c(1, 2)$  involving only the free contour propagator  $G_0^c(1, 2) = -i \langle \mathcal{T}_{\mathcal{C}} (\psi_{H_0}(1) \psi_{H_0}(2)) \rangle$  and the interaction vertices. Accordingly, non-equilibrium and equilibrium formalism are structurally equivalent, the only difference being the replacement of time integrals running on the real axis with contour ones. As in the equilibrium case, we can express the perturbative expansion of  $G^c(1, 2)$  diagrammatically through Feynman diagrams<sup>1</sup> and obtain the Dyson equation for the full contour propagator [48–51]:

$$\begin{aligned} G^c(1, 2) &= G_0^c(1, 2) + \int dx_3 \int_{\mathcal{C}} d\tau_3 \int dx_4 \int_{\mathcal{C}} d\tau_4 G_0^c(1, 3) \Sigma^c(3, 4) G^c(4, 2) \\ &= G_0^c(1, 2) + G_0^c(1, 3) \otimes \Sigma^c(3, 4) \otimes G^c(4, 2) \\ &= G_0^c(1, 2) + G^c(1, 3) \otimes \Sigma^c(3, 4) \otimes G_0^c(4, 2), \end{aligned} \quad (3.30)$$

where the symbol  $\otimes$  is understood as a convolution product, the subscript "0" indicates that the corresponding quantity refers to the non-interacting theory and all the quantities are evaluated along the contour. The function  $\Sigma^c$  is called (contour) self-energy and its expression depends on the interaction  $V(t)$  chosen. In Fig. 3.5 Dyson equation (3.30) is represented diagrammatically.

### 3.2.3 Langreth theorem

We now present a technique, based on the Langreth theorem, which allows us to convert the integrals along the contour into integrals on the real-time axis. In a generic perturbative expansion, one encounters, e.g., contour integrals of the form

$$D(\tau_1, \tau_2) = \int_{\mathcal{C}} d\tau A(\tau_1, \tau) B(\tau, \tau_2) = A(\tau_1, \tau) \otimes B(\tau, \tau_2), \quad (3.31)$$

where the contour  $\mathcal{C}$  can be the one depicted in Fig. 3.3 or Fig. 3.4. On this specific example, we illustrate the procedure for the associated lesser quantity  $D^<(\tau_1, \tau_2)$  in which, according to Eq. (3.22), we have  $\tau_1 \stackrel{\mathcal{C}}{<} \tau_2$ . First of all it is convenient to deform

<sup>1</sup>As in equilibrium formalism, the disconnected Feynman diagrams originating in the numerator of  $G^c$  are canceled by the vacuum diagrams from the denominator (see Eq. (3.27)).

$$\begin{aligned}
\text{Diagram of } G^c &= \text{Diagram of } G_0^c + \text{Diagram of } G_0^c \text{ with } \Sigma^c & \sum^c \text{Diagram of } G^c \\
&= \text{Diagram of } G_0^c + \text{Diagram of } G^c \text{ with } \Sigma^c & \sum^c \text{Diagram of } G_0^c
\end{aligned}$$

**Figure 3.5:** Diagrammatic representation of Dyson equation for the contour ordered Green's function  $G^c$ . The double arrow represents the full contour Green's function  $G^c$ , the single arrow the non-interacting Green's function  $G_0^c$  and the red circle the self-energy  $\Sigma^c$ .

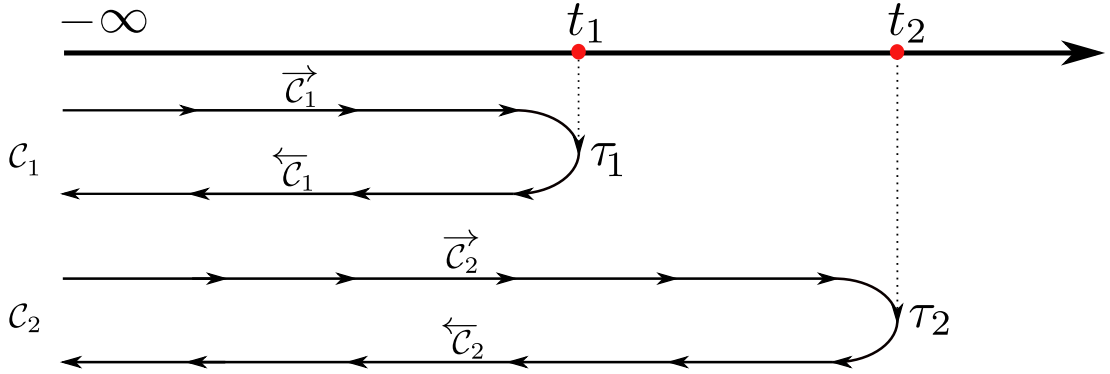


**Figure 3.6:** We write the contour  $\mathcal{C}$ , illustrated in Fig. 3.3 or Fig. 3.4, as  $\mathcal{C} = \mathcal{C}_1 + \mathcal{C}_2$ , where  $\mathcal{C}_i$ , with  $i = 1, 2$ , is the path going from  $t = -\infty$  to  $t = t_i$  and back. Each contour  $\mathcal{C}_i$  is then split into the forward branch  $\vec{\mathcal{C}}_i$ , from  $t = -\infty$  to  $t = t_i$ , and the backward branch  $\overleftarrow{\mathcal{C}}_i$ , from  $t = t_i$  to  $t = -\infty$ .

the contour  $\mathcal{C}$  into the equivalent contour  $\mathcal{C}_1 + \mathcal{C}_2$  as depicted in Fig. 3.6.

Equation (3.31), with  $\tau_1 \stackrel{c}{<} \tau_2$ , becomes

$$\begin{aligned}
D^<(\tau_1, \tau_2) &= \int_{\mathcal{C}_1} d\tau A(\tau_1, \tau)B(\tau, \tau_2) + \int_{\mathcal{C}_2} d\tau A(\tau_1, \tau)B(\tau, \tau_2) \\
&= \int_{\mathcal{C}_1} d\tau A(\tau_1, \tau)B^<(\tau, \tau_2) + \int_{\mathcal{C}_2} d\tau A^<(\tau_1, \tau)B(\tau, \tau_2),
\end{aligned} \tag{3.32}$$

because on the contour  $\mathcal{C}_1$  one has  $\tau \stackrel{c_1}{<} \tau_2$ , and, analogously,  $\tau_1 \stackrel{c_2}{<} \tau$  on the contour  $\mathcal{C}_2$ . By splitting the contours into the forward and backward parts  $\vec{\mathcal{C}}_i$  and  $\overleftarrow{\mathcal{C}}_i$ , respectively,

and by using the contour ordering on them, one has

$$D^<(\tau_1, \tau_2) = \int_{\vec{\mathcal{C}}_1} d\tau A^>(\tau_1, \tau) B^<(\tau, \tau_2) + \int_{\overleftarrow{\mathcal{C}}_1} d\tau A^<(\tau_1, \tau) B^<(\tau, \tau_2) \\ + \int_{\vec{\mathcal{C}}_2} d\tau A^<(\tau_1, \tau) B^<(\tau, \tau_2) + \int_{\overleftarrow{\mathcal{C}}_2} d\tau A^<(\tau_1, \tau) B^>(\tau, \tau_2). \quad (3.33)$$

Parameterizing the forward and backward contours as ( $i = 1, 2$ )

$$\vec{\mathcal{C}}_i = t \quad \text{with} \quad t \in [-\infty, t_i], \quad (3.34)$$

$$\overleftarrow{\mathcal{C}}_i = t \quad \text{with} \quad t \in [t_i, -\infty], \quad (3.35)$$

and noting that the contour variables  $\tau_i$  can now be identified by their corresponding values  $t_i$  on the real-time axis, Eq. (3.33) becomes

$$D^<(t_1, t_2) = \int_{-\infty}^{t_1} dt [A^>(t_1, t) - A^<(t_1, t)] B^<(t, t_2) + \int_{-\infty}^{t_2} dt A^<(t_1, t) [B^<(t_1, t) - B^>(t_1, t)] \\ = \int_{-\infty}^{+\infty} dt \theta(t_1 - t) [A^>(t_1, t) - A^<(t_1, t)] B^<(t, t_2) \\ + \int_{-\infty}^{+\infty} dt \theta(t_2 - t) A^<(t_1, t) [B^<(t_1, t) - B^>(t_1, t)]. \quad (3.36)$$

Introducing the retarded function

$$A^R(t_1, t_2) = \theta(t_1 - t_2) [A^>(t_1, t_2) - A^<(t_1, t_2)], \quad (3.37)$$

and the advanced function

$$A^A(t_1, t_2) = \theta(t_2 - t_1) [A^<(t_1, t_2) - A^>(t_1, t_2)], \quad (3.38)$$

one eventually finds the rule to express the lesser quantity  $D^<$  in Eq. (3.31) as

$$D^< = A^R(t_1, t) \circ B^<(t, t_2) + A^<(t_1, t) \circ B^A(t, t_2), \quad (3.39)$$

where  $\circ$  symbolizes convolution product in real time, i.e., integration over the internal real-time variable  $t$  from minus infinity to plus infinity. We report in table 3.1 other useful rules which can be proved analogously to Eq. (3.39). These equivalent expressions - known as Langreth theorem- allow one to turn any contour ordered quantity, such as the contour ordered Green's function we are interested in, into products of real-time quantities.

Contour	Real axis
$D = A \otimes B$	$D^{\gtrless} = A^R \circ B^{\gtrless} + A^{\gtrless} \circ B^A$ $D^R = A^R \circ B^R$ $D^A = A^A \circ B^A$
$D = A \otimes B \otimes C$	$D^{\gtrless} = A^R \circ B^R \circ C^{\gtrless} + A^R \circ B^{\gtrless} \circ C^A + A^{\gtrless} \circ B^A \circ C^A$

**Table 3.1:** List of rules based on Langreth theorem in order to express contour integrals in ones along real-time axis. On the left column we report quantities evaluated along the contour and on the right column the corresponding quantities on the real-axis. The symbol  $\otimes$  ( $\circ$ ) indicates contour (real-axis) convolution integral [48, 49].

### 3.2.4 Kinetic equations

Applying the last relation reported in table 3.1 to the Dyson equation (3.30), we can rewrite it for the real-time Green's function as

$$\begin{aligned}
G^{\gtrless} &= G_0^{\gtrless} + G_0^R \circ \Sigma^R \circ G^{\gtrless} + G_0^R \circ \Sigma^{\gtrless} \circ G^A + G_0^{\gtrless} \circ \Sigma^A \circ G^A \\
&= G_0^{\gtrless} + G^R \circ \Sigma^R \circ G_0^{\gtrless} + G^R \circ \Sigma^{\gtrless} \circ G_0^A + G^{\gtrless} \circ \Sigma^A \circ G_0^A.
\end{aligned} \tag{3.40}$$

We now express this equation in integro-differential form; the equation of motion for the Green's function are

$$(i\partial_t - h_0) G_0^{R/A}(t, t') = \delta(t - t'), \tag{3.41a}$$

$$(i\partial_t - h_0) G_0^{<, >}(t, t') = 0, \tag{3.41b}$$

$$G_0^{R/A}(t, t') (-i\partial_{t'} - h_0) = \delta(t - t'), \tag{3.41c}$$

$$G_0^{<, >}(t, t') (-i\partial_{t'} - h_0) = 0, \tag{3.41d}$$

where  $h_0$  denotes the single-particle Hamiltonian, i.e.,  $H_0 = \sum_i h_0 \psi^\dagger(i) \psi(i)$ . By acting with the operator  $(i\partial_t - h_0)$  from the left of the first equality in Eq. (3.40) and from the right of the second equality with  $(-i\partial_{t'} - h_0)$ , we obtain the Dyson equation for the real-time Green function in integro-differential form

$$\begin{aligned}
i\partial_t G^{\gtrless}(t, t') &= h_0 G^{\gtrless}(t, t') + \int_{-\infty}^{+\infty} dt'' [\Sigma^{\gtrless}(t, t'') G^A(t'', t') + \Sigma^R(t, t'') G^{\gtrless}(t'', t')], \\
-i\partial_{t'} G^{\gtrless}(t, t') &= G^{\gtrless}(t, t') h_0 + \int_{-\infty}^{+\infty} dt'' [G^R(t, t'') \Sigma^{\gtrless}(t'', t') + G^{\gtrless}(t, t'') \Sigma^A(t'', t')].
\end{aligned} \tag{3.42}$$

Equation (3.42) is the starting point in order to obtain, in the next Section, a master equation for the noisy quantum Ising chain from which all the relevant physical properties of the system then follow.

### 3.3 Prethermalization in a noisy quantum Ising chain

In this Section we briefly review the results of Ref. [34] about the kinetics of local observables and their correlation functions after a quench of the noisy quantum Ising chain discussed in Sec. 3.1. In order to evaluate these observables, in Sec. 3.3.1 a kinetic equation for the equal time non-equilibrium Green's function is obtained for the quench protocol discussed in Sec. 3.1 and illustrated in Fig. 3.1. This is achieved by deriving within the Keldysh contour technique a master equation, the solution of which eventually provides an analytic expression for the two-time functions of Bogolyubov fermions at equal time. These equations will then be used in order to calculate all the observables of interest and their the non-equilibrium dynamics, as discussed in Sec. 3.3.2. In the following we assume  $J = 1$  and we restore it in the calculations only when it is necessary.

#### 3.3.1 Master equation

Based on the solution of the quantum Ising chain discussed in Sec. 2.2, one can introduce the noise in the transverse field and write the noisy quantum Ising chain Hamiltonian (3.5) as

$$H(g, t) = 2 \sum_{k>0} \Psi_k^\dagger H_k(t) \Psi_k = 2 \sum_{k>0} \Psi_k^\dagger (H_k^0 + V_k(t)) \Psi_k, \quad (3.43)$$

where  $\Psi_k$  is the Nambu spinor (2.25) while, from Eq. (2.24),

$$H_k^0 = (g - \cos k)\sigma^z - (\sin k)\sigma^y \quad \text{and} \quad V_k(t) = \delta g(t)\sigma^z. \quad (3.44)$$

As explained in Sec. 3.2, we can set up a perturbative expansion for the contour ordered Green's function  $G^c(\tau, \tau')$  as

$$\begin{aligned} G^c(\tau, \tau') &= [G_k^c(\tau, \tau')]_{l,m} = -i \left\langle g_0 \left\langle GS \left| \mathcal{T}_C \left( \Psi_{k,l}(\tau) \Psi_{k,m}^\dagger(\tau') \right) \right| GS \right\rangle_{g_0} \right\rangle_{noise} \\ &= -i \left\langle \mathcal{T}_C \left( \Psi_{k,l}(\tau) \Psi_{k,m}^\dagger(\tau') \right) \right\rangle, \end{aligned} \quad (3.45)$$

where  $|GS\rangle_{g_0}$  is the ground state of the unperturbed Ising Hamiltonian (2.1) with  $g = g_0$ , the index  $l = 0, 1$  indicates the  $l$ -th component of the Nambu spinor  $\Psi_k$  and we take the expectation value over the initial pure state  $|GS\rangle_{g_0}$  and then we perform the average over the noise (3.6). The contour Green's function (3.45) satisfies the Dyson equation (3.30) diagrammatically illustrated in Fig. 3.7. In the following we will neglect noise crossed diagrams, computing the self-energy within the so called *self-consistent Born approximation* [49], controlled by the small parameter  $\gamma$

$$\gamma = \frac{\Gamma}{\Delta} \ll 1, \quad (3.46)$$

as illustrated in Fig. 3.7, with  $\Delta = |g - 1|$  half of the gap of the noiseless chain (2.56). This dimensionless parameter is, in a sense, the analogue of  $k_F l \gg 1$  in disordered electron systems, where the typical length scale associated to electron wavefunctions,

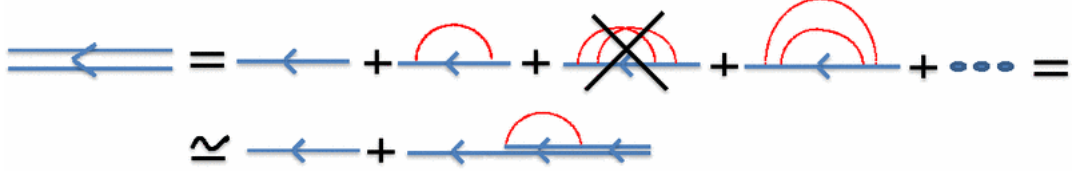


**Figure 3.7:** Diagrammatic representation of the Dyson equation (3.30) satisfied by the contour ordered Green's function (3.45) of the noisy quantum Ising chain. Crossed diagrams are neglected according to the self-consistent Born approximation Eq. (3.49). [34]

$\lambda_F \sim 1/k_F$  ( $k_F$  is the Fermi wave vector), is much smaller than the typical length associated to disorder,  $l$  (the average mean path), and correlations induced by the latter can be disregarded at leading order in  $k_F l \gg 1$ . This physical analogy is at the origin of the approximation  $\Gamma/\Delta \ll 1$ , since  $\Gamma$  and  $\Delta$  play a role analogous to  $l^{-1}$  and  $k_F$ , respectively.

The physically relevant information about the system are encoded in the real-time lesser Green's function  $G^<(t, t')$ , defined as

$$G^<(t, t') = [G_k^<(t, t')]_{l,m} = i \langle \Psi_{k,m}^\dagger(t') \Psi_{k,l}(t) \rangle. \quad (3.47)$$

The Dyson equation for the real-time Green's function can be written as in Eq. (3.42), i.e.,

$$\begin{aligned} i\partial_t G^<(t, t') &= H_k^0 G^<(t, t') + \int dt'' [\Sigma^<(t, t'') G^A(t'', t') + \Sigma^R(t, t'') G^<(t'', t')], \\ -i\partial_{t'} G^<(t, t') &= G^<(t, t') H_k^0 + \int dt'' [G^R(t, t'') \Sigma^<(t'', t') + G^<(t, t'') \Sigma^A(t'', t')], \end{aligned} \quad (3.48)$$

where  $H_k^0$  is given by Eq. (3.44).

Within the self-consistent Born approximation, the self energies are obtained by considering the lowest order self-energy diagram, i.e., the sunset diagram, and replacing in it the non-interacting propagator  $G_0$  with the full one  $G$ , as it is diagrammatically illustrated in Fig. 3.7:

$$\begin{aligned} \Sigma_{t,t'}^< &= \frac{\Gamma}{2} \delta(t-t') \sigma^z G_{t,t'}^< \sigma^z \\ \Sigma_{t,t'}^{R,A} &= \frac{\Gamma}{2} \delta(t-t') \sigma^z G_{t,t'}^{R,A} \sigma^z = \mp i \frac{\Gamma}{4} \delta(t-t') \mathbf{1}. \end{aligned} \quad (3.49)$$

The last equality in Eq. (3.49) follows from the fact that  $G_{t,t}^{R/A} = \mp i/2$ , as a consequence of the definitions (3.37) and (3.38), of the following convention for the step function  $\theta$ , i.e.,

$$\theta(x) = \begin{cases} 0, & x < 0, \\ 1/2, & x = 0, \\ 1, & x > 0, \end{cases} \quad (3.50)$$

and of the fundamental identity

$$\begin{aligned} G^<(t, t) - G^>(t, t) &= i\langle \Psi_{k,l}^\dagger(t) \Psi_{k,m}(t) \rangle + i\langle \Psi_{k,m}(t) \Psi_{k,l}^\dagger(t) \rangle = i \left\langle \left\{ \Psi_{k,l}^\dagger(t), \Psi_{k,m}(t) \right\} \right\rangle \\ &= i\delta_{l,m} = i\mathbf{1}. \end{aligned} \quad (3.51)$$

In the last line we used the anticommutation relation for Nambu spinors, i.e.,  $\{\Psi_{k,l}, \Psi_{k',m}^\dagger\} = \delta_{k,k'}\delta_{l,m}$ . In order to solve Eq. (3.48) we substitute Eq. (3.49) into it, subtract the two resulting equations and take the limit  $t \rightarrow t'$ ; defining the density matrix

$$\rho_k(t) = -iG_k^<(t, t) \quad (3.52)$$

we finally obtain the master equation [34]

$$\partial_t \rho_k = -i[H_k^0, \rho_k] + \frac{\Gamma}{2}(\sigma^z \rho_k \sigma^z - \rho_k), \quad (3.53)$$

where  $[H_k^0, \rho_k]$  on the right hand side is responsible for the free dynamics while the second one contains information about the dissipation due to the noise. We now apply to Eq. (3.53) a Bogolyubov rotation  $\mathcal{R}(\theta_k^g)$  (see Eqs. (2.26) and (2.28)), which diagonalizes the Ising model in the basis of the Bogolyubov fermions  $\gamma_k^g$ , finding

$$\partial_t \rho_k = -i[\widetilde{H}_k^0, \rho_k] + \frac{\Gamma}{2}(\sigma' \rho_k \sigma' - \rho_k), \quad (3.54)$$

where

$$\widetilde{H}_k^0 = \mathcal{R}^\dagger(\theta_k^g) H_k^0 \mathcal{R}(\theta_k^g) = \epsilon_k^g \sigma^z, \quad (3.55)$$

$$\sigma' = \mathcal{R}^\dagger(\theta_k^g) \sigma^z \mathcal{R}(\theta_k^g) = \cos(2\theta_k^g) \sigma^z + \sin(2\theta_k^g) \sigma^y. \quad (3.56)$$

The density matrix  $\rho_k$  is consequently expressed in the basis of the Bogolyubov fermions,

$$\rho_k(t) = \begin{pmatrix} \langle \gamma_k^{g\dagger}(t) \gamma_k^g(t) \rangle & \langle \gamma_k^{g\dagger}(t) \gamma_{-k}^{g\dagger}(t) \rangle \\ \langle \gamma_{-k}^g(t) \gamma_k^g(t) \rangle & \langle \gamma_{-k}^g(t) \gamma_{-k}^{g\dagger}(t) \rangle \end{pmatrix}, \quad (3.57)$$

where  $\langle \gamma_k^{g\dagger} \gamma_k^g \rangle$  are the populations of the energy levels of the noisy Hamiltonian with momentum  $k$  while  $\langle \gamma_k^{g\dagger} \gamma_{-k}^{g\dagger} \rangle$  represent the coherences.

Before solving Eq. (3.54), let us comment on the properties of the noise. In the base diagonalizing the final Hamiltonian,  $H_k(t)$  appears as

$$\begin{aligned} H_k(t) &= \epsilon_k^g \sigma^z + \delta g(t) (\sigma^z \cos 2\theta_k^g + \sigma^y \sin 2\theta_k^g) \\ &= \epsilon_k^g \sigma^z + \delta g_k^z(t) \sigma^z + \delta g_k^y(t) \sigma^y, \end{aligned} \quad (3.58)$$

where  $\delta g_k^z(t)$  and  $\delta g_k^y(t)$  satisfy

$$\begin{aligned}\langle \delta g_k^z(t) \delta g_k^z(t') \rangle &= \frac{\Gamma}{2} (\cos 2\theta_k^g)^2 \delta(t-t'), \\ \langle \delta g_k^y(t) \delta g_k^y(t') \rangle &= \frac{\Gamma}{2} (\sin 2\theta_k^g)^2 \delta(t-t'),\end{aligned}\tag{3.59}$$

where it should be easy to see that our model is equivalent to the QIC perturbed by two  $k$ -dependent delta correlated noises, one along the  $z$  direction and the other one along  $y$ . Moreover the noise along the  $y$  direction is correlated to the noise along the  $z$  direction

$$\langle \delta g_k^z(t) \delta g_k^y(t') \rangle = \frac{\Gamma}{2} \sin 2\theta_k^g \cos 2\theta_k^g \delta(t-t').\tag{3.60}$$

The usual way to solve a master equation like (3.54) is to decompose the density matrix  $\rho_k$  in the basis of the Pauli matrices, i.e.,

$$\rho_k = \frac{\mathbf{1}}{2} + \delta f_k \sigma^z + x_k \sigma^x + y_k \sigma^y,\tag{3.61}$$

where  $\delta f_k$  represents the population of the  $k$ -mode while  $x_k, y_k$  the coherences. These coefficients are real, being the density matrix  $\rho_k$  in Eq. (3.57) Hermitian. Upon inserting this decomposition in the master equation (3.54) we end up with a system of differential equations for the coefficients  $\delta f_k, x_k, y_k$  of the density matrix (3.61):

$$\begin{aligned}\partial_t(\delta f_k) &= -\Gamma \sin^2(2\theta_k^g) \delta f_k + \frac{\Gamma}{2} y_k \sin(4\theta_k^g), \\ \partial_t x_k &= -\Gamma x_k - 2\epsilon_k^g y_k, \\ \partial_t y_k &= \frac{\Gamma}{2} \sin(4\theta_k^g) \delta f_k + 2\epsilon_k^g x_k - \Gamma \cos^2(2\theta_k^g) y_k,\end{aligned}\tag{3.62}$$

where  $\theta_k^g$  and  $\epsilon_k^g$  are given in Eqs. (2.28) and (2.31), respectively. In the following we solve this system of equations in the limit  $\gamma = \Gamma/\Delta \ll 1$ , which allows us to neglect  $y$ - $z$  correlations; this approximation is checked numerically for different values of  $k$  in the Brillouin zone. Taking into account the various initial conditions in Eqs. (2.58) and (2.59), corresponding to an extensive amount of energy injected in the system by the quench of the transverse field, we immediately obtain [34]

$$\delta f_k(t) = \left[ \sin^2(\Delta\theta_k) - \frac{1}{2} \right] e^{-\Gamma t \sin^2(2\theta_k^g)},\tag{3.63}$$

where  $\Delta\theta_k$  is given in Eq. (2.38). For the coherences it is convenient to introduce the variable  $z_k = x_k - iy_k$  for which we obtain [34]

$$\partial_t z_k = (-2i\epsilon_k^g - \Gamma) z_k + \Gamma [1 - \cos^2(2\theta_k^g)] \frac{z_k - z_k^*}{2};\tag{3.64}$$

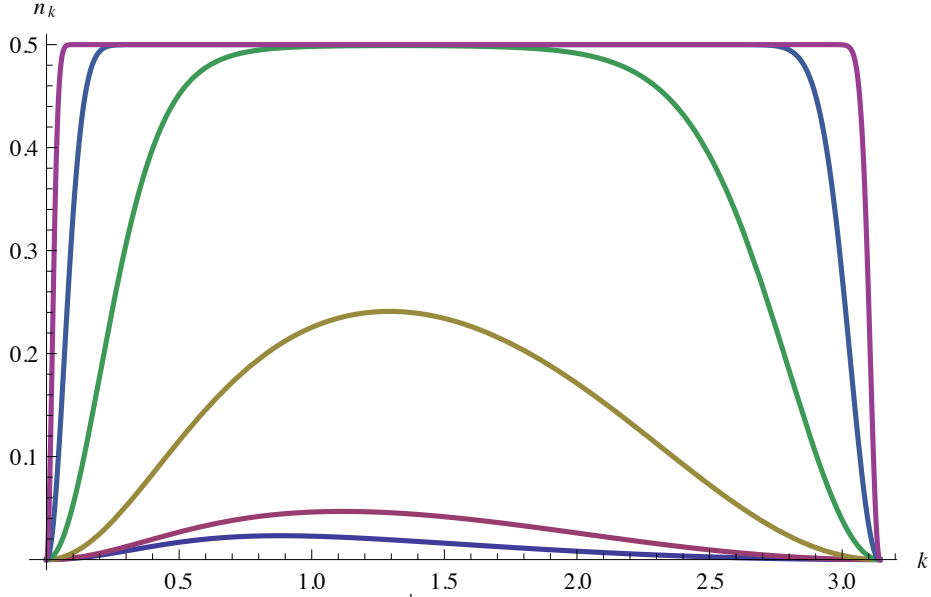


**Figure 3.8:** Populations  $n_k(t) = \langle \gamma_k^{g\dagger}(t) \gamma_k^g(t) \rangle$  of the energy levels of the noisy Hamiltonian (3.5) with momentum  $k$  as a function of wave vector  $k \in [0, \pi]$  at various times after the quench: from bottom to top,  $\Gamma t = 0.1, 1, 10, 10^2, 10^3$  and  $10^4$ . The quench occurs from  $g_0 = 2$  to  $g = 4$ . [Figure taken from Ref. [34]]

from this equation we see that the coherences decay exponentially fast as  $\Gamma t \gg 1$ , as one can see close to  $k \simeq 0$  or  $k \simeq \pi$ :

$$z_k \simeq z_k^0 e^{-2ic_k^g t} e^{-\Gamma t}. \quad (3.65)$$

On the other hand, we see from equation (3.63) that while the populations  $\delta f_k$  of most of the modes relax quickly to the thermal occupation  $n_k \simeq 1/2$  corresponding to infinite temperature on time scales of the order of  $1/\Gamma$ , this relaxation rate vanishes upon approaching the band edges  $k = 0$  and  $k = \pm\pi$  as illustrated in Fig. 3.8.

We report the expression for  $\delta f_k$  and  $z_k$  for  $k \simeq 0$ , as they will be useful later on in the calculation of the leading behavior of physical observables during thermalization dynamics discussed in the next Section:

$$\begin{aligned} \langle \gamma_k^{g\dagger} \gamma_k^g \rangle &= \frac{1}{2} + \frac{1}{2} \left( \frac{k^2}{2\Delta^2} \rho_-^2 - 1 \right) e^{-\Gamma k^2 t / \Delta^2}, \\ \langle \gamma_k^{g\dagger} \gamma_{-k}^{g\dagger} \rangle &= -\frac{ik}{2\Delta} \rho_- e^{-\alpha t - i\beta t}, \end{aligned} \quad (3.66)$$

where  $\rho_- \equiv 1 - \Delta/\Delta_0$  with  $\Delta_0 \equiv |g_0 - 1|$  and

$$\begin{aligned}\alpha &= \Gamma \left[ 1 - \frac{(k/\Delta)^2}{2} \right], \\ \beta &= 2\Delta \left[ 1 + \frac{(k/\Delta)^2}{2} \right].\end{aligned}\tag{3.67}$$

### 3.3.2 Thermalization dynamics of observables

Based on the expressions reported in the previous Section, we are now in the position to investigate the interplay between quench and noise in the time evolution of observables of interest: in particular we focus their dynamics from the initial state towards the asymptotic steady state, which is the infinite temperature state, where all fermion modes are equally occupied with  $n_k = 1/2$ , for all  $k$  in the Brillouin zone. We shall start the analysis by computing the energy absorbed by the system. We will then be concerned with the possible thermalization of the transverse magnetization correlator and, finally, we are going to look for signatures of the noise in the time evolution of the order parameter correlations.

#### Energy absorbed by the quantum Ising chain

The energy  $E(t)$  absorbed by the system during the noisy time-dependent protocol can be expressed as

$$E(t) = \langle \psi(t) | H(g, t) | \psi(t) \rangle\tag{3.68}$$

and this expression is for a certain realization of the noise  $\delta g$  and then it will have to be averaged over the distribution of the noise. The state of the chain at time  $t$ ,  $|\psi(t)\rangle$ , is

$$|\psi(t)\rangle = \mathcal{U}_{H(g,t)}(t, 0) |GS\rangle_{g_0},\tag{3.69}$$

where  $\mathcal{U}_{H(g,t)}(t, 0)$  is given by Eq. (3.11) and we remind that  $|GS\rangle_{g_0}$  is the ground state of the unperturbed Ising Hamiltonian (2.1) with  $g = g_0$  in which the chain is initially prepared. Substituting into Eq. (3.68) the expression for the Hamiltonian Eq. (3.5), we get

$$\begin{aligned}E(t) &= \langle \psi(t) | \left( H_0(g) + \delta g(t) \sum_i \sigma_i^z \right) | \psi(t) \rangle \\ &= \langle \psi(t) | H_0(g) | \psi(t) \rangle + \delta g(t) \langle \psi(t) | \sum_{i=1}^L \sigma_i^z | \psi(t) \rangle,\end{aligned}\tag{3.70}$$

where  $H_0(g)$  is given in Eq. (2.1). Let us now assume that at time  $\tau$  and onwards the noise is turned off. Accordingly, in the thermodynamic limit  $L \rightarrow \infty$ , the total energy

acquired at time  $\tau$  by the system is

$$E(\tau) = L \int_0^\pi \frac{dk}{2\pi} \epsilon_k^g \left( \langle \gamma_k^{g\dagger}(\tau) \gamma_k^g(\tau) \rangle - \langle \gamma_{-k}^g(\tau) \gamma_{-k}^{g\dagger}(\tau) \rangle \right). \quad (3.71)$$

We can now use the expectation values for the two-point functions of the Bogolyubov fermions derived in the previous Section (see Eqs. (3.61) and (3.63)) in order to evaluate this expression as a function of  $\tau$ . By using Eqs. (3.61) and (3.63), Eq. (3.71) can be written as

$$E(\tau) = L \int_0^\pi \frac{dk}{2\pi} 2\epsilon_k^g \delta f_k = -L \int_0^\pi \frac{dk}{2\pi} \epsilon_k^g \cos(2\Delta\theta_k) e^{-\Gamma\tau \sin^2(2\theta_k^g)}. \quad (3.72)$$

At short times  $\tau \ll \Gamma^{-1}$ , the energy  $E(\tau)$  is equal to the one  $E_Q$  injected in an ordinary quench plus small corrections [34]

$$E(\tau) = E_Q + L \int_0^\pi \frac{dk}{2\pi} \epsilon_k^g \cos(2\Delta\theta_k) \sin^2(2\theta_k^g) \Gamma\tau, \quad (3.73)$$

as one can readily verify by expanding the exponential in Eq. (3.72) and where

$$E_Q = -\frac{L}{2\pi} \int_0^\pi dk \epsilon_k^g \cos(2\Delta\theta_k) \quad (3.74)$$

is the energy injected in the system by a sudden quench  $g_0 \mapsto g$  with no noise on the transverse field.

For  $\tau \gg \Gamma^{-1}$ , Eq. (3.72) is actually dominated by the modes with smallest relaxation rate, i.e.,  $k \simeq 0$  and  $k = \pi$ , with the final result [34]

$$E(\tau)_{\Gamma\tau \gg 1} \simeq -\frac{L}{2\sqrt{\pi}} \frac{g^2 + 1}{\sqrt{\Gamma\tau}}. \quad (3.75)$$

Accordingly, the energy approaches its asymptotic value with an asymptotic algebraic behavior  $(\Gamma\tau)^{-1/2}$ , which is the signature of the slow relaxation of the  $k \simeq 0$  and  $k = \pi$  modes.

### Evolution of the spatial density of kinks

An interesting quantity for highlighting the dynamics of thermalization is the spatial density of kinks  $n_{kink}$ , defined as

$$n_{kink} \equiv \frac{1}{2L} \sum_{i=1}^L \langle (1 - \sigma_i^x \sigma_{i+1}^x) \rangle. \quad (3.76)$$

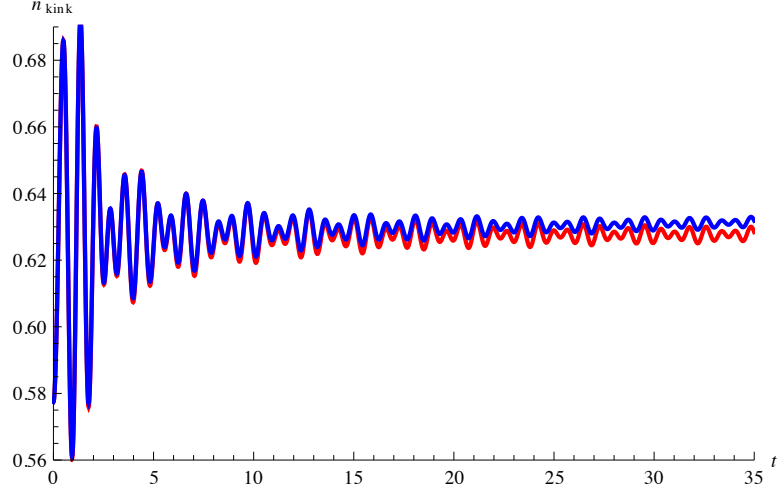


**Figure 3.9:** Density of kinks  $n_{kink}$  as a function of the time  $t$  elapsed after the quench from  $g_0 = 1.1$  to  $g = 4$  in the presence of a noise of strength  $\Gamma = 0.01$ . While the red line shows the value attained by  $n_{kink}$  without noise and predicted by the GGE, the full time evolution (blue line) shows first a saturation towards the GGE value for  $J^{-1} \ll t \ll \Gamma^{-1}$  and then a runaway towards the infinite temperature state. [Figure taken from Ref. [34]]

Simple algebraic manipulations yield [34]

$$\begin{aligned} n_{kink}(t) &= \frac{1}{2L} \sum_k (1 + 2\langle \gamma_k^{g\dagger} \gamma_k \rangle_{g=0}) = \\ &= \frac{1}{2L} \sum_k \left( 2 + 2\delta f_k(t) \cos(2\Delta\alpha_k) + 2y_k(t) \sin(2\Delta\alpha_k) \right). \end{aligned} \quad (3.77)$$

This result has been obtained by expressing the Bogolyubov fermions at  $g = 0$  in terms of fermions diagonalizing the Hamiltonian with  $g \neq 0$ , consequently  $\Delta\alpha_k = \theta_k^{g=0} - \theta_k^g$  is the difference between the two corresponding Bogolyubov angles. It is clear from this expression that the number of kinks  $n_{kink}$  can be written as the sum of two terms,  $n_{kink}(t) \equiv n_{drift}(t) + \Delta n(t)$ , where  $n_{drift}$  due to populations  $\delta f_k$  (plus the constant term) and describing the heating of the system towards the asymptotic steady state at infinite temperature;  $\Delta n(t)$ , instead, is responsible for dephasing, it is exclusively due to coherences, and it is at the origin of an intermediate stage of the dynamics of  $n_{kink}$ , which we shall relate to *prethermalization* [28–30].

It turns out that the dynamics of  $n_{kink}(t)$  towards the asymptotic state can be divided into three stages as summarized in Fig. 3.9:

1. first of all, the system relaxes towards the asymptotic steady state of the QIC after a quench of the transverse field without noise, which is the GGE of the QIC and which accounts for the conserved quantities of the model, i.e., the occupation number of the fermions  $n_k = \gamma_k^{g\dagger} \gamma_k^g$ . This happens through inhomogeneous dephasing, arising from the overlap of a continuum of frequencies in Eq. (3.77) and leading to a  $(Jt)^{-3/2}$  decay in the  $Jt \gg 1$  limit. This result can be easily derived

by applying a stationary phase approximation to Eq. (3.77) for  $Jt \gg 1$  but in the temporal range  $\Gamma t \ll 1$  where the noise is not effective. Though the term *prethermalization* has been introduced for closed quantum many-body systems driven out of equilibrium by a quench, the appearance in the dynamics of an intermediate stage described by a suitable chosen GGE observed here is very similar to what has been found in closed systems [29, 30], justifying the use of this term also in this context.

2. The second stage of the dynamics consists in a noise-induced dephasing, where coherences are suppressed by the noise exponentially in time for  $\Gamma t \gg 1$ , as the leading  $e^{-\Gamma t}$  behavior discussed before indicates.
3. The third stage corresponds to the heating up of the model and an equidistribution of the populations. This drives, e.g., the number of kinks towards the final stage of the dynamics corresponding to an infinite temperature state. This happens following the same  $(\Gamma t)^{-1/2}$  behavior as the energy, and it is due again to the presence of slow relaxing modes dominating the dynamics towards thermalization.

As a last remark, it should be noticed that the appearance of a prethermalization stage strictly depends on the different behaviors of populations and coherences during the dynamics. This implies that whether an observable will show *prethermalization* or not will depend crucially on its expression in the Bogolyubov basis. This is the reason behind the absence of a prethermal stage in the dynamics of  $E(t)$ .

### On-site transverse magnetization

A *prethermal* plateau is also observed in the dynamics of the on-site transverse magnetization  $\langle \sigma_i^z(t) \rangle$ , which possess a similar expression to Eq. (3.77) in the Bogolyubov basis

$$m^z \equiv \langle \sigma_i^z \rangle = - \int_0^\pi \frac{dk}{2\pi} 4 [\delta f_k(t) \cos(2\theta_k^g) - \sin(2\theta_k^g) y_k(t)], \quad (3.78)$$

where  $\delta f_k$  and  $y_k(t)$  are given in Eqs. (3.63) and (3.64), respectively. The prethermal plateau is in correspondence of the expectation value of  $\sigma_i^z$  evaluated in the GGE of the QIC without noise (see Eq. (2.64))

$$\langle \sigma_i^z \rangle_{GGE} = \int_0^\pi \frac{dk}{2\pi} 2 \cos(2\Delta\theta_k) \cos(2\theta_k^g), \quad (3.79)$$

with  $\Delta\theta_k$  given in Eq. (2.38), and it is approached algebraically as  $(Jt)^{-3/2}$ , in the limit  $Jt \gg 1$ , as in a quenched QIC [16]. On the other hand, the on-site transverse magnetization will approach its equilibrium expectation value  $\langle \sigma_i^z \rangle_{T=\infty} = 0$  at infinite temperature as a power law, i.e., as  $(\Gamma t)^{-1/2}$  for  $t \gg \Gamma^{-1}$ , when quantum coherent effects have been already exponentially suppressed by the noise. Accordingly, the non-equilibrium dynamics of this observable is exactly the same as the one observed for the number of kinks. In the next Section we are going to consider two-points correlation

function of the transverse magnetization in order to unveil novel behaviors behind the interplay of noise and quench.

### Correlator of the transverse magnetization

We now investigate the equal-time correlation function of the transverse magnetization, computed at different spin sites

$$C^{zz}(r, t) = \langle \sigma_{i+r}^z(t) \sigma_i^z(t) \rangle - \langle \sigma_i^z(t) \rangle^2. \quad (3.80)$$

Due to translational invariance, for future convenience we can set  $i = 0$ . The expression for  $C^{zz}(r, t)$  can be written as a sum of three terms [34]

$$C^{zz}(r, t) = \langle \sigma_r(t) \sigma_0(t) \rangle_{pop.} + \langle \sigma_r(t) \sigma_0(t) \rangle_{coh.} + \langle \sigma_r(t) \sigma_0(t) \rangle_{mix.}, \quad (3.81)$$

where

$$\begin{aligned} \langle \sigma_r(t) \sigma_0(t) \rangle_{pop.} = & 4 \int_{-\pi}^{\pi} \frac{dk}{2\pi} \int_{-\pi}^{\pi} \frac{dk'}{2\pi} e^{i(k-k')r} \left\{ \sin(2\theta_k^g) \sin(2\theta_{k'}^g) \delta f_k(t) \delta f_{k'}(t) \right. \\ & \left. + \left[ \frac{1}{2} + \cos(2\theta_{k'}^g) \delta f_{k'}(t) \right] \left[ \frac{1}{2} - \cos(2\theta_k^g) \delta f_k(t) \right] \right\}, \end{aligned} \quad (3.82)$$

$$\begin{aligned} \langle \sigma_r(t) \sigma_0(t) \rangle_{coh.} = & 4 \int_{-\pi}^{\pi} \frac{dk}{2\pi} \int_{-\pi}^{\pi} \frac{dk'}{2\pi} e^{i(k-k')r} \left\{ -\sin(2\theta_k^g) \sin(2\theta_{k'}^g) y_k(t) y_{k'}(t) \right. \\ & \left. + [x_k(t) + i y_k(t) \cos(2\theta_k^g)] \times [x_{k'}(t) - i y_{k'}(t) \cos(2\theta_{k'}^g)] \right\}, \end{aligned} \quad (3.83)$$

$$\begin{aligned} \langle \sigma_r(t) \sigma_0(t) \rangle_{mix.} = & 4 \int_{-\pi}^{\pi} \frac{dk}{2\pi} \int_{-\pi}^{\pi} \frac{dk'}{2\pi} e^{i(k-k')r} \left\{ i \delta f_k(t) \sin(2\theta_k^g) [x_{k'}(t) - i y_{k'}(t) \cos(2\theta_{k'}^g)] \right. \\ & - i \delta f_{k'}(t) \sin(2\theta_{k'}^g) [x_k(t) + i y_k(t) \cos(2\theta_k^g)] \\ & \left. + \sin(2\theta_k^g) \delta f_{k'}(t) y_k(t) \cos(2\theta_{k'}^g) + \sin(2\theta_{k'}^g) \delta f_k(t) y_{k'}(t) \cos(2\theta_k^g) \right\}. \end{aligned} \quad (3.84)$$

Looking the expression of the coherences in Eq. (3.64), it should be clear that we can extract from the integrals in Eqs. (3.83) and (3.84) a prefactor with a purely time dependent exponential decay in time, which allows us to neglect these terms for  $t \gg \Gamma^{-1}$ , as

$$\begin{aligned} \langle \sigma_r(t) \sigma_0(t) \rangle_{coh.} & \propto e^{-2\Gamma t}, \\ \langle \sigma_r(t) \sigma_0(t) \rangle_{mix.} & \propto e^{-\Gamma t}. \end{aligned} \quad (3.85)$$

The behavior of the equal-time correlation function of the transverse magnetization is analyzed in great detail in Ref.[34], where one can find all the necessary details of the calculation. The final result, illustrated in Fig. 3.10, is that the dynamics is characterized by the propagation of two “wave” fronts: at earlier times,  $t \ll \Gamma^{-1}$ , a first front

appears at  $r \simeq Jt$ , controlled by the velocity of the quasi-particles emitted after a quench ( $v \simeq J$ ), which separates unconnected space-time regions,  $r \gg Jt$ , where  $\sigma_i^z$  correlations behave as in the QIC without quench, from a region of space-time connected points  $r \ll Jt$ , where the stationary correlation function is the same as in a quenched QIC [16]. This is consistent with the Lieb-Robinson bound [55], as already found for other systems [56] and by various authors for the sudden quench of the QIC [16, 38]. The effects of the noise are hardly relevant at early times, as observed for the evolution of  $n_{kink}$ .

At longer times  $t \gg \Gamma^{-1}$ , instead, we find a diffusive spreading of correlations for  $\Delta r \ll \Gamma t$ , as the square of distance  $r$  scales as the time  $t$ , while for unconnected space-time points with  $\Delta r \gg \Gamma t$  the stationary correlation function crosses over to the asymptotic expression of the correlation function in a quenched QIC without noise [16]. This scenario can be summarized in the following expressions for the correlation function [34]:

$$C^{zz}(r, t \ll \Gamma^{-1}) \simeq \begin{cases} \frac{1}{2\pi r^2} \exp[-2\Delta_0 r], & r \gg vt, \\ \frac{1}{r^\alpha} \exp[-r/\xi_z], & r \ll vt, \end{cases} \quad (3.86)$$

where  $\xi_z$  is the correlation length associated with a simple *quantum quench* of the transverse field and  $\alpha$  an exponent, calculated in Ref. [16]. At long times  $t \gg \Gamma^{-1}$ , the noise becomes relevant and the second crossover, between the quenched QIC correlation function and a *diffusive* behavior emerges

$$C^{zz}(r, t \gg \Gamma^{-1}) \simeq \begin{cases} \frac{1}{r^\alpha} \exp[-r/\xi_z], & \gamma t \ll r \ll vt, \\ -\frac{1}{\pi} \frac{\Delta^2}{4} \frac{1}{\Gamma t} \exp\left[-\frac{(\Delta r)^2}{2\Gamma t}\right], & r \ll \gamma t, \end{cases} \quad (3.87)$$

where  $\gamma = \Gamma/\Delta$  is the small parameter introduced in Eq. (3.46), which controls the accuracy of the self-consistent Born approximation (3.49).

### Correlator of the order parameter

The last observable analyzed in Ref. [34] is the order parameter correlation function  $C^{xx}(r, t)$  at equal-times, defined as

$$C^{xx}(r, t) = \langle \sigma_{i+r}^x(t) \sigma_i^x(t) \rangle - \langle \sigma_i^x(t) \rangle^2, \quad (3.88)$$

in order to see if the diffusive behavior observed for correlation of the transverse magnetization is a general signature of the effect of the noise in correlation functions. The way to compute this function is to express it in the form of a Toeplitz determinant and to evaluate it for spins at a separation  $r \rightarrow \infty$  by using the Fisher-Hartwig conjecture (see Ref. [34] for details). For a quench without external noise the stationary correlation

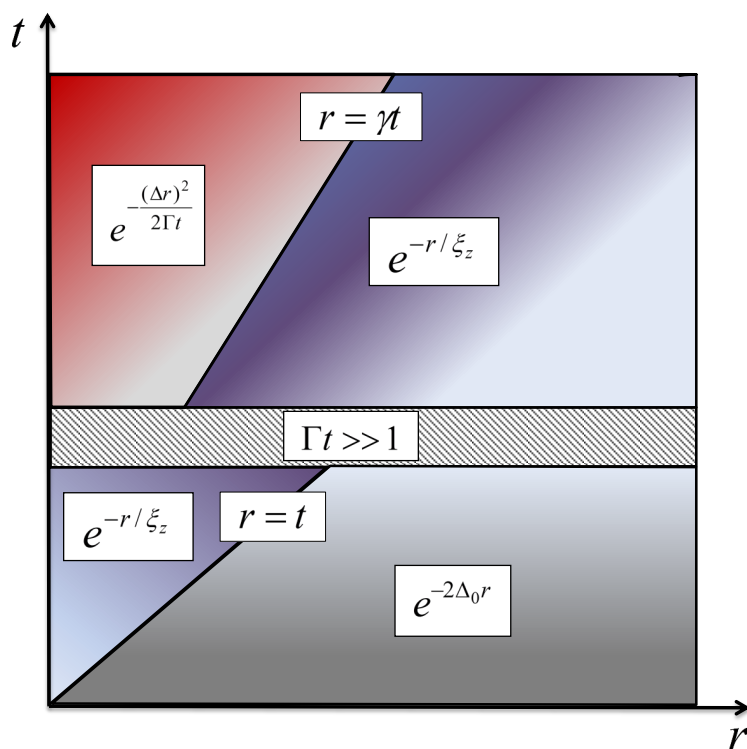


**Figure 3.10:** Spreading of quantum and thermal correlations in the noisy quantum Ising chain ( $J = 1$ ) of Eq. (3.5): the correlator of the transverse magnetization (see Eq. (3.80)) has a first crossover when ballistic quasi-particles, carrying quantum correlations, propagate at the distance  $r$ . Thermal correlations propagate at a second stage, leading to a crossover towards a diffusive form. [Figure taken from Ref. [34]]

function has in general an exponential form  $C^{xx}(r, t) \sim \exp(-r/\xi_Q)$ , with a correlation length  $\xi_Q$  predicted by the generalized Gibbs ensemble [16]. Turning on the noise, the correlation function takes the form [34]

$$C^{xx}(r, t) \underset{r \rightarrow \infty}{\sim} r^{-1/2} e^{-r/\xi(t)}, \quad (3.89)$$

where

$$\frac{1}{\xi(t)} = \frac{1}{\xi_{quench.}} + \frac{1}{\xi(t)_{noise}} \quad \text{with} \quad \frac{1}{\xi(t)_{noise}} = \frac{\Gamma t}{2g^2}. \quad (3.90)$$

In this way the equal-time correlation function of the transverse magnetization and of the order parameter show very different behavior (compare Eq. (3.87) with Eq. (3.89)), similarly to what happens for quenches in the QIC [36, 37]; indeed, the correlation function of the order parameter displays the same exponential form as in the absence of the noise and the spreading of quantum and thermal correlations does not result in a diffusive form, but rather it modifies the value of the correlation length which, at later times, decreases as  $1/\Gamma t$  as time increases.

## CHAPTER 4

# DYNAMIC CORRELATIONS OF THE NOISY QUANTUM ISING CHAIN AND EFFECTIVE TEMPERATURES

In the published studies of the noisy quantum Ising chain (NQIC) only equal-time quantities were considered [34]; in this Chapter we extend the calculation to two-time quantities and, in particular, we determine the correlation and linear response functions, which are needed in order to define effective temperatures. First of all, in Sec. 4.1 we analyze a simplified model consisting of a two-level system driven out of equilibrium by a time-dependent noise which heats it up. Based on the fluctuation-dissipation relations we are able to extract a parameter, which we call effective temperature, indicating that the two-level system is always out of equilibrium during the evolution, while the system approaches an infinite-temperature thermal state only at infinitely long times. Then in Sec. 4.2 we focus on the analysis of two-time quantities of the NQIC. Using Keldysh diagrammatic technique, we are able to solve analytically the Dyson equations for the Greens functions within the self-consistent Born approximation which is valid for sufficiently weak noise. From these solutions, in Sec. 4.3 we determine the expression of the correlator of the transverse magnetization. Finally, in Sec. 4.4 we obtain the correlation and linear response functions of the transverse spins in the long-time limit and we analyze these expression in order to understand how the equal-time correlator of the transverse magnetization changes at different times.

### 4.1 A toy model: two-level system

#### 4.1.1 The model and Green's function

Motivated by Eqs. (3.58) and (3.59), from which we see that the noisy quantum Ising chain is equivalent to the quantum Ising chain perturbed by two  $k$ -dependent delta correlated noises, one along the  $z$  direction and the other one along  $y$ , we introduce a simplified model, consisting of a two-level system subject to a time-dependent noise [57].

The Hamiltonian of the model is

$$H = \sum_{i,j=1,2} c_i^\dagger [H_0 + V(t)]_{ij} c_j, \quad (4.1)$$

where the operators  $c_i, c_i^\dagger$  obey standard anticommutation relations,

$$H_0 = \frac{\hbar}{2} \sigma^z \quad (4.2)$$

is time-independent and

$$V(t) = \sum_{i=x,y,z} \xi_i(t) \sigma^i. \quad (4.3)$$

is a stochastic noise. By imposing the constrain

$$\sum_{i=1,2} c_i^\dagger c_i = 1, \quad (4.4)$$

the Hamiltonian in Eq. (4.1) is equivalent to a 1/2 spin subject to a fluctuating magnetic field. We assume that the noise terms are uncorrelated, i.e.,  $\langle \xi_i(t) \xi_j(t') \rangle = 0$  for  $i \neq j$ , with zero average  $\langle \xi_i(t) \rangle = 0$  and the correlations of the noise in the same direction are

$$\langle \xi_z(t) \xi_z(t') \rangle = \frac{\Gamma_z}{2} \delta(t - t'), \quad (4.5)$$

$$\langle \xi_x(t) \xi_x(t') \rangle = \frac{\Gamma_r}{4} \delta(t - t'), \quad (4.6)$$

$$\langle \xi_y(t) \xi_y(t') \rangle = \frac{\Gamma_r}{4} \delta(t - t'). \quad (4.7)$$

We can treat this problem in the Keldysh formalism and set up a perturbation theory as explained in Sec. 3.2. We solve the Dyson equations (3.42) for the lesser and greater Green's functions  $G^{\lessgtr}(t, t')$  averaged over the noise

$$G^<(t, t') = i \langle c_j^\dagger(t') c_i(t) \rangle \quad \text{and} \quad G^>(t, t') = -i \langle c_i(t) c_j^\dagger(t') \rangle, \quad (4.8)$$

using the self-consistent Born approximation (see Sec. 3.3):

$$\begin{aligned} \Sigma^{\lessgtr}(t, t') &= \delta(t - t') \left[ \frac{\Gamma_z}{2} \sigma^z G^{\lessgtr}(t, t') \sigma^z + \frac{\Gamma_r}{4} (\sigma^x G^{\lessgtr}(t, t') \sigma^x + \sigma^y G^{\lessgtr}(t, t') \sigma^y) \right], \\ \Sigma^{R/A}(t, t') &= \mp i \delta(t - t') \left( \frac{\Gamma_z}{4} + \frac{\Gamma_r}{4} \right) \mathbf{1}. \end{aligned} \quad (4.9)$$

The solution of the Green's functions (4.8) in the approximation (4.9) is (see Appendix B for details)

$$\begin{aligned} G^<(t, t') &= i \mathcal{H}(t) \left[ e^{-(\frac{\Gamma_z + \Gamma_r}{4})|t-t'|} \frac{\mathbf{1}}{2} + e^{-\Gamma_r \left(\frac{t+t'}{2}\right) - (\frac{\Gamma_z - \Gamma_r}{4})|t-t'|} \delta f_0 \sigma^z \right. \\ &\quad \left. + e^{-(\Gamma_z + \frac{\Gamma_r}{2}) \left(\frac{t+t'}{2}\right) + \frac{\Gamma_z}{4}|t-t'|} (z_0 \sigma^+ + z_0^* \sigma^-) \right] \mathcal{H}^\dagger(t'), \end{aligned} \quad (4.10)$$

$$G^<(t, t') - G^>(t, t') = i e^{-\left(\frac{\Gamma_z + \Gamma_x}{4}\right)|t-t'|} \mathcal{H}(t) \mathcal{H}^\dagger(t'), \quad (4.11)$$

where we introduce the matrices  $\sigma^\pm$  and the time-dependent unitary matrix  $\mathcal{H}(t)$  defined respectively as

$$\sigma^\pm = \frac{\sigma^x \pm i\sigma^y}{2} \quad \text{and} \quad \mathcal{H}(t) = \begin{pmatrix} e^{-i\frac{\hbar}{2}t} & 0 \\ 0 & e^{i\frac{\hbar}{2}t} \end{pmatrix}. \quad (4.12)$$

We emphasize that the equal-time Green's function  $G^<$  of this model is similar to the one discussed in Chapter 3. The coefficients  $\delta f_0, z_0$  are fixed by the initial conditions of the evolution, depending on the initial state of the system assumed. We note that Eqs. (4.10) and (4.11) are not time-translation invariant, in contrast to what happens at equilibrium, because the system is driven out of equilibrium by the noise.

#### 4.1.2 Equilibrium and fluctuation-dissipation theorem

In order to compare with the case discussed above, here we consider the same two-level system but in absence of the noise (i.e., with  $V = 0$  in Eq. (4.1) and then given by Eq. (4.2)) and evolving from an equilibrium initial state at temperature  $\beta_0$ . We find that the corresponding Green's functions are related by the fluctuation-dissipation theorem (see Eq. (1.62)) which involve the temperature  $\beta_0$ . The time-independent Hamiltonian is

$$H_0 = \sum_{i,j=1,2} \frac{\hbar}{2} c_i^\dagger \sigma_{ij}^z c_j, \quad (4.13)$$

and we impose the constrain in Eq. (4.4). A suitable basis of the Hilbert space is given by

$$|n_1 = 1, n_2 = 0\rangle \quad \text{and} \quad |n_1 = 0, n_2 = 1\rangle, \quad (4.14)$$

where  $n_i = c_i^\dagger c_i$  is the number operator of the  $i$ -th level. The time evolution of the fermionic operators  $c_i$  are easily obtained from the Heisenberg equations of motion ( $\hbar = 1$ )

$$\frac{dc_i(t)}{dt} = i[H_0, c_i(t)] = -i \sum_{m=1,2} \frac{\hbar}{2} \sigma_{im}^z c_m(t), \quad (4.15)$$

which can be solved:

$$\begin{aligned} c_{1/2}(t) &= c_{1/2}(0) e^{\mp i\frac{\hbar}{2}t}, \\ c_{1/2}^\dagger(t) &= c_{1/2}^\dagger(0) e^{\pm i\frac{\hbar}{2}t}. \end{aligned} \quad (4.16)$$

Due to the equilibrium nature of the initial state the Green's functions of the two-level system follow from Eqs. (4.14) and (4.16):

$$\begin{aligned} G^<(t, t') &= \frac{i}{Z_0} \text{Tr} \left[ e^{-\beta_0 H_0} c_j^\dagger(t') c_i(t) \right] = \frac{i}{Z_0} \begin{pmatrix} e^{-\frac{\beta_0 \hbar}{2} - \frac{i\hbar}{2}(t-t')} & 0 \\ 0 & e^{+\frac{\beta_0 \hbar}{2} + \frac{i\hbar}{2}(t-t')} \end{pmatrix}, \\ G^>(t, t') &= -\frac{i}{Z_0} \text{Tr} \left[ e^{-\beta_0 H_0} c_i(t) c_j^\dagger(t') \right] = -\frac{i}{Z_0} \begin{pmatrix} e^{\frac{\beta_0 \hbar}{2} - \frac{i\hbar}{2}(t-t')} & 0 \\ 0 & e^{-\frac{\beta_0 \hbar}{2} + \frac{i\hbar}{2}(t-t')} \end{pmatrix}, \end{aligned} \quad (4.17)$$

where the partition function is  $Z_0 = 2 \cosh\left(\frac{\beta_0 \hbar}{2}\right)$ . Using Eq. (4.17), we can find the expressions of the Keldysh function  $G^K(t, t')$ , defined as the sum of the lesser  $G^<$  and greater  $G^>$  Green's function:

$$G^K(t, t') = G^>(t, t') + G^<(t, t') = i \tanh\left(\frac{\beta_0 \hbar}{2}\right) \begin{pmatrix} -e^{-\frac{i\hbar}{2}(t-t')} & 0 \\ 0 & e^{\frac{i\hbar}{2}(t-t')} \end{pmatrix}, \quad (4.18)$$

while the difference between the retarded  $G^R$  and advanced  $G^A$  Green's functions (see Eqs. (3.37) and (3.38)) turns out to be:

$$G^R(t, t') - G^A(t, t') = G^>(t, t') - G^<(t, t') = -i \begin{pmatrix} e^{-\frac{i\hbar}{2}(t-t')} & 0 \\ 0 & e^{\frac{i\hbar}{2}(t-t')} \end{pmatrix}. \quad (4.19)$$

A simple relation between  $G^K$  and  $G^R - G^A$  exists taking, in fact, their Fourier transform  $G^K(\omega)$  and  $G^R(\omega) - G^A(\omega)$ , respectively, defined by Eq. (1.59), of Eqs. (4.18) and (4.19). One finds

$$\begin{aligned} G^K(\omega) &= i \tanh\left(\frac{\beta_0 \hbar}{2}\right) \begin{pmatrix} -\delta(\omega - \frac{\hbar}{2}) & 0 \\ 0 & \delta(\omega + \frac{\hbar}{2}) \end{pmatrix}, \\ G^R(\omega) - G^A(\omega) &= -i \begin{pmatrix} \delta(\omega - \frac{\hbar}{2}) & 0 \\ 0 & \delta(\omega + \frac{\hbar}{2}) \end{pmatrix}, \end{aligned} \quad (4.20)$$

and therefore they satisfy the fluctuation-dissipation theorem in frequency-space (1.62)

$$G^K(\omega) = \tanh(\beta_0 \omega) [G^R(\omega) - G^A(\omega)]. \quad (4.21)$$

Analogously to what was done in Sec. 2.4 we would like to use a relationship analogous to Eq. (4.21) in order to define a sort of non-equilibrium effective temperature, the properties of which will eventually indicate whether the system reaches an equilibrium state or not. This attempt is described below.

### 4.1.3 Effective temperatures

In order to understand the role played by the noise in the dynamics of the two-level system discussed above and how it affects the effective temperature possibly associated with it, we consider the case in which the system is initially at equilibrium with inverse

temperature  $\beta_0$  and follows its heating up due to the noise. The dynamics for times  $t > 0$  is governed by the Hamiltonian (4.1) and the Green's functions are given by Eqs. (4.10) and (4.11) with the initial thermal condition (4.18, 4.19), which yield

$$G^R(t, t') - G^A(t, t') = -i e^{-\frac{\Gamma_z + \Gamma_r}{4}|t-t'|} \mathcal{H}(t) \mathcal{H}^\dagger(t'), \quad (4.22)$$

$$G^K(t, t') = -i \tanh\left(\frac{\beta_0 h}{2}\right) e^{-\Gamma_r\left(\frac{t+t'}{2}\right) - \left(\frac{\Gamma_z - \Gamma_r}{4}\right)|t-t'|} \mathcal{H}(t) \sigma^z \mathcal{H}^\dagger(t'), \quad (4.23)$$

with the matrix  $\mathcal{H}$  defined in Eq. (4.12). Following the line of argument presented in Sec. 1.6 we want to define an effective temperature through the fluctuation-dissipation relation (4.21). However, we cannot do a Fourier transform because the Green's function (4.22) and (4.23) are not time translation invariant. We note that Eqs. (4.22) and (4.23) can be expressed in terms of Wigner variable  $T$  and  $\tau$

$$T = \frac{t + t'}{2} \quad \text{and} \quad \tau = t - t'; \quad (4.24)$$

instead of doing a Fourier transform, we then perform a Wigner transform, defined as

$$f(\omega, \tau) = \int_{-2T}^{2T} d\tau' e^{i\omega\tau'} f(\tau, T). \quad (4.25)$$

In order to simplify the notation we use the same symbol for the function and its transform, as the difference is made clear by their argument. In other words we are keeping  $T$  fixed and then Fourier transform with respect to the variable  $\tau$ . To compute the Wigner transform of Eqs. (4.22) and (4.23), we need the following result

$$\int_{-2T}^{2T} d\tau e^{i(\omega+a)\tau - b|\tau|} = \frac{2b - e^{-2bT} \{2b \cos[2(\omega+a)T] - 2(\omega+a) \sin[2(\omega+a)T]\}}{b^2 + (\omega+a)^2}, \quad (4.26)$$

and, accordingly,

$$\begin{aligned} G_{11}^K(\omega, T) &= \mp 8i \tanh\left(\frac{\beta_0 h}{2}\right) \times \\ &\quad \frac{(\Gamma_z - \Gamma_r) e^{-\Gamma_r T} - e^{-\frac{\Gamma_z + \Gamma_r}{2} T} \{(\Gamma_z - \Gamma_r) \cos[(2\omega \mp h)T] - 2(2\omega \mp h) \sin[(2\omega \mp h)T]\}}{(\Gamma_z - \Gamma_r)^2 + 4(2\omega \mp h)^2}, \\ (G^R - G^A)(\omega, T)_{11} &= \\ &= -8i \times \frac{\Gamma_z + \Gamma_r - e^{-\frac{\Gamma_z + \Gamma_r}{2} T} \{(\Gamma_z + \Gamma_r) \cos[(2\omega \mp h)T] - 2(2\omega \mp h) \sin[(2\omega \mp h)T]\}}{(\Gamma_z + \Gamma_r)^2 + 4(2\omega \mp h)^2}, \end{aligned} \quad (4.27)$$

where  $G_{11}^K$  and  $(G^R - G^A)_{11}$  indicate, respectively, the diagonal elements of the matrix  $G^K$  and  $G^R - G^A$ . The off-diagonal elements vanishes because of the initial thermal condition (4.18, 4.19). We define an effective temperature  $\beta_{eff}$ , in general dependent

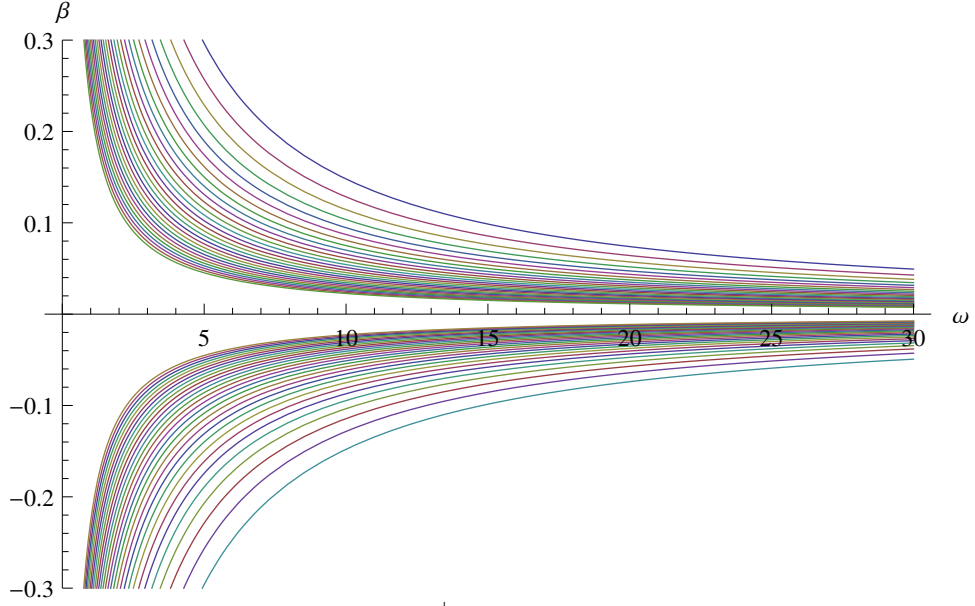


**Figure 4.1:** Effective temperatures  $\beta_{eff}^{\pm}(\omega, T)$  (see Eq. (4.29)) as a function of  $\omega$  for fixed  $T$  for  $\beta_0 = 10$ ,  $h = 2$ ,  $\Gamma_z = 5$ ,  $\Gamma_r = 0.01$ .  $T$  ranges from 10 to 150 at step of 5 units moving from the topmost (lowermost) to the lowermost (topmost) curves for  $\beta > 0$  ( $\beta < 0$ ). This qualitative behavior is observed independently of the choice of  $\beta_0$ .

on the frequency  $\omega$  and on the time  $T$ , such that

$$G^K(\omega, T) = \tanh \left[ \beta_{eff}^{\pm}(\omega, T)\omega \right] \left[ G^R(\omega, T) - G^A(\omega, T) \right]. \quad (4.28)$$

Clearly a lack of dependence on  $\omega$  and  $T$  (at least within some range) provides a strong evidence in favor of the fact that the system has reached equilibrium. As peculiarity of this model, we note that we have to define two different effective temperatures  $\beta_{eff}^{\pm}$ , one for each level, otherwise Eq. (4.28) can never be satisfied. From Eqs. (4.27) and (4.28) we obtain the two effective temperatures

$$\beta_{eff}^{\pm}(\omega, T) = \pm \frac{1}{\omega} \operatorname{arctanh} \left\{ \tanh \left( \frac{\beta_0 h}{2} \right) \left[ \frac{(\Gamma_z + \Gamma_r)^2 + 4(2\omega \mp h)^2}{(\Gamma_z - \Gamma_r)^2 + 4(2\omega \mp h)^2} \right] P_{\Gamma_z, \Gamma_r}^{\pm}(\omega, T) \right\}, \quad (4.29)$$

and we have defined

$$P_{\Gamma_z, \Gamma_r}^{\pm}(\omega, T) \equiv \frac{(\Gamma_z - \Gamma_r) e^{-\Gamma_r T} - e^{-\frac{\Gamma_z + \Gamma_r}{2} T} \{ (\Gamma_z - \Gamma_r) \cos[(2\omega \mp h)T] - 2(2\omega \mp h) \sin[(2\omega \mp h)T] \}}{\Gamma_z + \Gamma_r - e^{-\frac{\Gamma_z + \Gamma_r}{2} T} \{ (\Gamma_z + \Gamma_r) \cos[(2\omega \mp h)T] - 2(2\omega \mp h) \sin[(2\omega \mp h)T] \}}. \quad (4.30)$$

The effective temperature  $\beta_{eff}^{\pm}(\omega, T)$  is illustrated in Fig. 4.1 as a function of  $\omega$  for various fixed values of  $T$ : we note that  $\beta_{eff}^{\pm}(\omega, T)$  never displays a plateau upon changing  $\omega$ , which means that the system can never be thought of as being at thermal equilibrium. Actually this conclusion is independent of the value of  $T$ . The two-level system is always driven out of equilibrium by the noise and only in the infinite-time limit it reaches a thermal equilibrium state with infinite temperature, signaled by the fact that  $\beta_{eff}(T = \infty) = 0$ . The presence of a negative temperature  $\beta_{eff}$  is not worrying being

the system out of equilibrium. Clearly, this model is very simple and the lack of an even apparent thermalization is not really surprising. It is interesting then to test if in the noisy quantum Ising chain, the quantum many-body effects and the presence of many levels in interaction can lead a different scenario.

## 4.2 Green's functions of noisy quantum Ising chain

In Chapter 3, we presented a discussion of one-time quantities for a noisy quantum Ising chain; in this Section we extend the calculation to two-time quantities and find the correlation and linear response functions of the transverse spins. The model is characterized by the Hamiltonian (3.5) with Gaussian noise in the transverse field  $\delta g(t)$  with amplitude  $\Gamma$  (see Eq. (3.6)) and the quench protocol considered is illustrated in Fig. 3.1. In order to calculate the two-time correlation functions of the transverse spins of the chain we need to determine first the lesser Green's function  $G^<(t, t')$  at different real times expressed in terms of the post-quench Bogolyubov fermions  $\{\gamma_k^g, \gamma_k^{g\dagger}\}$ , i.e.,

$$G^<(t, t') = i \begin{bmatrix} \langle \gamma_k^{g\dagger}(t') \gamma_k^g(t) \rangle & \langle \gamma_k^{g\dagger}(t') \gamma_{-k}^{g\dagger}(t) \rangle \\ \langle \gamma_{-k}^g(t') \gamma_k^g(t) \rangle & \langle \gamma_{-k}^g(t') \gamma_{-k}^{g\dagger}(t) \rangle \end{bmatrix}. \quad (4.31)$$

Analogously to what was done in Chapter 3, the analysis starts from the Dyson equations (3.48): within the self-consistent Born approximation (3.49), valid for sufficiently weak noise  $\Gamma \ll \Delta$ , we obtain (see Appendix C for the details of the analysis)

$$\begin{aligned} G_{22}^<(\tau, T) &= i e^{\mp i \epsilon_k^g \tau} \left[ \frac{1}{2} e^{-\frac{\Gamma}{4} |\tau|} \pm \left( \sin^2(\Delta \theta_k) - \frac{1}{2} \right) e^{-\Gamma T \sin^2(2\theta_k^g) - \frac{\Gamma}{4} |\tau| \cos(4\theta_k^g)} \right], \\ G_{12}^<(\tau, T) &= -i P_{k,\Omega}^\pm(\tau, T) e^{\mp i \epsilon_k^g |\tau| + \frac{\Gamma}{4} |\tau| \cos^2(2\theta_k^g) - \frac{\Gamma}{2} T [1 + \cos^2(2\theta_k^g)]}, \end{aligned} \quad (4.32)$$

where  $\epsilon_k^g$ ,  $\theta_k^g$  and  $\Delta \theta_k$  are given in Eqs. (2.28), (2.31) and (2.38), while

$$\begin{aligned} P_{k,\Omega}^\pm(\tau, T) &= \sin(2\Delta \theta_k) \left\{ 2 \frac{\epsilon_k^g}{\Omega} \sin\left(\frac{\Omega}{2} \left(T - \frac{|\tau|}{2}\right)\right) \right. \\ &\quad \left. \pm \frac{i}{2} \left[ \frac{\Gamma}{\Omega} \sin^2(2\theta_k^g) \sin\left(\frac{\Omega}{2} \left(T - \frac{|\tau|}{2}\right)\right) + \cos\left(\frac{\Omega}{2} \left(T - \frac{|\tau|}{2}\right)\right) \right] \right\}. \end{aligned} \quad (4.33)$$

In this expression  $\Omega = \sqrt{|\Gamma^2 \sin^4(2\theta_k^g) - 16(\epsilon_k^g)^2|}$ . The greater Green's function  $G^>(t, t')$  can be obtained from the lesser one  $G^<(t, t')$  (4.32) through Eq. (C.6) reported in Appendix C:

$$G^<(t, t') - G^>(t, t') = i e^{-\frac{\Gamma}{4} |t-t'|} \begin{pmatrix} e^{-i \epsilon_k^g (t-t')} & 0 \\ 0 & e^{i \epsilon_k^g (t-t')} \end{pmatrix}. \quad (4.34)$$

As in Sec. 4.1  $\tau$  and  $T$  in the previous expressions are the Wigner variables (4.24).

### 4.3 Correlator of the transverse magnetization

In the previous Section we obtained the Green's function of the Bogolyubov fermions  $\{\gamma_k^g, \gamma_k^{g\dagger}\}$ ; starting from this quantity we can calculate the correlation function of the transverse magnetization at different times for two transverse spins at a distance  $r$

$$C^{zz}(r, t, t') = \langle \sigma_r^z(t) \sigma_0^z(t') \rangle - \langle \sigma_r^z(t) \rangle \langle \sigma_0^z(t') \rangle. \quad (4.35)$$

In order to do this, we first apply the Jordan-Wigner transformation (2.13-2.23) to the spin operators  $\sigma_j^z$  and then, by using the Bogolyubov rotation (2.26), we express the correlator in terms of the fermionic operators  $\{\gamma_k^g, \gamma_k^{g\dagger}\}$

$$\begin{aligned} C^{zz}(r, t, t') &= 4 \left[ \langle c_r^\dagger(t) c_r(t) c_0^\dagger(t') c_0(t') \rangle - \langle c_r^\dagger(t) c_r(t) \rangle \langle c_0^\dagger(t') c_0(t') \rangle \right] \\ &= \frac{4}{L^2} \sum_{k_1, k_2, k_3, k_4} e^{i(k_2 - k_1)r} \left[ \langle c_{k_1}^\dagger(t) c_{k_2}(t) c_{k_3}^\dagger(t') c_{k_4}(t') \rangle - \langle c_{k_1}^\dagger(t) c_{k_2}(t) \rangle \langle c_{k_3}^\dagger(t') c_{k_4}(t') \rangle \right] \\ &= \frac{4}{L^2} \sum_{k_1, k_2, k_3, k_4} e^{i(k_2 - k_1)r} \left\{ \left\langle \left[ u_{k_1}^g \gamma_{k_1}^{g\dagger}(t) + i v_{k_1}^g \gamma_{-k_1}^g(t) \right] \left[ u_{k_2}^g \gamma_{k_2}^g(t) - i v_{k_2}^g \gamma_{-k_2}^{g\dagger}(t) \right] \times \right. \right. \\ &\quad \times \left[ u_{k_3}^g \gamma_{k_3}^{g\dagger}(t') + i v_{k_3}^g \gamma_{-k_3}^g(t') \right] \left[ u_{k_4}^g \gamma_{k_4}^g(t') - i v_{k_4}^g \gamma_{-k_4}^{g\dagger}(t') \right] \left. \right\rangle - \\ &\quad - \left\langle \left[ u_{k_1}^g \gamma_{k_1}^{g\dagger}(t) + i v_{k_1}^g \gamma_{-k_1}^g(t) \right] \left[ u_{k_2}^g \gamma_{k_2}^g(t) - i v_{k_2}^g \gamma_{-k_2}^{g\dagger}(t) \right] \right\rangle \times \\ &\quad \times \left\langle \left[ u_{k_3}^g \gamma_{k_3}^{g\dagger}(t') + i v_{k_3}^g \gamma_{-k_3}^g(t') \right] \left[ u_{k_4}^g \gamma_{k_4}^g(t') - i v_{k_4}^g \gamma_{-k_4}^{g\dagger}(t') \right] \right\rangle \left. \right\} \quad (4.36) \end{aligned}$$

where  $L$  is the number of site in the chain (see Eq. (3.5)),  $r$  is the distance between the transverse spins  $\sigma_j^z$ , the wave vectors  $k_i$  belong to the NS sector (see Sec. 2.2.1) while  $u_k^g$  and  $v_k^g$  are given in Eq. (2.27). With an abuse of notation, we indicate with the same symbol both the fermions  $c_r$  in real space and their spatial Fourier transform  $c_k$ . According to Eq. (4.36), the transverse correlator  $C^{zz}$  is the Fourier transform of the difference between a 4-points Green's function of the fermions at different times and the product of 2-point Green functions at equal times. As we already know the 2-point function at equal times, we focus here on the 4-point Green function, which can be evaluated by using the following approximation:

$$\begin{aligned} \left\langle \gamma_{k_1}^\dagger(t) \gamma_{k_2}(t) \gamma_{k_3}^\dagger(t') \gamma_{k_4}(t') \right\rangle &\approx \left\langle \gamma_{k_1}^\dagger(t) \gamma_{k_2}(t) \right\rangle \left\langle \gamma_{k_3}^\dagger(t') \gamma_{k_4}(t') \right\rangle \\ &\quad - \left\langle \gamma_{k_1}^\dagger(t) \gamma_{k_3}^\dagger(t') \right\rangle \left\langle \gamma_{k_2}(t) \gamma_{k_4}(t') \right\rangle \\ &\quad + \left\langle \gamma_{k_1}^\dagger(t) \gamma_{k_4}(t') \right\rangle \left\langle \gamma_{k_2}(t) \gamma_{k_3}^\dagger(t') \right\rangle. \quad (4.37) \end{aligned}$$

Equation (4.37) is exact in the case of non-interacting theory, as it follows clearly from Wick theorem in Eq. (3.29). For interacting theory, as the one we are interested in, we instead should add correction terms, known as correlations, to Eq. (4.37); however in

the limit of sufficiently weak noise  $\Gamma \ll \Delta$  which we are considering these terms can be neglected. To improve this approximation one should consider also the correlations terms, known as Cooperons contribution. By using Eq. (4.37) for all 4-points terms in Eq. (4.36), defining

$$\rho_k^{ij}(t, t') = -iG_{ij}^<(t, t') \quad (4.38)$$

and using the definition of  $u_k^g$  and  $v_k^g$  in Eq. (2.27) we obtain

$$C^{zz}(r, t, t') = C_{diag}^{zz} + C_{non-diag}^{zz} + C_{mixed}^{zz}, \quad (4.39)$$

where we highlight the different contributions to the correlator given by

$$C_{diag}^{zz} = \frac{4}{L^2} \sum_{k_1, k_2} e^{i(k_2 - k_1)r} \left\{ \begin{aligned} & \cos(\theta_{k_1}^g + \theta_{k_2}^g) \left[ \cos \theta_{k_1}^g \cos \theta_{k_2}^g \rho_{k_1}^{11}(t', t) \rho_{k_2}^{22}(t', t) \right. \\ & \quad \left. - \sin \theta_{k_1}^g \sin \theta_{k_2}^g \rho_{k_1}^{22}(t', t) \rho_{k_2}^{11}(t', t) \right] \\ & + \sin(\theta_{k_1}^g + \theta_{k_2}^g) \left[ \cos \theta_{k_1}^g \sin \theta_{k_2}^g \rho_{k_1}^{11}(t', t) \rho_{k_2}^{11}(t', t) \right. \\ & \quad \left. + \sin \theta_{k_1}^g \cos \theta_{k_2}^g \rho_{k_1}^{22}(t', t) \rho_{k_2}^{22}(t', t) \right] \end{aligned} \right\}, \quad (4.40a)$$

$$C_{non-diag}^{zz} = \frac{4}{L^2} \sum_{k_1, k_2} e^{i(k_2 - k_1)r} \left\{ \begin{aligned} & \cos(\theta_{k_1}^g + \theta_{k_2}^g) \left[ \cos \theta_{k_1}^g \cos \theta_{k_2}^g \rho_{k_1}^{12}(t', t) \rho_{k_2}^{21}(t', t) \right. \\ & \quad \left. - \sin \theta_{k_1}^g \sin \theta_{k_2}^g \rho_{k_1}^{21}(t', t) \rho_{k_2}^{12}(t', t) \right] \\ & + \sin(\theta_{k_1}^g + \theta_{k_2}^g) \left[ \cos \theta_{k_1}^g \sin \theta_{k_2}^g \rho_{k_1}^{12}(t', t) \rho_{k_2}^{12}(t', t) \right. \\ & \quad \left. + \sin \theta_{k_1}^g \cos \theta_{k_2}^g \rho_{k_1}^{21}(t', t) \rho_{k_2}^{21}(t', t) \right] \end{aligned} \right\}, \quad (4.40b)$$

$$C_{mixed}^{zz} = \frac{4i}{L^2} \sum_{k_1, k_2} e^{i(k_2 - k_1)r} \left\{ \begin{aligned} & \cos(\theta_{k_1}^g + \theta_{k_2}^g) \times \\ & \left[ \cos \theta_{k_1}^g \sin \theta_{k_2}^g \left( \rho_{k_1}^{12}(t', t) \rho_{k_2}^{11}(t', t) + \rho_{k_1}^{11}(t', t) \rho_{k_2}^{12}(t', t) \right) \right. \\ & \quad \left. + \sin \theta_{k_1}^g \cos \theta_{k_2}^g \left( \rho_{k_1}^{22}(t', t) \rho_{k_2}^{21}(t', t) + \rho_{k_1}^{21}(t', t) \rho_{k_2}^{22}(t', t) \right) \right] \\ & + \sin(\theta_{k_1}^g + \theta_{k_2}^g) \times \\ & \left[ \sin \theta_{k_1}^g \sin \theta_{k_2}^g \left( \rho_{k_1}^{22}(t', t) \rho_{k_2}^{12}(t', t) + \rho_{k_1}^{21}(t', t) \rho_{k_2}^{11}(t', t) \right) \right. \\ & \quad \left. - \cos \theta_{k_1}^g \cos \theta_{k_2}^g \left( \rho_{k_1}^{12}(t', t) \rho_{k_2}^{22}(t', t) + \rho_{k_1}^{11}(t', t) \rho_{k_2}^{21}(t', t) \right) \right] \end{aligned} \right\}, \quad (4.40c)$$

where  $L$  is the chain length (see Eq. (3.5)),  $r$  is the distance between the transverse spins  $\sigma_j^z$ , the Bogolyubov angles  $\theta_k^g$  are given by Eq. (2.28), while Eqs. (4.32) and (4.38) define

the elements  $\rho_k^{ij}(t, t')$ . The subscripts "diag", "non-diag" and "mixed" of  $C^{zz}$  indicate that the expression of the corresponding contribution to  $C^{zz}$  involves only the diagonal, the non-diagonal, or the mixed components, respectively, of the Green's function  $G_k^<$  investigated in Sec. 4.2.

## 4.4 Long-time behavior

### 4.4.1 Two-time correlation and linear response functions

In this Section we want to study the correlator of the transverse spins  $C^{zz}$  within the long-time limit defined by the condition

$$t, t' \gg \Gamma^{-1} \quad \text{with fixed } \tau = t - t'. \quad (4.41)$$

We are interested in this time range because the noise has come into play and the equal-time correlator of the transverse magnetization shows a diffusive behavior as highlighted in Eq. (3.87) and discussed in Sec. 3.3; here we want to investigate how the correlator  $C^{zz}$  changes at different times. In the other time range,  $t, t' \ll \Gamma^{-1}$ , we know from Eq. (3.87) that the equal-time correlator of transverse magnetization agrees with the GGE predictions for a quantum Ising chain following a quantum quench and we expect that the different time behavior within this time range resembles the one found in Ref. [38]. In this limit we can neglect the non-diagonal and mixed contributions (4.40b-4.40c) in Eq. (4.39) because they are exponentially suppressed for  $\Gamma T \gg 1$ ; in fact; from Eqs. (4.32), (4.40b) and (4.40c)

$$C_{out-diag}^{zz} \propto e^{-\Gamma T} \quad \text{and} \quad C_{mixed}^{zz} \propto e^{-\Gamma T}. \quad (4.42)$$

Accordingly, in the following we will concentrate only on the diagonal term  $C_{diag}^{zz}$ . By exchanging the indices  $k_1 \leftrightarrow k_2$ , the correlator  $C^{zz}$  in Eq. (4.40a) can be expressed as

$$C^{zz} = \frac{4}{L^2} \sum_{k_1, k_2} \left\{ \cos(\theta_{k_1}^g + \theta_{k_2}^g) \times \right. \\ \left[ e^{i(k_2 - k_1)r} \cos \theta_{k_1}^g \cos \theta_{k_2}^g - e^{-i(k_2 - k_1)r} \sin \theta_{k_1}^g \sin \theta_{k_2}^g \right] \rho_{k_1}^{11}(t', t) \rho_{k_2}^{22}(t', t) \\ + \sin(\theta_{k_1}^g + \theta_{k_2}^g) \cos \theta_{k_1}^g \sin \theta_{k_2}^g \times \\ \left. \left[ e^{i(k_2 - k_1)r} \rho_{k_1}^{11}(t', t) \rho_{k_2}^{11}(t', t) + e^{-i(k_2 - k_1)r} \rho_{k_1}^{22}(t', t) \rho_{k_2}^{22}(t', t) \right] \right\}, \quad (4.43)$$

Now we write the diagonal term as (see Eq. (4.32))

$$\rho_k^{11}(t, t') = e^{\mp i \epsilon_k^g \tau} \left[ \frac{1}{2} e^{-\frac{\Gamma}{4} |\tau|} \pm \delta h_k(\tau, T) \right], \quad (4.44)$$

where we defined

$$\delta h_k(\tau, T) \equiv \left[ \sin^2(\Delta\theta_k) - \frac{1}{2} \right] \exp \left[ -\Gamma T \sin^2(2\theta_k^g) - \frac{\Gamma}{4} |\tau| \cos(4\theta_k^g) \right] \quad (4.45)$$

and  $\theta_k^g$  are the Bogolyubov angles (2.28),  $\Delta\theta_k$  is given by Eq. (2.38) and  $\tau$  and  $T$  are the Wigner variables (4.24). In particular, the expression in Eq. (4.45) for  $k \simeq 0$ , which is useful in order to calculate the leading behavior of the two-time correlator (analogous to Eq. (3.66)), becomes:

$$\delta h_k(\tau, T) \underset{k \simeq 0}{\simeq} \frac{1}{2} \left( \frac{k^2}{2\Delta^2} \rho_-^2 - 1 \right) \exp \left[ -\frac{\Gamma}{4} |\tau| - \Gamma \left( T - \frac{|\tau|}{2} \right) \frac{k^2}{\Delta^2} \right], \quad (4.46)$$

where  $\Delta = |g - 1|$  is half of the gap (2.56) of the quantum Ising chain and  $\rho_-$  is given in Eq. (3.66). By replacing Eq. (4.44) in Eq. (4.43) and by using the elementary trigonometric addition formulas and Eq. (2.29), we obtain, in the thermodynamic limit  $1/L \sum_k \rightarrow \int_{-\pi}^{\pi} dk / (2\pi)$ , the real part of the correlator  $C^{zz}$

$$\begin{aligned} \text{Re } C^{zz}(r, \tau, T) = e^{-\frac{\Gamma}{2} |\tau|} & \left\{ |A_1(r, \tau) + A_2(r, \tau)|^2 - 4 [\text{Re } B_1(r, \tau)]^2 \right\} \\ & - 4 \left\{ |C_1(r, \tau, T) - C_2(r, \tau, T)|^2 - 4 [\text{Im } D_1(r, \tau, T)]^2 \right\}, \end{aligned} \quad (4.47)$$

and its imaginary part

$$\begin{aligned} \text{Im } C^{zz}(r, \tau, T) = 4 e^{-\frac{\Gamma}{4} |\tau|} \text{Im} & \left\{ C_1(r, \tau, T) [A_1^*(r, \tau) + A_2^*(r, \tau)] \right. \\ & + C_2^*(r, \tau, T) [A_1(r, \tau) + A_2(r, \tau)] - \\ & - D_1(r, \tau, T) [B_1^*(r, \tau) - B_1(-r, \tau)] \\ & \left. + D_1(-r, \tau, T) [B_1(r, \tau) - B_1^*(-r, \tau)] \right\}. \end{aligned} \quad (4.48)$$

The functions  $A_1, A_2, B_1, C_1, C_2, D_1$  introduced above can be written as

$$A_1(r, \tau) = \int_0^{\pi} \frac{dk}{\pi} \left( \frac{1}{2} + \frac{g - \cos k}{\epsilon_k^g} \right) \cos(kr) e^{-i\epsilon_k^g \tau}, \quad (4.49)$$

$$A_2(r, \tau) = \int_0^{\pi} \frac{dk}{\pi} \left( \frac{1}{2} - \frac{g - \cos k}{\epsilon_k^g} \right) \cos(kr) e^{i\epsilon_k^g \tau}, \quad (4.50)$$

$$B_1(r, \tau) = -i \int_0^{\pi} \frac{dk}{\pi} \frac{\sin k}{\epsilon_k^g} \sin(kr) e^{-i\epsilon_k^g \tau}, \quad (4.51)$$

$$C_1(r, \tau, T) = \int_0^{\pi} \frac{dk}{\pi} \left( \frac{1}{2} + \frac{g - \cos k}{\epsilon_k^g} \right) \delta h_k(\tau, T) \cos(kr) e^{-i\epsilon_k^g \tau}, \quad (4.52)$$

$$C_2(r, \tau, T) = \int_0^\pi \frac{dk}{\pi} \left( \frac{1}{2} - \frac{g - \cos k}{\epsilon_k^g} \right) \delta h_k(\tau, T) \cos(kr) e^{i\epsilon_k^g \tau}, \quad (4.53)$$

$$D_1(r, \tau, T) = -i \int_0^\pi \frac{dk}{\pi} \frac{\sin k}{\epsilon_k^g} \delta h_k(\tau, T) \sin(kr) e^{-i\epsilon_k^g \tau}, \quad (4.54)$$

where  $\delta h_k$  is given by Eq. (4.45),  $\epsilon_k^g$  is the dispersion relation Eq. (2.31)  $\tau$  and  $T$  are the Wigner variables (4.24). In order to make the integrals run only on half the original Brillouin zone we used the fact that  $\delta h_k = \delta h_{-k}$ . The fluctuations  $C_+^{zz}$  and linear response function  $R^{zz}$  for the system in the long-time limit (4.41) can be found from Eqs. (1.57) and (1.58) based on Eqs. (4.47) and (4.48), i.e.,

$$C_+^{zz}(r, \tau, T) = \text{Re } C^{zz}(r, \tau, T), \quad (4.55)$$

$$R^{zz}(r, \tau, T) = -2\theta(\tau) \text{Im } C^{zz}(r, \tau, T). \quad (4.56)$$

In general,  $C^{zz}$  contains a stationary and a non-stationary part where the former depends only on  $\tau$ , while the latter also on  $T$ .

#### 4.4.2 Non-stationary two-time correlation function

We now focus on the non-stationary part of Eq. (4.55)

$$[C_+^{zz}(r, \tau, T)]_{non-stat} = -4 \left\{ |C_1(r, \tau, T) - C_2(r, \tau, T)|^2 - 4 [\text{Im } D_1(r, \tau, T)]^2 \right\}, \quad (4.57)$$

in order to see how the diffusive behavior displayed by one-time quantities and discussed in Sec. 3.3 changes at different times. The integrals (4.52), (4.53) and (4.54) can be computed by approximating the integrands around  $k \simeq 0$  and  $k \simeq \pm\pi$ . Indeed, in the time range  $\Gamma T \gg 1$  we are interested (see Eq. (4.41)), they as well the function  $\delta h_k$  are dominated by the slowest modes  $k \simeq 0$  and  $k \simeq \pm\pi$ , as it can be seen from Eq. (4.45). We focus only on the contribution from the mode  $k \simeq 0$  because the modes  $k \simeq \pm\pi$  are due only to the presence of the lattice and are generically responsible for oscillating corrections to the leading behavior, which we neglect for the time being. For concreteness we assume that the time  $t'$  is smaller than  $t$

$$t' < t \quad \text{so that} \quad T - \frac{|t|}{2} = \min(t, t') = t' \quad \text{and} \quad \tau = t - t' > 0, \quad (4.58)$$

by plugging in Eq. (4.57) the integrals (D.5 - D.6 - D.7), evaluated in Appendix D, we find that the non-stationary part of the correlation function, within the space-time range

$$\Delta r \ll \sqrt{\Gamma^2 t'^2 + \Delta^2 \tau^2} \quad \text{with} \quad t, t' \gg \Gamma^{-1}, \quad (4.59)$$

is given by

$$[C_+^{zz}(r, t', \tau)]_{non-stat} = -\frac{1}{\pi} \frac{\Delta^2}{4} \frac{e^{-\frac{\Gamma}{2}\tau}}{\sqrt{\Gamma^2 t'^2 + \Delta^2 \tau^2}} \times \exp \left[ -\frac{\Gamma t' (\Delta r)^2}{2(\Gamma^2 t'^2 + \Delta^2 \tau^2)} \right], \quad (4.60)$$

where we remind  $r$  is the distance between the transverse spins,  $\Gamma$  the amplitude noise given by Eq. (3.6) and  $\Delta = g - 1$  is half of the gap (2.56) of the quantum Ising chain. At equal times,  $\tau = 0$ , Eq. (4.60) reduces to the diffusive correlator given by Eq. (3.87). At short time differences, i.e., for

$$\Delta\tau \ll \Gamma t', \tag{4.61}$$

the space-time part of Eq. (4.60) shows a diffusive behavior analogous to the one of the equal-time correlator (3.87) and, in fact, the square of the distance  $r$  scales as the time  $t'$

$$r^2 \sim t'. \tag{4.62}$$

In other words, the behavior of this quantity at short time difference compared to the time elapsed from the quench is not able to display a qualitative different scaling. On the contrary, for much longer time differences, i.e, for

$$\Delta\tau \gg \Gamma t', \tag{4.63}$$

the two-time correlator (4.60) changes completely its qualitative behavior and the space  $r$  scale linearly, i.e., ballistically with the time  $\tau$

$$r \sim \tau. \tag{4.64}$$

The non-stationary correlation function (4.57) is illustrated in Fig. 4.2 as a function of  $\Gamma t'$  for various fixed values of  $\Delta\tau$ . It is evident the presence of two regions; as long as  $\Delta\tau \ll \Gamma t'$  the non-stationary correlation function  $[C_+^{zz}]_{non-stat}$  is qualitative similar to the equal-time one. Instead, for longer time differences,  $\Delta\tau \gg \Gamma t'$ , it crosses to a different qualitative behavior and the "propagation" from diffusive becomes ballistic. Clearly, this crossover is totally new and it cannot be observed at equal times. Note that this behavior is independent of some features of the quench, as it does not depend on the pre-quench Hamiltonian. However, the very fact that this quantity shows a dependence on  $t'$  indicates that the very presence of an initial condition plays an essential role in determining this genuinely non-equilibrium feature. We emphasize that this crossover is different from the one observed in Eq. (3.87). Indeed, by looking at Eq. (3.87) we see that the equal-time correlator  $C^{zz}(r, t)$  in the long-time limit,  $t \gg \Gamma^{-1}$ , crosses from a diffusive form to the one predicted by the GGE, in which it retains memory of the initial conditions. Instead, as mentioned above, in Eq. (4.60) there is no reference to the initial state; in the time range considered the quench has no more effect on the system and only the noise affects the dynamics, in this way the crossover observed at different times is due entirely to the noise.

#### 4.4.3 Effective temperature

Based on the expressions for  $\text{Re } C^{zz}$  and  $\text{Im } C^{zz}$  in Eqs. (4.47) and (4.48), respectively, we can calculate the corresponding response and correlation function according to Eqs. (4.55) and (4.56). In turn, they can be used in order to define an effective

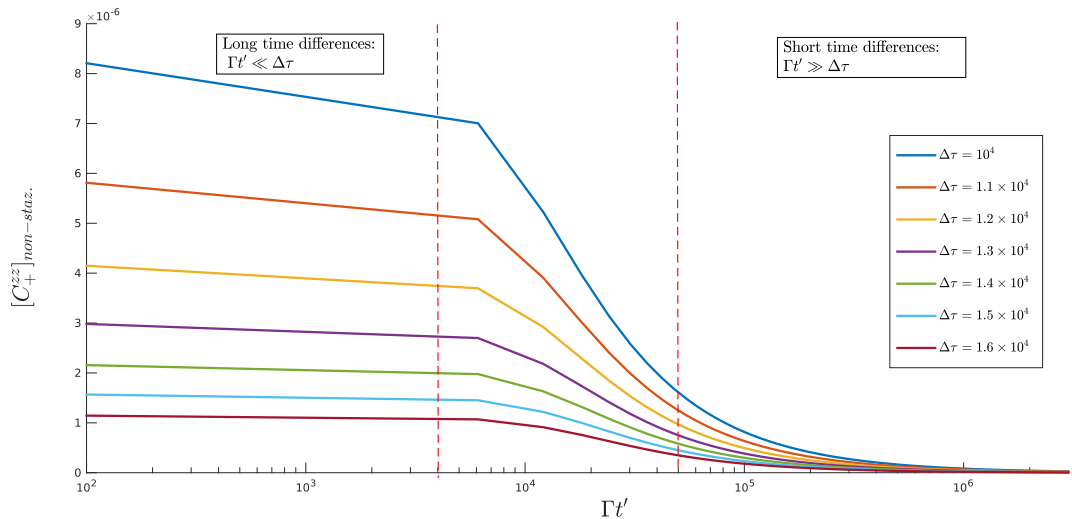


**Figure 4.2:** Non-stationary correlation function  $[C_+^{zz}]_{non-stat.}$  given by Eq. (4.57) as a function of  $\Gamma t'$  with fixed  $\Delta r = 5$  and  $\Gamma/\Delta = 5 \times 10^{-4}$ .  $\Gamma t'$  assumes values in  $[10^2, 3 \times 10^6]$  (note  $x$ -axis is in log-scale).  $\Delta\tau$  ranges from  $10^4$  to  $1.6 \times 10^4$  at step of  $10^3$ . It is evident the existence of two region where the correlation function shows a qualitative different behavior. At short time differences  $\Delta\tau \ll \Gamma t'$  (right region), the system is not able to distinguish two-time quantities from the corresponding at one-time. Instead, for much longer time differences  $\Delta\tau \gg \Gamma t'$  (left region) a new and different behavior, peculiar of two-time correlator, emerges.

temperature for the noisy quantum Ising chain. In order to simplify the analysis of Eqs. (4.55) and (4.56), we focus on the autocorrelation function  $C^{zz}(r = 0, t, t')$ , i.e., on the correlation between the values of the same spin at two different times. From the discussion in Sec. 3.3, we know that in the long-time limit (4.41) the coherences are suppressed by the noise, i.e., the quantum effects are negligible and it is therefore legitimate to expect the emergence of a sort of classical dynamics which can be eventually characterized by an effective temperature derived from the classical fluctuation-dissipation theorem (1.61). First of all, we note that the integrals (4.51) and (4.54) vanishes for  $r = 0$ . Accordingly, Eqs. (4.55) and (4.56) can be written as

$$C_+^{zz}(r = 0, \tau, T) = e^{-\frac{\Gamma}{2}|\tau|} |A_1(0, \tau) + A_2(0, \tau)|^2 - 4 |C_1(0, \tau, T) - C_2(0, \tau, T)|^2, \quad (4.65)$$

$$R^{zz}(r = 0, \tau, T) = -8\theta(\tau) e^{-\frac{\Gamma}{4}|\tau|} \text{Im} \{ [A_1(0, \tau) + A_2(0, \tau)] [C_2^*(0, \tau, T) - C_1^*(0, \tau, T)] \}, \quad (4.66)$$

From Eqs. (D.5), (D.6), (D.10) and (D.11) reported in Appendix D, we find that for  $\tau \gg 1$ , Eqs. (4.65) and (4.66) are equal to

$$C_+^{zz}(r = 0, t', \tau \gg 1) = \frac{\Delta}{4\pi} e^{-\frac{\Gamma}{2}\tau} \left[ \frac{1}{\tau} - \frac{\Delta}{\sqrt{\Gamma^2 t'^2 + \Delta^2 \tau^2}} \right], \quad (4.67)$$

$$R^{zz}(r = 0, t', \tau \gg 1) = -\frac{\Delta^{3/2}}{\pi} \frac{e^{-\frac{\Gamma}{2}\tau}}{\sqrt{\tau}} \text{Im} \left[ \frac{1}{\sqrt{\Delta\tau + i\Gamma t'}} \right]. \quad (4.68)$$

At short time differences, i.e., for  $\Delta\tau \ll \Gamma t'$ , we can expand Eqs. (4.67) and (4.68) and find at the lowest order

$$C_+^{zz}(r=0, t', 1 \ll \tau \ll (\Gamma t')/\Delta) \simeq \frac{\Delta}{4\pi} \frac{e^{-\frac{\Gamma}{2}\tau}}{\tau}, \quad (4.69)$$

$$R^{zz}(r=0, t', 1 \ll \tau \ll (\Gamma t')/\Delta) \simeq \frac{\Delta^{3/2}}{\pi} \frac{e^{-\frac{\Gamma}{2}\tau}}{\sqrt{2\tau}} \frac{1}{\sqrt{\Gamma t'}}. \quad (4.70)$$

From the classical fluctuation-dissipation theorem (1.61), we can define a time-dependent inverse effective temperature  $\beta_{eff}(t', \tau)$  as

$$\beta_{eff}(t', \tau) \equiv -\frac{R^{zz}(t', \tau)}{\frac{d}{d\tau} C_+^{zz}(t', \tau)}. \quad (4.71)$$

Accordingly, from Eqs. (4.69) to (4.71) we obtain that, in the long-time limit (4.41) and for sufficiently short time differences  $\Delta\tau \ll \Gamma t'$ , the inverse effective temperature is

$$\beta_{eff}(t', \tau) \sim \sqrt{\frac{\Delta\tau}{\Gamma t'}}. \quad (4.72)$$

Equation (4.72) means that within the regime of short time differences investigated here the temperature is large and it increases with no bound as a function of  $t'$  with fixed  $\tau$ : eventually the system "thermalizes" at an infinite effective temperature. This picture agrees with that of Sec. 4.4.2: at short time differences compared to the time elapsed from the quench two-time quantities behave as they do at equal time, according to the analysis of equal-time quantities presented in Sec. 3.3, the system is continually heated up by the noise which drives it towards the infinite temperature state.

In the opposite limit of large time separations,  $\Delta\tau \gg \Gamma t'$ , Eqs. (4.67) and (4.68) take, instead, the form

$$C_+^{zz}(r=0, t', (\Gamma t')/\Delta \ll \tau) \simeq \frac{\Delta}{4\pi} \frac{e^{-\frac{\Gamma}{2}\tau}}{2\tau} \left(\frac{\Gamma t'}{\Delta\tau}\right)^2, \quad (4.73)$$

$$R^{zz}(r=0, t', (\Gamma t')/\Delta \ll \tau) \simeq \frac{\Delta}{2\pi} \frac{e^{-\frac{\Gamma}{2}\tau}}{\tau} \left(\frac{\Gamma t'}{\Delta\tau}\right). \quad (4.74)$$

Also in this case, we can extract an inverse effective temperature from Eqs. (4.73) and (4.74) through Eq. (4.72), which turns out to be

$$\beta_{eff}(t', \tau) \sim \frac{\Delta\tau}{\Gamma t'}. \quad (4.75)$$

The inverse effective temperatures in Eqs. (4.72) and (4.75) depend on the same parameter  $\Delta\tau/\Gamma t'$  via two different functional forms in the two different limiting cases of small and large values. Within the regime of large time separations  $\Delta\tau \gg \Gamma t'$  investigated here, the effective temperature (4.75) is small. It seems that the system somehow remembers the initial zero temperature, but currently the physical interpretation of this

fact is unclear and perspective of this work is to investigate in detail the very nature of the novel behaviors which emerge at different times and the possible crossovers between the various regime. Moreover, we have to explore the limits of validity of Born approximation used until now and to confirm its validity within the regime in which the new behavior emerges.

Understanding the non-equilibrium dynamics of quantum many-body systems poses fundamental challenges which are presently motivating a growing theoretical and experimental activity in statistical physics and condensed matter, with recent and impressive advances. Due to the lack of general principles to treat systems out of equilibrium, insight coming from the study of specific models is still very valuable. In this thesis we focus on the non-equilibrium dynamics of a noisy quantum Ising chain (NQIC), consisting of a quantum Ising chain perturbed by a time-dependent delta correlated noise in the transverse field and driven out of equilibrium also by a sudden quench of the static component of the transverse field. We know from the investigation of various one-time observables [34] that the system first attains an intermediate prethermal state and then it is driven towards an infinite-temperature thermal state. Moreover, at longer times, when the noise has come into play, the equal-time correlator of the transverse magnetization shows a diffusive behavior. However, in the literature only one-time quantities were considered; the aim of this thesis is to extend the calculation to two-time quantities and, in particular, determine its correlation and linear response functions. Two-time quantities are, in fact, very important because they carry additional information on how the dynamics occurs and, moreover, they offer the possibility to study fluctuation-dissipation relations out of equilibrium and introduce effective temperatures on their basis [38].

After the general introduction to the topic of the non-equilibrium dynamics of quantum many-body systems in Chapter 1, Chapter 2 presents the necessary background about the quantum Ising chain (QIC) which the NQIC we are interested in is based on. The latter model is then discussed in detail in Chapter 3. The core of the thesis is presented in Chapter 4 where, first of all, we analyze a simplified model consisting of a two-level system driven out of equilibrium by a time-dependent noise which heats the system. From the fluctuation-dissipation relations we are able to extract a parameter, which we call effective temperature and which signals that the two-level system is always out of equilibrium during the evolution, while it reaches an infinite-temperature thermal state

only in the infinite-time limit. Then we focus on the analysis of two-time quantities of the NQIC. Using Keldysh diagrammatic technique, we are able to solve analytically the Dyson equations for the Greens function in the self-consistent Born approximation, valid for sufficiently weak noise. From the solution of the Greens function we can find expressions of the correlation and linear response functions of transverse spins at different times. These expressions results to be very rich as they show a variety of possible regimes; therefore we focus on the long-time limit in which the noise has come in play leaving the analysis of the other regimes to future studies. We find that at short time differences compared to the time elapsed from the quench, the two-time correlator of the transverse magnetization shows a diffusive behavior analogous to the one of the equal-time correlator. On the contrary, for much longer time differences, the qualitative behavior of the two-time correlator changes completely and the "propagation" becomes ballistic. Clearly, this crossover is totally new and cannot be detected in one-time quantities. Finally, we extract from the classical fluctuation-dissipation relations an effective temperature; in the case of short time differences compared to the time elapsed from the quench we find a temperature which as time goes by grows towards infinity, as we expect from the picture emerging from the analysis of the two-time correlator of the transverse magnetization. Instead, in the opposite case of much longer time differences we find an effective temperature that tends to zero: at the present we are not able to rationalize this fact and therefore more studies are required. The investigation of the non-equilibrium dynamics of a noisy quantum Ising chain is by no means concluded. Indeed, future perspectives include a complete and detailed analysis of the dynamics correlations calculated in this thesis within the various regions of the space-time diagram, the computation of two-time quantities for other observables, the improvement of the Born approximation used, for example including the Cooperons contributions in the two-time correlations, and understanding how these corrections affect the results found so far.

In this Appendix we provide some details about the Bogolyubov rotations which is extensively used in this thesis. The operator  $H_k = (g - \cos k)\sigma^z - (\sin k)\sigma^y$  which appears in Eq. (2.25) is self-adjoint and therefore its eigenvalues are real and the eigenvectors form an orthonormal basis. The eigenvalue equation

$$H_k \begin{pmatrix} u_k^g \\ -iv_k^g \end{pmatrix} = \epsilon_k^g \begin{pmatrix} u_k^g \\ -iv_k^g \end{pmatrix} \quad (\text{A.1})$$

gives the Bogolyubov equations, where  $u_k^g$  and  $v_k^g$  are real functions of  $k$

$$(g - \cos k)u_k^g + (\sin k)v_k^g = \epsilon_k^g u_k^g, \quad (\text{A.2})$$

$$(\sin k)u_k^g + (\cos k - g)v_k^g = \epsilon_k^g v_k^g. \quad (\text{A.3})$$

Note that if  $(u_k^g, -iv_k^g)$  is an eigenvector of  $H_k$  with eigenvalue  $\epsilon_k^g$  then  $(-iv_k^g, u_k^g)$  is eigenvector with eigenvalue  $-\epsilon_k^g$ . This can be written in the compact form:

$$H_k \begin{pmatrix} u_k^g & -iv_k^g \\ -iv_k^g & u_k^g \end{pmatrix} = \begin{pmatrix} u_k^g & -iv_k^g \\ -iv_k^g & u_k^g \end{pmatrix} \begin{pmatrix} \epsilon_k^g & 0 \\ 0 & -\epsilon_k^g \end{pmatrix} = \mathcal{R}(\theta_k^g) \epsilon_k^g \sigma^z, \quad (\text{A.4})$$

where  $\mathcal{R}^\dagger(\theta_k^g)$  is the Bogolyubov rotation operator. Moreover we assume the matrix  $\mathcal{R}(\theta_k^g)$  to be unitary; in order to satisfy this condition the coefficient  $u_k^g, v_k^g$  have to fulfill

$$(u_k^g)^2 + (v_k^g)^2 = 1 \quad (\text{A.5})$$

and therefore it is convenient to parametrize the coefficients as

$$u_k^g = \cos \theta_k^g \quad \text{and} \quad v_k^g = \sin \theta_k^g, \quad (\text{A.6})$$

where  $\theta_k^g$  is the so-called Bogolyubov angle. In terms of the rotations  $\mathcal{R}_k$  written above, the Hamiltonian  $H_k$  can be expressed as

$$H_k = \begin{pmatrix} u_k^g & -iv_k^g \\ -iv_k^g & u_k^g \end{pmatrix} \begin{pmatrix} \epsilon_k^g & 0 \\ 0 & -\epsilon_k^g \end{pmatrix} \begin{pmatrix} u_k^g & iw_k^g \\ iw_k^g & u_k^g \end{pmatrix}; \quad (\text{A.7})$$

in order to diagonalize it, it is natural to define the Bogolyubov fermions  $\{\gamma_k^g, \gamma_k^{g\dagger}\}$  in terms of the original Nambu spinor  $\{\Psi_k, \Psi_k^\dagger\}$  and fermions  $\{c_k, c_k^\dagger\}$  introduced in Sec. 2.2:

$$\begin{pmatrix} \gamma_k^g \\ \gamma_{-k}^{g\dagger} \end{pmatrix} = \begin{pmatrix} u_k^g & iw_k^g \\ iw_k^g & u_k^g \end{pmatrix} \begin{pmatrix} c_k \\ c_{-k}^\dagger \end{pmatrix} = \mathcal{R}^\dagger(\theta_k^g) \Psi_k \quad (\text{A.8})$$

The Bogolyubov fermions satisfy the canonical anticommutation relations because we assumed  $\mathcal{R}(\theta_k^g)$  to be unitary.

The eigenvalue  $\epsilon_k^g$  can be determined by looking for the roots of the characteristic polynomial

$$\det(H_k - \lambda \mathbf{1}) = \lambda^2 - (g - \cos k)^2 - \sin^2 k = 0, \quad (\text{A.9})$$

$$\lambda_\pm = \pm \epsilon_k^g = \pm \sqrt{(g - \cos k)^2 + \sin^2 k}. \quad (\text{A.10})$$

Now let us focus on the Bogolyubov Eqs. (A.2) and (A.3) and multiply them by  $u_k^g = \cos \theta_k^g$ :

$$(g - \cos k) \cos^2 \theta_k^g + \sin k \sin \theta_k^g \cos \theta_k^g = \epsilon_k^g \cos^2 \theta_k^g, \quad (\text{A.11})$$

$$(\cos k - g) \sin^2 \theta_k^g + \sin k \sin \theta_k^g \cos \theta_k^g = \epsilon_k^g \sin^2 \theta_k^g. \quad (\text{A.12})$$

By subtracting the first from the second we obtain the relation

$$\cos(2\theta_k^g) = \frac{g - \cos k}{\epsilon_k^g}, \quad (\text{A.13})$$

which determines the Bogolyubov angle as a function of  $k$  and of the transverse field  $g$ . By adding, instead, the two equations we have

$$\sin(2\theta_k^g) = \frac{\sin k}{\epsilon_k^g} \quad (\text{A.14})$$

and therefore the Bogolyubov angle  $\theta_k^g$  fulfills

$$\tan(2\theta_k^g) = \frac{\sin(2\theta_k^g)}{\cos(2\theta_k^g)} = \frac{\sin k}{g - \cos k}. \quad (\text{A.15})$$

For  $k > 0$  this relation has to be inverted with  $2\theta_k^g \in [0, \pi]$ , whereas the values of  $\theta_k^g$  for  $k < 0$  are obtained by using the property  $\theta_{-k}^g = -\theta_k^g$ .

## APPENDIX B

### GREEN'S FUNCTIONS OF TWO-LEVEL SYSTEM

In this Appendix we present the calculations to find the Green's functions  $G^{\gtrless}(t, t')$ , reported in Eqs. (4.10) and (4.11), of the two-level system. The starting point is the Dyson equations (3.42) for the Green's functions (4.8) and, as we do in Chapter 3 and we will do in the next Sections, we compute the self-energy within the self-consistent Born approximation (4.9). By substituting Eq. (4.9) into Eq. (3.42), we obtain two matrix differential equations

$$i\partial_t G^{\gtrless}(t, t') = \left[ h_0 - i \left( \frac{\Gamma_z + \Gamma_r}{4} \right) \right] G^{\gtrless}(t, t') + \theta(t' - t) \left[ \frac{\Gamma_z}{2} \sigma^z G^{\gtrless}(t, t) \sigma^z + \frac{\Gamma_r}{4} (\sigma^x G^{\gtrless}(t, t) \sigma^x + \sigma^y G^{\gtrless}(t, t) \sigma^y) \right] [G^<(t, t') - G^>(t, t')], \quad (\text{B.1a})$$

$$-i\partial_{t'} G^{\gtrless}(t, t') = G^{\gtrless}(t, t') \left[ h_0 + i \left( \frac{\Gamma_z + \Gamma_r}{4} \right) \right] - \theta(t - t') [G^<(t, t') - G^>(t, t')] \left[ \frac{\Gamma_z}{2} \sigma^z G^{\gtrless}(t, t) \sigma^z + \frac{\Gamma_r}{4} (\sigma^x G^{\gtrless}(t, t) \sigma^x + \sigma^y G^{\gtrless}(t, t) \sigma^y) \right], \quad (\text{B.1b})$$

where  $h_0 = (h/2)\sigma^z$  is given in Eq. (4.2) and we used the definition of retarded and advanced function (3.37 - 3.38). First of all, we need to calculate the equal-time Green's function. We define the density matrix  $\rho(t)$

$$\rho(t) = -iG^<(t, t), \quad (\text{B.2})$$

then by subtracting the first equation in Eq. (B.1) from the second one and taking the limit  $t \rightarrow t'$ , we obtain the master equation for the density matrix

$$\partial_t \rho(t) = -i[h_0, \rho] + \frac{\Gamma_z}{2} (\sigma^z \rho \sigma^z - \rho) + \frac{\Gamma_r}{4} (\sigma^x \rho \sigma^x + \sigma^y \rho \sigma^y - 2\rho), \quad (\text{B.3})$$

where we used Eqs. (3.50) and (3.51). Equation (B.3) is solved, as in Sec. 3.3, decomposing the density matrix on the Pauli basis

$$\rho(t) = \frac{1}{2}\mathbf{1} + \delta f(t)\sigma^z + z\sigma^+ + z^*\sigma^-, \quad (\text{B.4})$$

then by plugging this decomposition in Eq. (B.3) to finally find the easily solvable equations

$$\begin{aligned} \partial_t \delta f(t) &= -\Gamma_r \delta f(t), \\ \partial_t z(t) &= -ihz - \left( \Gamma_z + \frac{\Gamma_r}{2} \right) z(t). \end{aligned} \quad (\text{B.5})$$

The initial conditions depend on the assumed initial state of the system. From these equations, we can observe that the two-level system considered has a dephasing rate  $\Gamma_\phi$  given by

$$\Gamma_\phi = \Gamma_z + \frac{\Gamma_r}{2}. \quad (\text{B.6})$$

We now substitute Eq. (B.4) into Eq. (B.1) and using the  $\sigma$ -matrix multiplication rules

$$\begin{aligned} \sigma^y \sigma^z \sigma^y &= -\sigma^z \\ \sigma^x \sigma^\pm \sigma^x &= \sigma^\pm \\ \sigma^y \sigma^\pm \sigma^y &= -\sigma^\mp \\ \sigma^z \sigma^\pm \sigma^z &= -\sigma^\pm \end{aligned} \quad (\text{B.7})$$

we obtain the differential equations

$$\begin{aligned} i\partial_t G^\geq(t, t') &= \left[ \frac{h}{2}\sigma^z - i \left( \frac{\Gamma_z + \Gamma_r}{4} \right) \right] G^\geq(t, t') + i\theta(t' - t) \left\{ \mp \left( \frac{\Gamma_z + \Gamma_r}{4} \right) \right. \\ &\quad \left. + \left( \frac{\Gamma_z - \Gamma_r}{2} \right) \delta f(t)\sigma^z - \frac{\Gamma_z}{2} [z(t)\sigma^+ + z^*(t)\sigma^-] \right\} [G^<(t, t') - G^>(t, t')], \end{aligned} \quad (\text{B.8a})$$

$$\begin{aligned} -i\partial_{t'} G^\geq(t, t') &= G^\geq(t, t') \left[ \frac{h}{2}\sigma^z + i \left( \frac{\Gamma_z + \Gamma_r}{4} \right) \right] - i\theta(t - t') [G^<(t, t') - G^>(t, t')] \\ &\quad \left\{ \mp \left( \frac{\Gamma_z + \Gamma_r}{4} \right) + \left( \frac{\Gamma_z - \Gamma_r}{2} \right) \delta f(t')\sigma^z - \frac{\Gamma_z}{2} [z(t')\sigma^+ + z^*(t')\sigma^-] \right\}. \end{aligned} \quad (\text{B.8b})$$

The next step is to subtract the equation for  $G^<$  from the one for  $G^>$ , such that to find the differential equation ruling the evolution of  $G^< - G^>$  and then substitute its expression on the r.h.s of Eq. (C.1), where this difference naturally appears. Adopting

this strategy, one finds:

$$\partial_t [G^<(t, t') - G^>(t, t')] = \left[ -i\frac{\hbar}{2}\sigma^z - \left( \frac{\Gamma_z + \Gamma_r}{4} \right) \text{sgn}(t - t') \right] \times [G^<(t, t') - G^>(t, t')], \quad (\text{B.9a})$$

$$\partial_{t'} [G^<(t, t') - G^>(t, t')] = [G^<(t, t') - G^>(t, t')] \times \left[ i\frac{\hbar}{2}\sigma^z - \left( \frac{\Gamma_z + \Gamma_r}{4} \right) \text{sgn}(t - t') \right], \quad (\text{B.9b})$$

where  $\text{sgn}(t)$  indicates the sign function, i.e.,  $\text{sgn}(t) = 1$  if  $t > 0$  and  $\text{sgn}(t) = -1$  if  $t < 0$ . The solution of Eq. (B.9) is

$$G^<(t, t') - G^>(t, t') = i e^{-(\frac{\Gamma_z + \Gamma_r}{4})|t - t'|} \mathcal{H}(t - t'), \quad (\text{B.10})$$

where the matrix  $\mathcal{H}$  is defined in Eq. (4.12). We are able to obtain from Eqs. (B.8) and (B.10) a set of differential equation for  $G^<$  involving only  $G^<$ , and so for  $G^>$ , i.e.,

$$\begin{aligned} \partial_t G^{\gtrless}(t, t') &= \left[ -i\frac{\hbar}{2}\sigma^z - \left( \frac{\Gamma_z + \Gamma_r}{4} \right) \right] G^{\gtrless}(t, t') + i\theta(t' - t) e^{-(\frac{\Gamma_z + \Gamma_r}{4})|t - t'|} \\ &\quad \left\{ \mp \left( \frac{\Gamma_z + \Gamma_r}{4} \right) + \left( \frac{\Gamma_z - \Gamma_r}{2} \right) \delta f(t) \sigma^z - \frac{\Gamma_z}{2} [z(t) \sigma^+ + z^*(t) \sigma^-] \right\} \mathcal{H}(t - t'), \end{aligned} \quad (\text{B.11a})$$

$$\begin{aligned} \partial_{t'} G^{\gtrless}(t, t') &= G^{\gtrless}(t, t') \left[ i\frac{\hbar}{2}\sigma^z - \left( \frac{\Gamma_z + \Gamma_r}{4} \right) \right] + i\theta(t - t') e^{-(\frac{\Gamma_z + \Gamma_r}{4})|t - t'|} \\ &\quad \mathcal{H}(t - t') \left\{ \mp \left( \frac{\Gamma_z + \Gamma_r}{4} \right) + \left( \frac{\Gamma_z - \Gamma_r}{2} \right) \delta f(t') \sigma^z - \frac{\Gamma_z}{2} [z(t') \sigma^+ + z^*(t') \sigma^-] \right\}, \end{aligned} \quad (\text{B.11b})$$

with the functions  $\delta f$  and  $z$  given in Eq. (B.5). To solve Eq. (B.11), we firstly consider the case  $t > t'$ ; in this way Eq. (B.11a) can be easily solved to yield

$$G^<(t > t', t') = e^{-(\frac{\Gamma_z + \Gamma_r}{4})t} \mathcal{H}(t) N(t'), \quad (\text{B.12})$$

where  $N(t')$  is a matrix which depend on the time  $t'$ . By substituting this solution in Eq. (B.11b), and by using the expressions for the functions  $\delta f(t')$  and  $z(t')$  (see Eq. (B.5)), one finds an inhomogeneous differential equation for the matrix  $N(t')$  which can be solved via elementary method:

$$N(t') = e^{-(\frac{\Gamma_z + \Gamma_r}{4})t'} A \mathcal{H}^\dagger(t') + i \left[ e^{(\frac{\Gamma_z + \Gamma_r}{4})t'} \frac{\mathbf{1}}{2} + e^{(\frac{\Gamma_z - 3\Gamma_r}{4})t'} \delta f_0 \sigma^z + e^{-(\frac{3\Gamma_z + \Gamma_r}{4})t'} (z_0 \sigma^+ + z_0^* \sigma^-) \right], \quad (\text{B.13})$$

where  $A$  is a matrix of constant coefficients and  $\delta f_0$ ,  $z_0$  are the initial conditions of Eq. (B.5) depending on the assumed initial state. Combining Eqs. (B.12) and (B.13),

the Green's function turns out to be

$$G^<(t > t', t') = e^{-\left(\frac{\Gamma_z + \Gamma_r}{4}\right)(t+t')} \mathcal{H}(t) A \mathcal{H}^\dagger(t') + i \mathcal{H}(t) \left[ e^{-\left(\frac{\Gamma_z + \Gamma_r}{4}\right)(t-t')} \frac{\mathbf{1}}{2} + e^{-\frac{\Gamma_z}{4}(t-t') - \frac{\Gamma_r}{4}(t+3t')} \delta f_0 \sigma^z + e^{-\frac{\Gamma_z}{4}(t+3t') - \frac{\Gamma_r}{4}(t+t')} (z_0 \sigma^+ + z_0^* \sigma^-) \right] \mathcal{H}^\dagger(t'). \quad (\text{B.14})$$

For the remaining case  $t < t'$ , one can proceed as before, concluding that

$$G^<(t < t', t') = e^{-\left(\frac{\Gamma_z + \Gamma_r}{4}\right)(t+t')} \mathcal{H}(t) B \mathcal{H}^\dagger(t') + i \mathcal{H}(t) \left[ e^{-\left(\frac{\Gamma_z + \Gamma_r}{4}\right)(t'-t)} \frac{\mathbf{1}}{2} + e^{-\frac{\Gamma_z}{4}(t'-t) - \frac{\Gamma_r}{4}(t'+3t)} \delta f_0 \sigma^z + e^{-\frac{\Gamma_z}{4}(t'+3t) - \frac{\Gamma_r}{4}(t+t')} (z_0 \sigma^+ + z_0^* \sigma^-) \right] \mathcal{H}^\dagger(t') \quad (\text{B.15})$$

and  $B$  is a matrix of constant coefficients. In order to equal-time condition (B.4) holds, we have to impose  $A = B = 0$  and finally find the solution of the two-time Green's functions reported in Eqs. (4.10) and (4.11).

## APPENDIX C

# GREEN'S FUNCTION OF THE NOISY QUANTUM ISING CHAIN

In this Appendix we report the details of the determination of the Green's function Eqs. (4.32) and (4.34). We start from the Dyson equations (3.48) for the Green's function (3.47); one can show that the crossed diagrams are negligible [34] and therefore the self-energy can be computed within the self-consistent Born approximation Eq. (3.49). By substituting Eq. (3.49) into Eq. (3.48) and by using the definition of the retarded/advanced Green function Eqs. (3.37) and (3.38), we obtain two matrix differential equations

$$i\partial_t G^{\geq}(t, t') = \left[ H_k^0 - i\frac{\Gamma}{4} \right] G^{\geq}(t, t') + \frac{\Gamma}{2} \theta(t' - t) \sigma^z G^{\geq}(t, t) \sigma^z [G^<(t, t') - G^>(t, t')], \quad (\text{C.1a})$$

$$-i\partial_{t'} G^{\geq}(t, t') = G^{\geq}(t, t') \left[ H_k^0 + i\frac{\Gamma}{4} \right] - \frac{\Gamma}{2} \theta(t - t') [G^<(t, t') - G^>(t, t')] \sigma^z G^{\geq}(t', t') \sigma^z, \quad (\text{C.1b})$$

where  $H_k^0$  is given by Eq. (3.44). The next step is to subtract the equation for  $G^<$  from the one for  $G^>$ , such that to find the differential equation ruling the evolution of  $G^< - G^>$  and then substitute its expression on the r.h.s of Eq. (C.1), where this difference naturally appears. Adopting this strategy, one finds:

$$\partial_t [G^<(t, t') - G^>(t, t')] = - \left[ iH_k^0 + \frac{\Gamma}{4} \text{sgn}(t - t') \right] \times [G^<(t, t') - G^>(t, t')], \quad (\text{C.2a})$$

$$\partial_{t'} [G^<(t, t') - G^>(t, t')] = [G^<(t, t') - G^>(t, t')] \times \left[ iH_k^0 + \frac{\Gamma}{4} \text{sgn}(t - t') \right], \quad (\text{C.2b})$$

where  $\text{sgn}(t)$  indicates the sign function, i.e.,  $\text{sgn}(t) = 1$  if  $t > 0$  and  $\text{sgn}(t) = -1$  if  $t < 0$ . Now we apply a Bogolyubov rotation  $\mathcal{R}(\theta_k^0)$  (see Eq. (2.26)), in order to diagonalize  $H_k^0$

and express  $G^{\geq}$  in terms of the Bogolyubov fermions  $\{\gamma_k^g, \gamma_k^{g\dagger}\}$ :

$$H_k^0 \longmapsto \mathcal{R}^\dagger(\theta_k^g) H_k^0 \mathcal{R}(\theta_k^g) = \epsilon_k^g \sigma^z, \quad (\text{C.3})$$

with  $\epsilon_k^g$  defined in Eq. (2.31) and

$$G^<(t, t') \longmapsto \mathcal{R}^\dagger(\theta_k^g) G^<(t, t') \mathcal{R}(\theta_k^g) \equiv G_b^<(t, t') = i \begin{bmatrix} \langle \gamma_k^{g\dagger}(t') \gamma_k^g(t) \rangle & \langle \gamma_k^{g\dagger}(t') \gamma_{-k}^{g\dagger}(t) \rangle \\ \langle \gamma_{-k}^g(t') \gamma_k^g(t) \rangle & \langle \gamma_{-k}^g(t') \gamma_{-k}^{g\dagger}(t) \rangle \end{bmatrix}. \quad (\text{C.4})$$

We denoted by  $G_b^<$  the Green function in the Bogolyubov basis; in order to simplify the notation in the following we omit the subscript "b" and we indicate it simply by  $G^<$ .

After the rotation, Eq. (C.2) become

$$\partial_t [G^<(t, t') - G^>(t, t')] = - \left[ i\epsilon_k^g \sigma^z + \frac{\Gamma}{4} \text{sgn}(t - t') \right] \times [G^<(t, t') - G^>(t, t')], \quad (\text{C.5a})$$

$$\partial_{t'} [G^<(t, t') - G^>(t, t')] = [G^<(t, t') - G^>(t, t')] \times \left[ i\epsilon_k^g \sigma^z + \frac{\Gamma}{4} \text{sgn}(t - t') \right], \quad (\text{C.5b})$$

which can be solved by imposing the fundamental condition  $G^<(t, t) - G^>(t, t) = i\mathbf{1}$  (see Eq. (3.51)), with the result:

$$G^<(t, t') - G^>(t, t') = i e^{-\frac{\Gamma}{4}|t-t'|} \begin{bmatrix} \exp[-i\epsilon_k^g(t-t')] & 0 \\ 0 & \exp[i\epsilon_k^g(t-t')] \end{bmatrix}. \quad (\text{C.6})$$

By expressing Eq. (C.1) in the Bogolyubov basis and by substituting Eq. (C.6), we have

$$\partial_t G^<(t, t') = - \left( i\epsilon_k^g \sigma^z + \frac{\Gamma}{4} \right) G^<(t, t') + \frac{\Gamma}{2} \theta(t' - t) e^{\frac{\Gamma}{4}(t-t')} \sigma G^<(t, t) \sigma e^{-i\epsilon_k^g \sigma^z (t-t')}, \quad (\text{C.7a})$$

$$\partial_{t'} G^<(t, t') = G^<(t, t') \left( i\epsilon_k^g \sigma^z - \frac{\Gamma}{4} \right) + \frac{\Gamma}{2} \theta(t - t') e^{-\frac{\Gamma}{4}(t-t')} e^{-i\epsilon_k^g \sigma^z (t-t')} \sigma G^<(t', t) \sigma, \quad (\text{C.7b})$$

with the equal time condition given in Eqs. (3.61), (3.63) and (3.64) while  $\sigma$  is defined in Eq. (3.56). In the following we focus only on the lesser function  $G^<(t, t')$  because the greater one can be easily found by using Eq. (C.6). Moreover, we note that the Green function appearing on the r.h.s of Eq. (C.7) is at equal times, for which we already have a solution (Eqs. (3.61), (3.63) and (3.64)). From Eq. (3.53), one therefore finds

$$\begin{aligned} \frac{\Gamma}{2} \sigma G^<(t, t) \sigma &= i \partial_t \rho_k(t) - 2i\epsilon_k^g (x_k \sigma^y - y_k \sigma^x) + i \frac{\Gamma}{2} \rho_k(t) \\ &= i \frac{\Gamma}{2} \left[ \frac{\mathbf{1}}{2} + \sigma^z \cos(4\theta_k^g) \delta f_k(t) - \sigma^x x_k(t) - \sigma^y \cos(4\theta_k^g) y_k(t) \right], \end{aligned} \quad (\text{C.8})$$

where the functions  $\delta f_k(t)$ ,  $x_k(t)$  and  $y_k(t)$  are respectively given by Eqs. (3.63) and (3.64) and  $\theta_k^g$  are the Bogolyubov angles (see Eq. (2.28)). By substituting into Eq. (C.7) we

obtain two inhomogeneous differential equations

$$\begin{aligned} \partial_t G^<(t, t') &= - \left[ i\epsilon_k^g \sigma^z + \frac{\Gamma}{4} \right] G^<(t, t') + i\frac{\Gamma}{2} \theta(t' - t) e^{\frac{\Gamma}{4}(t-t')} \times \\ &\quad \times \left[ \frac{\mathbf{1}}{2} + \cos(4\theta_k^g) \delta f_k(t) \sigma^z - x_k(t) \sigma^x - \cos(4\theta_k^g) y_k(t) \sigma^y \right] e^{-i\epsilon_k^g \sigma^z (t-t')}, \end{aligned} \quad (\text{C.9a})$$

$$\begin{aligned} \partial_{t'} G^<(t, t') &= G^<(t, t') \left[ i\epsilon_k^g \sigma^z - \frac{\Gamma}{4} \right] + i\frac{\Gamma}{2} \theta(t - t') e^{-\frac{\Gamma}{4}(t-t')} \times \\ &\quad \times e^{-i\epsilon_k^g \sigma^z (t-t')} \left[ \frac{\mathbf{1}}{2} + \cos(4\theta_k^g) \delta f_k(t') \sigma^z - x_k(t') \sigma^x - \cos(4\theta_k^g) y_k(t') \sigma^y \right]. \end{aligned} \quad (\text{C.9b})$$

In order to solve Eq. (C.9) let us assume first that  $t > t'$ : Eq. (C.9a) simplifies as

$$\partial_t G^<(t > t', t') = - \left[ i\epsilon_k^g \sigma^z + \frac{\Gamma}{4} \right] G^<(t, t') \implies G^<(t > t', t') = e^{-(i\epsilon_k^g \sigma^z + \frac{\Gamma}{4})t} A(t'), \quad (\text{C.10})$$

where  $A(t')$  is a matrix which depend on the time  $t'$  and the momentum  $k$ . Substituting Eq. (C.10) into Eq. (C.9b) we find the following inhomogeneous differential equation for  $A(t')$ :

$$\begin{aligned} \partial_{t'} A(t') &= A(t') \left[ i\epsilon_k^g \sigma^z - \frac{\Gamma}{4} \right] + i\frac{\Gamma}{2} e^{(i\epsilon_k^g \sigma^z + \frac{\Gamma}{4})t'} \times \\ &\quad \times \left[ \frac{\mathbf{1}}{2} + \cos(4\theta_k^g) \delta f_k(t') \sigma^z - x_k(t') \sigma^x - \cos(4\theta_k^g) y_k(t') \sigma^y \right]. \end{aligned} \quad (\text{C.11})$$

By making explicit the matrix structure, we obtain for the diagonal elements  $A_{ii}$  of the matrix  $A$ :

$$\partial_{t'} A_{\frac{11}{22}}(t') = A_{\frac{11}{22}}(t') \left[ \pm i\epsilon_k^g - \frac{\Gamma}{4} \right] + i\frac{\Gamma}{2} e^{(\pm i\epsilon_k^g + \frac{\Gamma}{4})t'} \left[ \frac{1}{2} \pm \cos(4\theta_k^g) \delta f_0 e^{-\Gamma t' \sin^2 2\theta_k^g} \right], \quad (\text{C.12})$$

where we used Eq. (3.63), with the initial condition  $\delta f_0 = \sin^2(\Delta\theta_k) - \frac{1}{2}$  while  $\Delta\theta_k$  is given by Eq. (2.38). Equation (C.12) can be solved via elementary methods which yield

$$A_{\frac{11}{22}}(t') = C_{\frac{11}{22}} e^{(\pm i\epsilon_k^g - \frac{\Gamma}{4})t'} + \frac{i}{2} e^{(\pm i\epsilon_k^g + \frac{\Gamma}{4})t'} \pm i \left[ \sin^2(\Delta\theta_k) - \frac{1}{2} \right] e^{[\pm i\epsilon_k^g + \frac{\Gamma}{2} \cos(4\theta_k^g) - \frac{\Gamma}{4}]t'}, \quad (\text{C.13})$$

where  $C_{11/22}$  are arbitrary  $k$ -dependent integration constants which can be fixed on the basis of the initial conditions. Eventually, by using Eqs. (C.10) and (C.13), the diagonal elements of  $G^<(t > t', t')$  are given by

$$G_{22}^<(t > t', t') = C_{11}^{22} e^{\mp i\epsilon_k^g(t-t') - \frac{\Gamma}{4}(t+t')} + \frac{i}{2} e^{(\mp i\epsilon_k^g - \frac{\Gamma}{4})(t-t')} \pm i \left[ \sin^2(\Delta\theta_k) - \frac{1}{2} \right] e^{\mp i\epsilon_k^g(t-t') - \frac{\Gamma}{4}(t+t') + \frac{\Gamma}{2}t' \cos(4\theta_k^g)}. \quad (\text{C.14})$$

For the non-diagonal elements (still under the assumption  $t > t'$ ), from Eq. (C.11) we have

$$\partial_{t'} A_{12}^{21}(t') = A_{12}^{21}(t') \left[ \mp i\epsilon_k^g - \frac{\Gamma}{4} \right] + i \frac{\Gamma}{2} e^{(\pm i\epsilon_k^g + \frac{\Gamma}{4})t'} [-x_k(t') \pm i \cos(4\theta_k^g) y_k(t')]. \quad (\text{C.15})$$

The solution of Eq. (3.64) with initial condition  $x_k(0) = 0, y_k(0) = \frac{\sin 2(\Delta\theta_k)}{2}$ , coming from Eq. (2.59), are

$$x_k(t) = -2 \frac{\epsilon_k^g}{\Omega} \sin(2\Delta\theta_k) \sin\left(\frac{\Omega}{2}t\right) e^{-\frac{\Gamma}{2}[1+\cos^2(2\theta_k^g)]t}, \quad (\text{C.16a})$$

$$y_k(t) = \frac{\sin(2\Delta\theta_k)}{2} \left[ \cos\left(\frac{\Omega}{2}t\right) + \frac{\Gamma}{\Omega} \sin^2(2\theta_k^g) \sin\left(\frac{\Omega}{2}t\right) \right] e^{-\frac{\Gamma}{2}[1+\cos^2(2\theta_k^g)]t}, \quad (\text{C.16b})$$

where we define

$$\Omega \equiv \sqrt{|\Gamma^2 \sin^4(2\theta_k^g) - 16\epsilon_k^2|}. \quad (\text{C.17})$$

From Eqs. (C.15) and (C.16) we obtain

$$A_{12}^{21}(t') = C_{12}^{21} e^{(\mp i\epsilon_k^g - \frac{\Gamma}{4})t'} - i \sin(2\Delta\theta_k) \times \left\{ 2 \frac{\epsilon_k^g}{\Omega} \sin\left(\frac{\Omega}{2}t'\right) \pm \frac{i}{2} \left[ \frac{\Gamma}{\Omega} \sin^2(2\theta_k^g) \sin\left(\frac{\Omega}{2}t'\right) + \cos\left(\frac{\Omega}{2}t'\right) \right] \right\} \quad (\text{C.18})$$

and therefore, by combining Eqs. (C.10) and (C.18), the non-diagonal elements of the lesser Green function  $G^<$  are

$$G_{21}^<(t > t', t') = C_{12}^{21} e^{(\mp i\epsilon_k^g - \frac{\Gamma}{4})(t+t')} - i \sin(2\Delta\theta_k) e^{\mp i\epsilon_k^g(t-t') - \frac{\Gamma}{4}(t+t') - \frac{\Gamma}{2} \cos^2(2\theta_k^g)t'} \times \left\{ 2 \frac{\epsilon_k^g}{\Omega} \sin\left(\frac{\Omega}{2}t'\right) \pm \frac{i}{2} \left[ \frac{\Gamma}{\Omega} \sin^2(2\theta_k^g) \sin\left(\frac{\Omega}{2}t'\right) + \cos\left(\frac{\Omega}{2}t'\right) \right] \right\}, \quad (\text{C.19})$$

with arbitrary  $k$ -dependent integration constants  $C_{12/21}$ . For the remaining case  $t < t'$ , one can proceed as before, concluding that

$$G_{11}^<(t < t', t') = D_{11}^{22} e^{\mp i\epsilon_k^g(t-t') - \frac{\Gamma}{4}(t+t')} + \frac{i}{2} e^{(\mp i\epsilon_k^g + \frac{\Gamma}{4})(t-t')} \pm i \left[ \sin^2(\Delta\theta_k) - \frac{1}{2} \right] e^{\mp i\epsilon_k^g(t-t') - \frac{\Gamma}{4}(t+t') + \frac{\Gamma}{2}t \cos(4\theta_k^g)}, \quad (\text{C.20a})$$

$$G_{12}^<(t < t', t') = D_{12}^{21} e^{(\mp i\epsilon_k^g - \frac{\Gamma}{4})(t+t')} - i \sin(2\Delta\theta_k) e^{\pm i\epsilon_k^g(t-t') - \frac{\Gamma}{4}(t+t') - \frac{\Gamma}{2} \cos^2(2\theta_k^g)t} \times$$

$$\left\{ 2 \frac{\epsilon_k^g}{\Omega} \sin\left(\frac{\Omega}{2}t\right) \pm \frac{i}{2} \left[ \frac{\Gamma}{\Omega} \sin^2(2\theta_k^g) \sin\left(\frac{\Omega}{2}t\right) + \cos\left(\frac{\Omega}{2}t\right) \right] \right\}, \quad (\text{C.20b})$$

where  $D_{ij}$  are the elements of the  $k$ -dependent constant matrix  $D$  determined on the basis of the initial conditions. Combining Eqs. (C.14), (C.19) and (C.20) and requiring that  $G^<(t, t')$  satisfies the equal-time condition given by Eqs. (3.61), (3.63) and (3.64), we have to impose  $C = D = 0$  and finally find the solution anticipated in Eq. (4.32).

## APPENDIX D

### EVALUATION OF INTEGRALS

In this Appendix we present the details of the calculation via a saddle-point approximation of the integrals  $C_1$ ,  $C_2$  and  $D_1$  defined in eqs. (4.52), (4.53) and (4.54). The strategy consists in approximating the integrand of these integrals around  $k \simeq 0$  and  $k \simeq \pm\pi$ . Indeed, in the time range  $\Gamma T \gg 1$  we are interested in, they and the function  $\delta h_k$  in Eq. (4.45) are dominated by the slowest modes  $k \simeq 0$  and  $k \simeq \pm\pi$ , as it can be seen from Eq. (4.45). We focus only on the contribution from the mode  $k \simeq 0$ ; the modes  $k \simeq \pm\pi$  are due to the presence of the lattice and typically give rise to oscillating corrections which we neglect for the being. From Eq. (4.46) and the dispersion relation (2.31) for slow mode  $k \simeq 0$ , one has

$$\epsilon_{k \simeq 0}^g = 2\sqrt{k^2 + (g-1)^2} = 2\sqrt{k^2 + \Delta^2}, \quad (\text{D.1})$$

where  $\Delta = g - 1$  is half of the gap (2.56) of the quantum Ising chain. Accordingly, we can write the integrals (4.52) as

$$C_1(r, \tau, T) \simeq -e^{-\frac{\Gamma}{4}|\tau|} \int_{-\infty}^{\infty} \frac{dk}{8\pi} \left( 1 + \frac{\Delta}{\sqrt{k^2 + \Delta^2}} \right) \times \exp \left[ -\Gamma \left( T - \frac{|\tau|}{2} \right) \frac{k^2}{\Delta^2} - ikr - 2i\Delta\sqrt{k^2 + \Delta^2}\tau \right], \quad (\text{D.2})$$

which, by performing the substitution  $k = \Delta q$ , takes the form

$$C_1(r, \tau, T) \simeq -e^{-\frac{\Gamma}{4}|\tau|} \int_{-\infty}^{\infty} \frac{dq}{8\pi} \Delta \left( 1 + \frac{1}{\sqrt{q^2 + 1}} \right) \times \exp \left[ -\Gamma \left( T - \frac{|\tau|}{2} \right) q^2 - i\Delta r q - 2i\Delta\tau\sqrt{q^2 + 1} \right]. \quad (\text{D.3})$$

From Eq. (D.3) it is clear that the exponential decay induced by a non-vanishing noise strength  $\Gamma \neq 0$  gives a natural cutoff which enforces the convergence of the integral; in particular the largest contribution to the integral comes from the modes with

$$q \ll \frac{1}{\sqrt{\Gamma \left(T - \frac{|\tau|}{2}\right)}} = \frac{1}{\sqrt{\Gamma \min(t, t')}}; \quad (\text{D.4})$$

recalling we have assumed in Eq. (4.41) that  $\Gamma \min(t, t') \gg 1$ , we can expand the integrand for small  $q$  and obtain, in the limit  $\Delta r \ll \Gamma \min(t, t')$ ,

$$\begin{aligned} C_1(r, \tau, T) &\simeq -e^{-\frac{\Gamma}{4}|\tau|} \int_{-\infty}^{\infty} \frac{dq}{8\pi} \Delta \left(2 - \frac{q^2}{2}\right) \\ &\quad \times \exp \left[ -\Gamma \left(T - \frac{|\tau|}{2}\right) q^2 - i\Delta r q - 2i\Delta\tau \left(1 + \frac{q^2}{2}\right) \right] \\ &= -\frac{\Delta}{4\pi} \sqrt{\frac{\pi}{\Gamma \left(T - \frac{|\tau|}{2}\right) + i\Delta\tau}} \\ &\quad \times \exp \left\{ -\frac{\Gamma}{4}|\tau| - 2i\Delta\tau - \frac{(\Delta r)^2}{4[\Gamma \left(T - \frac{|\tau|}{2}\right) + i\Delta\tau]} \right\} + O \left( \frac{\Delta r}{\Gamma \min(t, t')} \right)^{3/2}, \end{aligned} \quad (\text{D.5})$$

where we have performed the Gaussian integration and neglected higher-order terms coming from the quadratic terms  $\propto q^2$ . In the limit  $\Delta r \ll \Gamma \min(t, t')$  the integrals  $C_2$  and  $D_1$  given by Eqs. (4.53) and (4.54), respectively, can be neglected; indeed proceeding as before one finds

$$\begin{aligned} C_2(r, \tau, T) &\simeq -\frac{\Delta}{16\pi} e^{-\frac{\Gamma}{4}|\tau| + 2i\Delta\tau} \int_{-\infty}^{\infty} dq q^2 \times \exp \left[ -\Gamma \left(T - \frac{|\tau|}{2} - \frac{i\Delta\tau}{\Gamma}\right) q^2 - i\Delta r q \right] \\ &= O \left( \left( \frac{\Delta r}{\Gamma \min(t, t')} \right)^{3/2} \right), \end{aligned} \quad (\text{D.6})$$

$$\begin{aligned} D_1(r, \tau, T) &\simeq -\frac{\Delta}{8\pi} e^{-\frac{\Gamma}{4}|\tau| - 2i\Delta\tau} \int_{-\infty}^{\infty} dq \left( q - \frac{q^3}{2} \right) \times \exp \left[ -\Gamma \left(T - \frac{|\tau|}{2} + \frac{i\Delta\tau}{\Gamma}\right) q^2 - i\Delta r q \right] \\ &= O \left( \frac{\Delta r}{\Gamma \min(t, t')} \right). \end{aligned} \quad (\text{D.7})$$

Now we want to evaluate the integrals  $A_1$  and  $A_2$  reported in Eqs. (4.49) and (4.50) for  $r = 0$  in the limit  $\tau \gg 1$ . Since we are considering  $\tau \gg 1$ , these integrals are dominated by the slowest modes  $k \simeq 0$  and  $k \simeq \pm\pi$ . Therefore they can be computed by approximating the corresponding integrands around  $k \simeq 0$  (analogously to what we have done above, we neglect here the lattice corrections coming from the modes  $k \simeq \pm\pi$ ).

Consider the integral  $A_1(r = 0, \tau)$  in Eq. (4.49):

$$A_1(r = 0, \tau) = \int_{-\pi}^{\pi} \frac{dk}{2\pi} \left( \frac{1}{2} + \frac{g - \cos k}{\epsilon_k^g} \right) e^{-i\epsilon_k^g \tau} \simeq \int_{-\infty}^{\infty} \frac{dk}{2\pi} \left( \frac{1}{2} + \frac{\Delta}{2\sqrt{k^2 + \Delta^2}} \right) e^{-2i\sqrt{k^2 + \Delta^2}\tau}, \quad (\text{D.8})$$

where  $\epsilon_k^g$  is the dispersion relation (2.31),  $\Delta$  is half the gap (2.56) and we extend the domain of integration from the Brillouin zone to the entire real-axis. With the substitution  $q = k/\Delta$ , the integral (D.8) can be written as

$$\begin{aligned} A_1(r = 0, \tau) &= \int_{-\infty}^{\infty} \frac{dq}{2\pi} \frac{\Delta}{2} \left( 1 + \frac{1}{\sqrt{q^2 + 1}} \right) e^{-2i\Delta\tau\sqrt{q^2 + 1}} \\ &\simeq \frac{\Delta}{2} \int_{-\infty}^{\infty} \frac{dq}{2\pi} \left( 2 - \frac{q^2}{2} \right) e^{-2i\Delta\tau(1+q^2/2)}, \end{aligned} \quad (\text{D.9})$$

where in the last line we have expanded the integrand in power series around  $q = 0$ . The integral (D.9) is elementary and, after neglecting higher-order corrections coming from the quadratic term  $\propto q^2$ , we obtain

$$A_1(r = 0, \tau \gg 1) \simeq \sqrt{\frac{\Delta}{4\pi i\tau}} e^{-2i\Delta\tau}. \quad (\text{D.10})$$

The integral  $A_2(r = 0, \tau \gg 1)$  given by Eq. (4.50) can be evaluated along the same lines with the result

$$A_2(r = 0, \tau \gg 1) \simeq \frac{\Delta}{4} \int_{-\infty}^{\infty} \frac{dq}{2\pi} \frac{q^2}{2} e^{-2i\Delta\tau(1+q^2/2)} \simeq \frac{\Delta}{16\sqrt{\pi}} \left( \frac{i}{\Delta\tau} \right)^{3/2} e^{2i\Delta\tau}; \quad (\text{D.11})$$

note that it is negligible compared to Eq. (D.10) in the limit  $\tau \gg 1$ .

## REFERENCES

- [1] Immanuel Bloch, Jean Dalibard, and Wilhelm Zwerger. Many-body physics with ultracold gases. *Reviews of Modern Physics*, 80(3):885, 2008.
- [2] Anatoli Polkovnikov, Krishnendu Sengupta, Alessandro Silva, and Mukund Vengalattore. Colloquium: Nonequilibrium dynamics of closed interacting quantum systems. *Reviews of Modern Physics*, 83(3):863, 2011.
- [3] Markus Greiner, Olaf Mandel, Tilman Esslinger, Theodor W Hänsch, and Immanuel Bloch. Quantum phase transition from a superfluid to a mott insulator in a gas of ultracold atoms. *Nature*, 415(6867):39–44, 2002.
- [4] J Eisert, M Friesdorf, and Christian Gogolin. Quantum many-body systems out of equilibrium. *Nature Physics*, 11(2):124–130, 2015.
- [5] John von Neumann. Beweis des ergodensatzes und des H-theorems. *Zeitschrift fuer Physik*, 57:30–70, 1929.
- [6] Marcos Rigol, Vanja Dunjko, and Maxim Olshanii. Thermalization and its mechanism for generic isolated quantum systems. *Nature*, 452(7189):854–858, 2008.
- [7] Josh Deutsch. Quantum statistical mechanics in a closed system. *Physical Review A*, 43(4):2046, 1991.
- [8] Mark Srednicki. Chaos and quantum thermalization. *Physical Review E*, 50(2):888, 1994.
- [9] Robin Steinigeweg, Abdelah Khodja, Hendrik Niemeyer, Christian Gogolin, and Jochen Gemmer. Pushing the limits of the eigenstate thermalization hypothesis towards mesoscopic quantum systems. *Physical Review Letters*, 112(13):130403, 2014.
- [10] Marcos Rigol. Breakdown of thermalization in finite one-dimensional systems. *Physical Review Letters*, 103(10):100403, 2009.

- [11] Jean-Sebastien Caux and Jorn Mossel. Remarks on the notion of quantum integrability. *Journal of Statistical Mechanics: Theory and Experiment*, 2011(02):P02023, 2011.
- [12] Bill Sutherland. *Beautiful models: 70 years of exactly solved quantum many-body problems*. World Scientific, 2004.
- [13] Marcos Rigol, Vanja Dunjko, Vladimir Yurovsky, and Maxim Olshanii. Relaxation in a completely integrable many-body quantum system: an ab initio study of the dynamics of the highly excited states of 1d lattice hard-core bosons. *Physical Review Letters*, 98(5):050405, 2007.
- [14] Edwin T Jaynes. Information theory and statistical mechanics. *Physical review*, 106(4):620, 1957.
- [15] Miguel A Cazalilla. Effect of suddenly turning on interactions in the Luttinger model. *Physical Review Letters*, 97(15):156403, 2006.
- [16] Pasquale Calabrese, Fabian HL Essler, and Maurizio Fagotti. Quantum quench in the transverse field Ising chain: I. time evolution of order parameter correlators. *Journal of Statistical Mechanics: Theory and Experiment*, 2012(07):P07016, 2012.
- [17] Pasquale Calabrese, Fabian HL Essler, and Maurizio Fagotti. Quantum quenches in the transverse field Ising chain: II. stationary state properties. *Journal of Statistical Mechanics: Theory and Experiment*, 2012(07):P07022, 2012.
- [18] Martin Eckstein and Marcus Kollar. Nonthermal steady states after an interaction quench in the Falicov-Kimball model. *Physical Review Letters*, 100(12):120404, 2008.
- [19] Marcus Kollar and Martin Eckstein. Relaxation of a one-dimensional mott insulator after an interaction quench. *Physical Review A*, 78(1):013626, 2008.
- [20] Toshiya Kinoshita, Trevor Wenger, and David S Weiss. A quantum newton's cradle. *Nature*, 440(7086):900–903, 2006.
- [21] Elliott H Lieb and Werner Liniger. Exact analysis of an interacting Bose gas. I. the general solution and the ground state. *Physical Review*, 130(4):1605, 1963.
- [22] Elliott H Lieb. Exact analysis of an interacting Bose gas. II. the general solution and the ground state. *Physical Review*, 130(4):1616, 1963.
- [23] Corinna Kollath, Andreas M Läuchli, and Ehud Altman. Quench dynamics and nonequilibrium phase diagram of the Bose-Hubbard model. *Physical Review Letters*, 98(18):180601, 2007.
- [24] Mari Carmen Bañuls, J Ignacio Cirac, and Matthew B Hastings. Strong and weak thermalization of infinite nonintegrable quantum systems. *Physical Review Letters*, 106(5):050405, 2011.

- [25] Christian Gogolin, Markus P Müller, and Jens Eisert. Absence of thermalization in nonintegrable systems. *Physical Review Letters*, 106(4):040401, 2011.
- [26] Bram Wouters, Jacopo De Nardis, Michael Brockmann, Davide Fioretto, Marcos Rigol, and J-S Caux. Quenching the anisotropic heisenberg chain: exact solution and generalized Gibbs ensemble predictions. *Physical Review Letters*, 113(11):117202, 2014.
- [27] B Pozsgay, M Mestyán, MA Werner, M Kormos, G Zaránd, and G Takács. Correlations after quantum quenches in the  $X X Z$  spin chain: Failure of the generalized Gibbs ensemble. *Physical Review Letters*, 113(11):117203, 2014.
- [28] Jürgen Berges, Sz Borsányi, and Christof Wetterich. Prethermalization. *Physical Review Letters*, 93(14):142002, 2004.
- [29] Michael Moeckel and Stefan Kehrein. Interaction quench in the Hubbard model. *Physical Review Letters*, 100(17):175702, 2008.
- [30] Marcus Kollar, F Alexander Wolf, and Martin Eckstein. Generalized Gibbs ensemble prediction of prethermalization plateaus and their relation to nonthermal steady states in integrable systems. *Physical Review B*, 84(5):054304, 2011.
- [31] Ryan Barnett, Anatoli Polkovnikov, and Mukund Vengalattore. Prethermalization in quenched spinor condensates. *Physical Review A*, 84(2):023606, 2011.
- [32] Matteo Marcuzzi, Jamir Marino, Andrea Gambassi, and Alessandro Silva. Prethermalization in a nonintegrable quantum spin chain after a quench. *Physical Review Letters*, 111(19):197203, 2013.
- [33] Giuseppe Menegoz and Alessandro Silva. Prethermalization of weakly interacting bosons after a sudden interaction quench. *Journal of Statistical Mechanics: Theory and Experiment*, 2015(5):P05035, 2015.
- [34] Jamir Marino and Alessandro Silva. Relaxation, prethermalization, and diffusion in a noisy quantum Ising chain. *Physical Review B*, 86(6):060408, 2012.
- [35] Michael Gring, Maximilian Kuhnert, Tim Langen, Takuya Kitagawa, Bernhard Rauer, Matthias Schreitl, Igor Mazets, D Adu Smith, Eugene Demler, and Jörg Schmiedmayer. Relaxation and prethermalization in an isolated quantum system. *Science*, 337(6100):1318–1322, 2012.
- [36] Davide Rossini, Alessandro Silva, Giuseppe Mussardo, and Giuseppe E Santoro. Effective thermal dynamics following a quantum quench in a spin chain. *Physical Review Letters*, 102(12):127204, 2009.
- [37] Davide Rossini, Sei Suzuki, Giuseppe Mussardo, Giuseppe E Santoro, and Alessandro Silva. Long time dynamics following a quench in an integrable quantum spin chain: Local versus nonlocal operators and effective thermal behavior. *Physical Review B*, 82(14):144302, 2010.

- [38] Laura Foini, Leticia F Cugliandolo, and Andrea Gambassi. Dynamic correlations, fluctuation-dissipation relations, and effective temperatures after a quantum quench of the transverse field Ising chain. *Journal of Statistical Mechanics: Theory and Experiment*, 2012(09):P09011, 2012.
- [39] Leticia F Cugliandolo. The effective temperature. *Journal of Physics A: Mathematical and Theoretical*, 44(48):483001–483041, 2011.
- [40] Morikazu Toda, Ryogo Kubo, Nobuhiko Saitō, and Natsuki Hashitsume. *Statistical physics II: nonequilibrium statistical mechanics*, volume 30. Springer Science & Business Media, 1992.
- [41] Subir Sachdev. *Quantum phase transitions*. Wiley Online Library, 2007.
- [42] R Coldea, DA Tennant, EM Wheeler, E Wawrzynska, D Prabhakaran, M Telling, K Habicht, P Smeibidl, and K Kiefer. Quantum criticality in an Ising chain: experimental evidence for emergent E8 symmetry. *Science*, 327(5962):177–180, 2010.
- [43] Jonathan Simon, Waseem S Bakr, Ruichao Ma, M Eric Tai, Philipp M Preiss, and Markus Greiner. Quantum simulation of antiferromagnetic spin chains in an optical lattice. *Nature*, 472(7343):307–312, 2011.
- [44] Pascual Jordan and Eugene Wigner. Paulis equivalence prohibition. *Zeitschrift fuer Physik*, 47:631, 1928.
- [45] Maurizio Fagotti and Fabian HL Essler. Reduced density matrix after a quantum quench. *Physical Review B*, 87(24):245107, 2013.
- [46] Thomas Barthel and Ulrich Schollwöck. Dephasing and the steady state in quantum many-particle systems. *Physical Review Letters*, 100(10):100601, 2008.
- [47] Th Niemeijer. Some exact calculations on a chain of spins 12. *Physica*, 36(3):377–419, 1967.
- [48] Jørgen Rammer. *Quantum field theory of non-equilibrium states*. Cambridge University Press, 2007.
- [49] Hartmut Haug and Antti-Pekka Jauho. *Quantum kinetics in transport and optics of semiconductors*, volume 2. Springer, 2008.
- [50] Alex Kamenev. *Field theory of non-equilibrium systems*. Cambridge University Press, 2011.
- [51] Joseph Maciejko. *An introduction to nonequilibrium many-body theory*. Lecture Notes, 2007.
- [52] Alekseĭ Alekseevich Abrikosov, Lev Petrovich Gorkov, Igor Ekhtievich Dzyaloshinski, and Dzialoshinskiĭ Igor Ekhtievich. *Methods of quantum field theory in statistical physics*. Courier Corporation, 1975.

- [53] Alexander L Fetter and John Dirk Walecka. *Quantum theory of many-particle systems*. Courier Corporation, 2003.
- [54] Gian-Carlo Wick. The evaluation of the collision matrix. *Physical review*, 80(2):268, 1950.
- [55] Elliott H Lieb and Derek W Robinson. *The finite group velocity of quantum spin systems*. Springer, 2004.
- [56] Ludwig Mathey and Anatoli Polkovnikov. Light cone dynamics and reverse Kibble-Zurek mechanism in two-dimensional superfluids following a quantum quench. *Physical Review A*, 81(3):033605, 2010.
- [57] Alessandro Silva. Quench dynamics of the dissipative quantum Ising model I: Keldysh technique and simple applications to two level systems. *Unpublished notes*, 2007.